Not-In-Kind Technologies for Residential and Commercial Unitary Equipment

February 2000

Steve Fischer
Solomon Labinov
Oak Ridge National Laboratory
Oak Ridge, Tennessee

Prepared by the
OAK RIDGE NATIONAL LABORATORY
Oak Ridge, Tennessee 37831
managed by
LOCKHEED MARTIN ENERGY RESEARCH CORP.
for the
U.S. DEPARTMENT OF ENERGY
under contract number DE-AC05-96OR22464

ACKNOWLEDGEMENTS

The authors gratefully acknowledge the assistance and support they received from many individuals and organizations. This project would not have been possible without the funding provided by the Department of Energy and the individual efforts of Esher Kweller and John Ryan of DOE. Mr. Kweller, Van Baxter and Phil Fairchild of ORNL, and Karim Amrane of the Air Conditioning and Refrigeration Institute (ARI) provided the advice and direction necessary for a useful evaluation of alternative cycles and concise presentation of operating principles, advantages, disadvantages, and economic feasibility of each technology. Members of the ARI Research and Technology committee and ARTI 21-CR Alternative Cycles subcommittee were instrumental in encouraging DOE to undertake this effort and provided valuable information to the project. Steve Garrett at Penn State University, Carl Zimm at Astronautics of America, Jim Braun at Purdue University, Greg Swift at Los Alamos National Laboratory, Rick Murphy and Robert DeVault of Oak Ridge National Laboratory, and many others provided detailed information about their own research on heat pumping technologies.

ABSTRACT

This project was initiated by the Department of Energy in response to a request from the HVAC industry for consolidated information about alternative heating and cooling cycles and for objective comparisons of those cycles in space conditioning applications. Twenty-seven different heat pumping technologies are compared on energy use and operating costs using consistent operating conditions and assumptions about component efficiencies for all of them. This report provides a concise summary of the underlying principals of each technology, its advantages and disadvantages, obstacles to commercial development, and economic feasibility. Both positive and negative results in this study are valuable; the fact that many of the cycles investigated are not attractive for space conditioning avoids any additional investment of time or resources in evaluating them for this application. In other cases, negative results in terms of the cost of materials or in cycle efficiencies identify where significant progress needs to be made in order for a cycle to become commercially attractive.

Specific conclusions are listed for many of the technologies being promoted as alternatives to electrically-driven vapor compression heat pumps using fluorocarbon refrigerants. Although reverse Rankine cycle heat pumps using hydrocarbons have similar energy use to conventional electric-driven heat pumps, there are no significant energy savings due to the minor differences in estimated steady-state performance; higher costs would be required to accommodate the use of a flammable refrigerant. Magnetic and compressor-driven metal hydride heat pumps may be able to achieve efficiencies comparable to reverse Rankine cycle heat pumps, but they are likely to have much higher life cycle costs because of high costs for materials and peripheral equipment. Both thermoacoustic and thermionic heat pumps could have lower life cycle costs than conventional electric heat pumps because of reduced equipment and maintenance costs although energy use would be higher.

There are strong opportunities for gas-fired heat pumps to reduce both energy use and operating costs outside of the high cooling climates in the southeast, south central states, and the southwest. Diesel and IC (Otto) engine-driven heat pumps are commercially available and should be able to increase their market share relative to gas furnaces *on a life cycle cost basis*; the cost premiums associated with these products, however, make it difficult to achieve three or five year paybacks which adversely affects their use in the U.S. Stirling engine-driven and duplex Stirling heat pumps have been investigated in the past as potential gas-fired appliances that would have longer lives and lower maintenance costs than diesel and IC engine-driven heat pumps at slightly lower efficiencies. These potential advantages have not been demonstrated and there has been a low level of interest in Stirling engine-driven heat pumps since the late 1980's. GAX absorption heat pumps have high heating efficiencies relative to conventional gas furnaces and are viable alternatives to furnace/air conditioner combinations in all parts of the country outside of the southeast, south central states, and desert southwest. Adsorption heat pumps may be competitive with the GAX absorption system at a higher degree of mechanical complexity; insufficient information is available to be more precise in that assessment.

TABLE OF CONTENTS

LIST OF TABLES

LIST OF FIGURES

EXECUTIVE SUMMARY

This project was initiated by the Department of Energy in response to a request from the HVAC industry for consolidated information about alternative heating and cooling cycles and for objective comparisons of those cycles in space conditioning applications. In the past individual companies investigated, or re-investigated, alternative cycles for each new generation of R&D managers and engineers. There was a great deal of duplication of effort between companies and occasionally within companies. It was recognized by members of the Air Conditioning and Refrigeration Institute (ARI) Research and Technology committee, and by individuals in the HVAC industry, that a national laboratory is well suited to perform such an evaluation and to provide a reference document to the industry. This report should serve as a document that alleviates the needs of individual companies to investigate alternative cycles and to aid them in investigations of any cycles that they chose to pursue. In this context, both positive and negative results are valuable; the fact that many of the cycles investigated are not attractive for space conditioning avoids any additional investment of time or resources in evaluating them for this application. In other cases, negative results in terms of the cost of materials or in cycle efficiencies identify where significant progress needs to be made in order for a cycle to become commercially attractive.

ORNL worked with ARI and the ARTI 21-CR alternative cycles subcommittee to assemble a comprehensive list of technologies for evaluation and to create an outline for this report that provides a concise summary of the underlying principals of each technology, its advantages and disadvantages, obstacles to commercial development, and economic feasibility.

Information from over 300 sources, including technical journals and conference proceedings, personal contacts, patents, computer models, theses and dissertations, and product literature were collected and evaluated to compare the energy use of 27 possible heat pump cycles in the U.S. Modeled performance at the ARI rating conditions was used with TMY weather data for 117 cities to estimate gas and electricity use; state-wide average energy costs and DOE fuel escalation factors were used to estimate lifetime energy costs. Calculated steady-state and seasonal efficiencies are summarized in Tables 1 and 2.

It should be pointed out that while a broad selection of technologies are examined, the list is not all inclusive. There are heat pumping technologies under development that simply could not be fit into the framework of this project because of limitations on time and resources. Foremost among these, perhaps, is ground-coupled, or geothermal, heat pumps. These are very efficient, electrically-driven compression cycle heat pumps that have very low energy consumption but high first costs. Unfortunately, they could not be evaluated in this project because of the extensive analysis required to estimate their annual performance at different sites around the country. Such an evaluation would be very valuable. There is a similar situation with desiccant dehumidification systems. In most instances, desiccant systems are used in conjunction with a conventional vapor compression system. Evaluation of desiccant systems requires an hourly building simulation, similar to the intensive calculations required for geothermal heat pumps. This too is beyond the scope of this project.

Each of the alternative heat pump cycles that is considered is compared to either a conventional electric heat pump (HSPF 8.3, SEER 12) or a gas furnace with electric air conditioner (AFUE 80%,

Table 1 Seasonal and Steady-State Efficiencies for Electric-Driven Heat Pumps

Technology	HSPF (Btu/Wh)	SEER (Btu/Wh)	System COPs: Heating 47EF	Heating 17EF	Cooling 82EF	Cooling 95EF
a. Reverse Rankine Cycle						
R-22	9.0	11.9	3.90	2.60	4.02	3.20
R-290 (propane)	8.1	11.8	3.84	2.57	4.00	3.18
R-744 (transcritical CO_2)	7.8	9.5	3.78	2.32	3.21	2.26
b. Brayton Cycle						
Closed, Regenerative (current)	5.0	2.9	1.77	1.75	0.99	0.93
Closed, Regenerative (future)	5.2	3.3	1.87	1.80	1.12	1.06
c. Stirling Cycle	5.8	6.0	2.10	2.04	2.04	2.04
d. Vortex Tube	0.3	0.3	0.08	0.08	0.08	0.08
e. Thermoelectric						
Current Technology	3.9	2.5	1.40	1.09	0.86	0.62
Future Technology	5.8	8.3	2.30	1.73	2.79	2.40
f. Thermoacoustic	6.6	8.9	2.87	1.90	3.02	2.38
g. Pulse Tube	3.4	1.1	0.88	0.88	0.39	0.39
h. Malone Cycle	no data	no data	no data	no data	no data	no data
I. Magnetic Refrigeration	9.5	12.8	3.91	3.99	3.99	2.99
j. Compressor Driven Metal Hydride	6.0	10.5	2.75	1.44	3.54	2.87
k. Electro-Chemical Heat Pump	no data	no data	no data	no data	no data	no data

SEER 12). The calculated HSPF of the baseline electric heat pump in Table 1 is slightly higher than that of the actual equipment chosen for the baseline; comparisons throughout this report are of calculated results to calculated results unless otherwise noted. Only the magnetic heat pump is competitive with the baseline heat pump in energy use although Rankine cycle machines using propane or CO_2 are nearly as efficient as fluorocarbon systems. All of these electric driven systems have drawbacks that limit their viability as replacements for Rankine cycle fluorocarbon systems. GAX absorption, engine-driven, Vuilleumier cycle, and duplex Stirling gas-fired heat pumps are all viable alternatives to the gas furnace baseline. Insufficient data are available to compare adsorption concepts with the baseline systems.

Most of the gas-fired systems have significantly higher heating efficiencies than the baseline gas furnace / electric air conditioner combination but lower cooling gCOPs.

While the efficiencies provide insights into the relative energy costs of operating each system, they do not provide direct information on the ownership costs which require knowledge of manufacturing, installation, and maintenance costs in addition to operating efficiency and building loads. It is beyond the scope of this project to estimate the manufacturing and installation costs of the alternative technologies, but it is possible to look at limits of what those costs could be. The difference between the lifetime energy and maintenance costs for a new technology and a baseline system tells how much more, or how much less, the installed costs of the alternative system would need to be in order for that system to have the same ownership cost as the gas or electric baseline equipment.

Table 2 Seasonal and Steady-State Efficiencies for Gas-Fired Heat Pumps

Technology	HSPF gCOP	CSPF gCOP	Parasitics W/ton	System COPs: Heating 47EF	System COPs: Heating 17EF	System COPs: Cooling 82EF	System COPs: Cooling 95EF
l. Gas Furnace / Electric Air Conditioner	0.80	1.36	210	0.80	0.80	1.57	1.17
m. Engine-Driven Heat Pump							
Diesel Engine	1.55	1.27	185	2.07	1.53	1.35	1.05
IC (Otto) Engine	1.43	1.09	185	1.85	1.39	1.16	0.90
Stirling Engine	1.38	1.02	185	1.76	1.33	1.08	0.84
Brayton Engine	1.35	0.98	185	1.71	1.30	1.04	0.81
Rankine Engine	1.27	0.87	185	1.58	1.21	0.93	0.72
n. Fuel Cell Powered Heat Pump	1.5	1.7	0	2.02	1.38	1.75	1.35
o. Vuilleumier Cycle	1.2	0.7	320	1.30	1.32	0.71	0.63
p. Absorption Cycles							
Single-Effect	no data	0.56	230	no data	no data	0.58	0.53
GAX	1.36	0.67	245/100	1.52	1.50	0.71	0.64
Double-Effect	1.55	0.94	220	1.78	1.75	1.00	0.80
q. Adsorption Cycles							
Metal Hydride							
Carbon / Ammonia							
Organic Salts	no data	no data	no data	no data	no data	no data	no data
r. Duplex Stirling Heat Pump	1.3	0.91	310	1.57	1.48	0.96	0.96
s. Ejector Heat Pump	1.0	0.3	280	1.05	1.04	0.29	0.21

Notes: electric air conditioner SEER converted to gCOP by backing out fan and blower power and scaling based on 3413 Btu_{site} / 11,500 Btu_{plant}.

Fuel Cell Powered Rankine Cycle Heat Pumps: The combination of a fuel cell and an electric-driven Rankine cycle heat pump, with heat recovery, is the most efficient system considered in this project. The equipment and maintenance costs, however, need to be significantly below those achieved to date and the fuel cell functional lifetime significantly longer in order for this technology to be viable in large parts of the U.S. Assuming that target first costs ($/kW) can be achieved for low capacity fuel cells, the economics are marginal in the northeastern states and unacceptable elsewhere.

Figure 1 shows the "allowable installed cost premium" for the fuel cell powered heat pump relative to the gas furnace / electric air conditioner baseline (maximum increase in equipment and installation costs that yields the same life-cycle costs) for the lower 48 states (assuming that maintenance costs for the fuel cell system are $100 per year higher than those for the baseline gas furnace). The dashed lines separating the extreme southwest and the south eastern states indicates where the installed cost of the fuel cell powered heat pump could be $500 per ton higher than the installed cost of the gas baseline and the two systems would still have the same life cycle costs. Below the northern panhandle of Florida the fuel cell powered system would need to cost less than the gas baseline while in the northeast and along the northern Pacific coast installed costs could be more than $1500 per ton higher. Installed costs in New York could be up to $3000 per ton higher at this maintenance costs and still have the same life cycle cost as the gas furnace baseline.

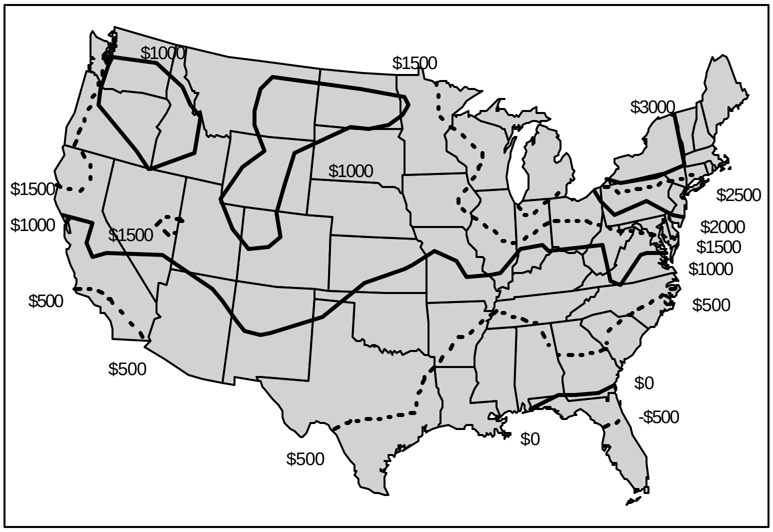

Fig. 1 Allowable installed cost premium ($/ton) for a fuel cell powered heat pump relative to the gas furnace baseline.

While the economics appear attractive, there are two noteworthy facts illustrated in Fig. 1. First, the “contours” on the map are widely separated so that underestimating the annual maintenance cost could have significant impacts; a small increase in maintenance costs will remove large portions of the country as viable markets. If the fuel cell has to be replaced once during the lifetime of the heat pump, then the “0" line shifts up above the current location of the $500 contour in Fig. 1; effectively reducing the potential market for the new system. Differences in local energy costs from the state-wide averages will also alter the comparisons significantly. Second, the incremental installed cost of this technology is approximately the cost of the fuel cell, projected to be $1000 to $1200 per kW of capacity. This cost will make fuel cell powered unitary heat pumps uneconomical in terms of life cycle cost except in the northeast and a narrow band along the northern Pacific coast. Factoring in uncertainties in the maintenance and non-energy operating costs restrict the potential market to New England and New York.

Engine-Driven Heat Pumps: Engine driven heat pumps compare favorably against the gas furnace / electric air conditioner baseline in all parts of the country except the southeast. An IC engine-driven heat pump could achieve the same life cycle cost as the gas furnace baseline at an installed cost several hundred dollars to as much as $2000 per ton higher than the gas furnace baseline depending on the region of the country and the differential in annual maintenance costs. These systems do not compare well in the southeast, south central, or southwestern states against the baseline gas furnace and electric air conditioner or in the southeast against the baseline electric heat pump.

Results for an IC engine-driven heat pump are shown in Fig. 2 relative to the gas furnace baseline assuming maintenance cost of $125/y (vs $100/y for the baseline system). The contours in this drawing show that the high efficiency and low operating costs of this system justify fairly high installed cost premiums (on a life cycle cost basis) in large parts of the country. The northeast and upper Midwest in particular could have strong markets for this product. The economic analysis also yields favorable results in the Pacific northwest, although a comparison should be made with an electric heat pump in much of the northwest because of the low electric rates in that area.

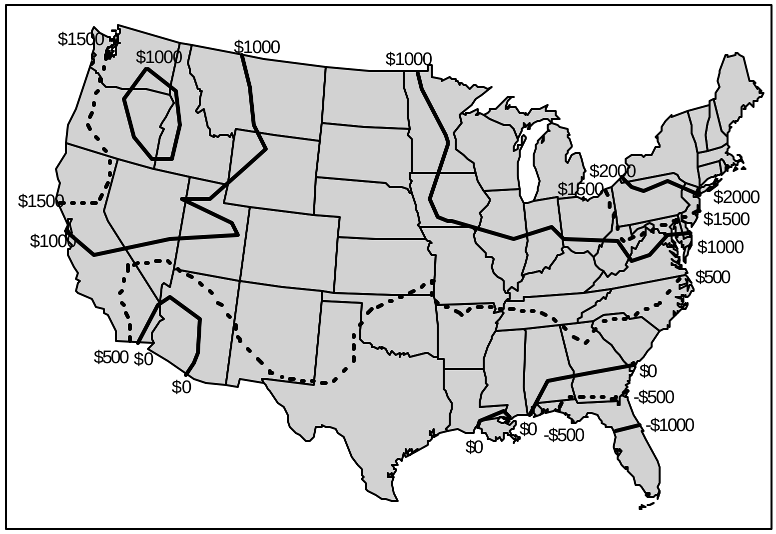

Fig. 2. Allowable installed cost premium ($/ton) for an IC engine-driven heat pump relative to the gas furnace baseline.

Absorption Cycle Heat Pumps: The GAX absorption cycle heat pump is an economically viable alternative to the gas furnace baseline in most of the U.S. Equal life cycle costs can be achieved at installed costs $500 to $1000 per ton higher than the gas furnace and electric air conditioner. The results of the economic evaluation of this technology relative to the gas furnace baseline are shown in Fig. 3 (assuming the same annual maintenance costs for the furnace and GAX heat pump). These data also show that this technology could have the same life cycle cost as the baseline systems at higher installed costs outside of the southeastern, south central, and desert southwest regions.

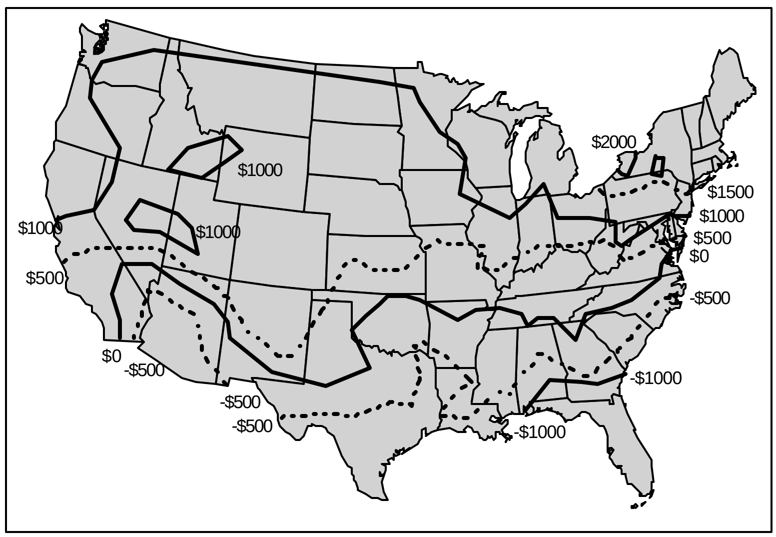

Fig. 3 Allowable installed cost premium ($/ton) for a GAX absorption heat pump relative to the gas furnace baseline.

For the most part, the remaining technologies listed in Tables 1 and 2 do not compare favorably with the electric and gas baseline heating and cooling systems.

Rankine cycle with propane: No reduction in operating costs relative to the baseline electric heat pump; first costs could be as much as 35% higher due to flammable refrigerant

Transcritical CO_2: Reduced efficiencies relative to the baseline electric heat pump would require medium to high reductions in installed costs in order to have 3 year or 5 year payback or for equivalent life cycle costs. Actual installed costs are likely to be similar to those for the baseline system.

Brayton Cycle: The significantly lower efficiencies of the Brayton cycle result in an extremely unfavorable comparison with the baseline electric heat pump; life cycle costs cannot be equal even if the Brayton cycle machines have 0 installed costs.

Stirling Cycle: The efficiencies are reduced relative to the baseline electric heat pump and installed costs would need to be more the $2000 per ton below the baseline costs to achieve equal life cycle costs. Manufacturing costs for the Stirling system are uncertain, but the estimated difference in lifetime energy costs exceeds the installed cost of the baseline system.

Magnetic Heat Pumps: Magnetic heat pumps have high theoretical efficiencies. The results of an economic evaluation with "reasonable" assumptions are shown in Fig. 4 (¼ hp pump, 175 W linear motor , $30/year maintenance differential). Installed costs can be $100 per ton higher than the electric heat pump baseline throughout most of the U.S. Cost increases of more than $200 per ton are supported in the northeast and parts of the Midwest with increases of up to $500 per ton in New York. Material costs will be a problem facing the commercialization of this technology in spite of the favorable economics shown in Fig. 4. The paramagnetic material alone would cost on the order of $6400 per ton of cooling capacity. The cost of superconducting magnet must also be considered.

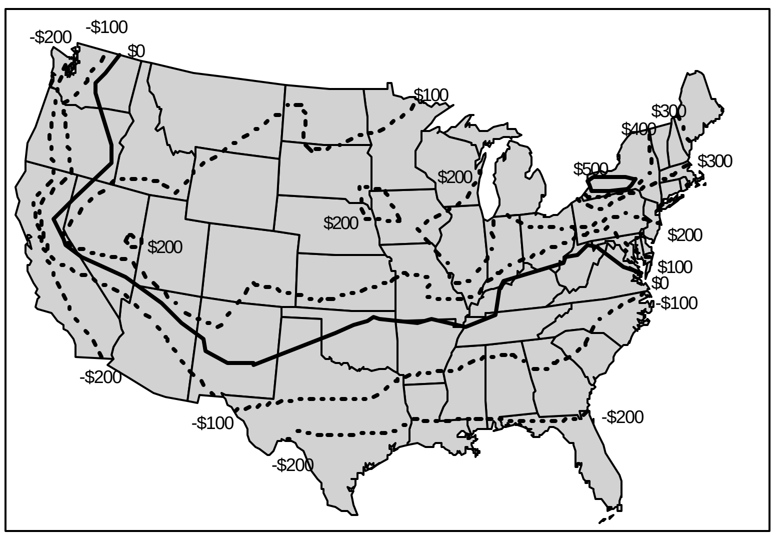

Fig. 4. Allowable installed cost premium ($/ton) for a magnetic heat pump relative to the electric heat pump baseline.

Thermoelectric and Thermionic Heating and Cooling: The best available thermoelectric cells have extremely low efficiencies and under the most favorable assumptions they would have lifetime operating costs in excess of $4000 per ton above the electric heat pump baseline. Either thermoelectric cells achieving the theoretical maximum efficiency or thermionic converters, however, could have the same life cycle cost as the baseline electric heat pump with reductions in installed costs of $300 to $600 per ton. That means they would have the same life cycle cost with an installed cost approximately 60% to 70% that of a conventional heat pump and a lower life cycle cost at an installed cost below that level. It is conceivable that such low costs could be achieved considering the dramatic reductions in manufacturing costs for other solid state electronics equipment.

Thermoacoustic Heat Pumps: In 1998, thermoacoustic heat pumps are projected to have efficiencies approximately 30% below those of conventional electric-driven heat pumps. The reduction in the number of moving parts may reduce equipment and maintenance costs sufficiently that thermoacoustic systems could have lower life cycle costs than the electric heat pump baseline, albeit at higher energy costs. Installed costs would need to be on the order of $600 to $1000 per ton below those of the baseline system however, which represents reductions on the order of 35% to 60% of the baseline costs.

Pulse-Tube Heat Pumps: This technology was developed for cryogenic applications and compares very unfavorably with the Rankine cycle heat pump at space conditioning temperature lifts. It is not suited to this application.

Malone Cycle Heat Pumps: Very little data are available to assess the potential of Malone cycles for space conditioning applications. Accurate thermodynamic and thermophysical data are needed for liquid CO_2 or propylene near their critical points in order to estimate COPs; these data are not available and efficiencies can not be estimated accurately.

Compressor Driven Metal Hydride: This technology has high cooling efficiencies, though about 10% below those of the baseline electric heat pump; the heating COPs are at best about 70% those of the electric heat pump. Cost reductions of more than $800 per ton would be necessary for this technology to compete with the electric baseline. Such savings are unlikely since this technology employs all of the major components of an electric heat pump and also requires the hydriding materials and secondary heat transfer loop.

Vuilleumier Cycle Heat Pumps: Vuilleumier cycle heat pumps are less efficient than “conventional” engine driven systems but they are inherently less complicated and could be viable products in predominantly heating climates. Both the installed cost and annual maintenance costs of the Vuilleumier cycle heat pump are unknown. Arguments can be made that both factors are lower than the corresponding values for the gas and electric baseline systems. A comparison of the Vuilleumier cycle heat pump with an engine-driven system shows that the Vuilleumier machine could have lower life cycle costs if the installed cost is $400 to $700 per ton less than that for the engine driven system and the annual maintenance costs are $50 lower.

Adsorption Cycle Heat Pumps: Insufficient data are available on COPs at the ARI rating conditions and independent cycle calculations could not be performed. Development of adsorption heat pumps appears to have ended without reaching commercialization.

Duplex Stirling Cycle Heat Pumps: Duplex Stirling heat pumps have attractive economics in the regions of the U.S. with relatively high heating loads, although the supportable increases in first costs are less favorable than they are for IC and diesel engine driven Rankine cycle heat pumps. The duplex Stirling systems have the potential to have lower maintenance costs than the other engine driven systems because they have many fewer moving parts, but thus far the high reliability and reduced maintenance have not been demonstrated. Further development is needed in regenerators, gas springs and bearings, and heat exchanger design for reduced log mean temperature differences. While actively pursued earlier, there have been no major development efforts undertaken since the late 1980s.

Ejector Heat Pumps: These systems have extremely low efficiencies and are not viable alternatives to the gas and electric baseline systems. They could be well suited to applications employing waste heat.

INTRODUCTION

Objectives

This project was initiated by the Department of Energy in response to a request from the HVAC industry for consolidated information about alternative heating and cooling cycles and for objective comparisons of those cycles in space conditioning applications. In the past individual companies investigated, or re-investigated, alternative cycles for each new generation of R&D managers and engineers. There was a great deal of duplication of effort between companies and occasionally within companies. It was recognized by members of the Air Conditioning and Refrigeration Institute (ARI) Research and Technology committee, and by individuals in the HVAC industry, that a national laboratory is well suited to perform such an evaluation and to provide a reference document to the industry. This report should serve as a document that alleviates the needs of individual companies to investigate alternative cycles and to aid them in investigations of any cycles that they chose to pursue. ORNL worked with ARI and the ARTI 21-CR alternative cycles subcommittee to assemble a comprehensive list of technologies for evaluation and to create an outline for this report that provides a concise summary of the underlying principals of each technology, its advantages and disadvantages, obstacles to commercial development, and economic feasibility.

Approximately 30 different heat pumping technologies have been identified as possible alternatives to conventional vapor compression systems in residential and commercial unitary equipment. Many of these technologies are addressed in the literature presenting performance data or relative comparisons, but the operating conditions and assumptions are frequently omitted from the publications or inconsistent with data in other publications or ARI rating conditions. This project is structured to identify those refrigeration technologies from the 30 that could become viable commercial products to compete with conventional vapor compression equipment in unitary applications. The evaluation, thus requires performance estimates for each technology at a uniform set of operating conditions as well as the application of some economic assumptions to determine "commercial viability." These requirements, coupled with the large number of technologies, made it impossible to include promising technologies such as geothermal or ground-coupled heat pumps and desiccant dehumidification systems in the analysis. No definitive conclusions are drawn about whether or not a particular technology will succeed in space conditioning applications, though sufficient information is presented to gauge the likelihood of the technology competing successfully against the established electric heat pump and gas furnace technologies.

Methodology

Unfortunately, very little operating data are available for most of the technologies considered in this evaluation. Consequently theoretical analyses are performed to estimate what the efficiency would be under assumed operating conditions and component efficiencies; these assumptions are stated clearly throughout this report. Wherever possible the modeled COPs are compared with reported data from the literature or from personal communications with experts in each field. This comparison of steady-state or seasonal efficiency acts either as corroboration of the theoretical calculations or as an indication of the shortcomings of this report; there are some of each.

By the very nature of heat pumps, there are times when an auxiliary heat source is required because the system capacity is insufficient to meet the load. Electric heat pumps provide backup heating to meet this excess demand with resistance heaters. Since there are so few gas-fired heat pumps commercially available, there is no “standard” for providing this supplementary heat. The analysis summarized in this report assumes that gas-fired heat pumps provide heat from three sources: (1) the outdoor heat source, (2) recovered waste heat, and (3) a gas burner with an 80% efficiency.

Economic Evaluations

The economic comparisons presented in this report are not direct cost comparisons between the alternative technologies and baseline electric-driven or gas-fired systems. It is far beyond the scope of this project to estimate the manufacturing cost of any of the alternative technologies. The comparisons, instead, are in terms of the approximate premium in installed cost for the alternative technology that would give it the same life-cycle cost as a baseline system; or alternatively, the required reduction in installed cost for a system which is less efficient than the baseline system. Qualitative statements are then made, where possible, about the alternative technology which add some perspective as to whether or not the installed cost premium is likely, or unlikely, to be possible. Installed cost premiums are specified throughout this report in terms of 1998 $/ton. Results are also presented for allowable cost premiums that would yield 3 and 5 year paybacks.

Each of the alternative technologies evaluated in this study is compared to either an electric heat pump or gas furnace / electric air conditioner baseline or both. The electric baseline is a commercially available three ton heat pump with rated performance HSPF of 8.3 and SEER of 12; while higher than the minimum standard SEER 10 heat pump, this unit is less efficient than the best available electric heat pump. The gas furnace baseline is defined as having an AFUE 80% efficiency and an SEER 12 air conditioner.

Binned weather data and building loads for 117 cities in the U.S. are used with modeled steady-state COPs to compute seasonal energy use in each city. The modeled COPs for the electric heat pump are very close to the manufacturer’s published values for the baseline unit. Each of the alternative technologies are assumed to have heat pumping and air conditioning capacities equal to those of the baseline heat pump; the capacity of gas-fired heat pumps is assumed to be augmented with heat recovery (up to 50% of the engine or absorber coolant and flue gas waste heat) to meet the building load. Cycling losses are computed using the C_d=0.25 for the fixed capacity heat pumps and C_d=0.10 for technologies with easily modulated capacity (e.g. engine-driven heat pumps, absorption systems).

The energy use data are used to compute lifetime operating costs for each system. Annual operating costs for 1998 are determined using statewide averages for gas and electricity rates for each of the 117 cities. This is a broad assumption and tremendous simplification; energy economics are city and utility area dependent and local rates should be used with estimated energy use data to determine more accurate economic comparisons. In this report, however, the present value of lifetime energy costs are computed using constant dollar energy costs from the Energy Information Administration, a discount rate of 4.1% and 3% for general inflation for an assumed 20 year equipment lifetime. The discount rate and rate of inflation are the values prescribed by DOE for life cycle cost analyses for federal projects.

The maintenance costs of the alternative cycles (relative to the baseline systems) and auxiliary energy use, unfortunately, are important if not crucial assumptions. In most instances results of the economic evaluation are presented across a range of “incremental” maintenance costs (e.g. $25 per year higher than the baseline electric heat pump). Estimates of the maintenance costs are used to identify a range of installed cost increases or decreases allowable for the alternative technology to have the same life cycle cost as one of the baseline systems. The allowable installed cost premiums are also listed for technologies that could possibly achieve three and five year paybacks. Pumping power for secondary heat transfer loops is assumed to be 100 W per ton of design capacity.

The simplified economic analysis presented in this report does not incorporate regional demographics. While the calculations are based on climate data for particular cities and state-wide average energy rate data, it is easiest to discuss the results in terms of geographic regions or individual states. For this purpose, the discussion of the economic analysis is frequently presented as a summary of results in the nine geographic regions encompassing the 117 cities used in the analysis:

- **Northeast**: New York, Pennsylvania, Massachusetts, Vermont, Maine, and New Jersey,
- **Southeast**: Florida, Georgia, South Carolina, North Carolina, Virginia, West Virginia, Kentucky, Tennessee, Alabama, Mississippi, and Louisiana,
- **South Central**: Texas, Oklahoma, Kansas, Missouri, and Arkansas,
- **Southwest**: Arizona and New Mexico,
- **Midwest**: Ohio, Michigan, Indiana, Illinois, Iowa, Wisconsin, and Minnesota,
- **Northern Plains**: Nebraska, North Dakota, and South Dakota,
- **Rocky Mountain**: Colorado, Wyoming, Montana, Utah, and Idaho,
- **Pacific Northwest**: Oregon and Washington,
- **California**: California and Nevada

These divisions are also illustrated in Fig.5. Regional and state-wide averages of three and five year payback and life cycle cost premiums are calculated for each state and region based on the number of the 117 cities located there.

The discussion of the economic analysis of each alternative technology includes comments of where the technology is most competitive with the baseline, some comments as to why it is appropriate in those cities (e.g. high heating loads, relative costs of gas and electricity), and what hardware differences need to be supported by the price differential (e.g. gas engine in place of an electric motor, increased heat transfer surfaces). There have been detailed costs analyses performed in both DOE and industry R&D projects for some of the technologies covered in this report. Where possible, the results obtained here are compared with those reported elsewhere to confirm or conflict with the findings reported here.

Fig. 5. Geographic regions for economic analysis.

Summary

Among the technologies which are not commercially available or do not have significant market share, there is current R&D activity in:

- thermionic and thermoelectric, primarily targeted at power generation,
- thermoacoustic heat pumps,
- compressor driven metal hydride heat pumps,
- transcritical CO_2 heat pumps,
- reverse Rankine cycle heat pumps using hydrocarbon refrigerants,
- GAX, open cycle, and triple-effect absorption heat pumps,
- adsorption cycles (ammoniated carbon, metal hydride, complex compounds/organic salts, open cycle),
- IC engine driven heat pumps,
- magnetic refrigeration, and
- compressor driven metal hydride heat pumps.

There is no significant known current R&D activity on:

- Stirling cycle refrigeration,
- Vuilleumier cycle cooling,

- Stirling, Brayton, or Rankine engine driven heat pumps,
- ejector heat pumps,
- pulse tube heat pumps, and
- vortex tubes.

The Brayton cycle is being applied in transportation systems (airplanes and the European high speed train). There is a low level of activity in Malone cycle cooling.

REVERSED RANKINE CYCLE HEAT PUMPS

Basic Concept Description

technology for electric-driven heat pumps and serves as a baseline for comparison of competing technologies. The schematic diagram in Fig. 6 illustrates the basic cycle. A hermetic compressor is used to compress a gas to a high temperature and pressure as shown in Figs. 7 and 8. Heat is rejected either to the ambient or to the conditioned space (depending on the mode of operation), cooling the gas and causing it to condense. The resulting hot, high pressure liquid is then expanded causing it to flash to a low pressure, low temperature mixture of liquid and vapor. This two-phase mixture is evaporated absorbing heat from the ambient (heating mode) or conditioned space (cooling mode) to form a low pressure, low temperature vapor that is returned to the compressor.

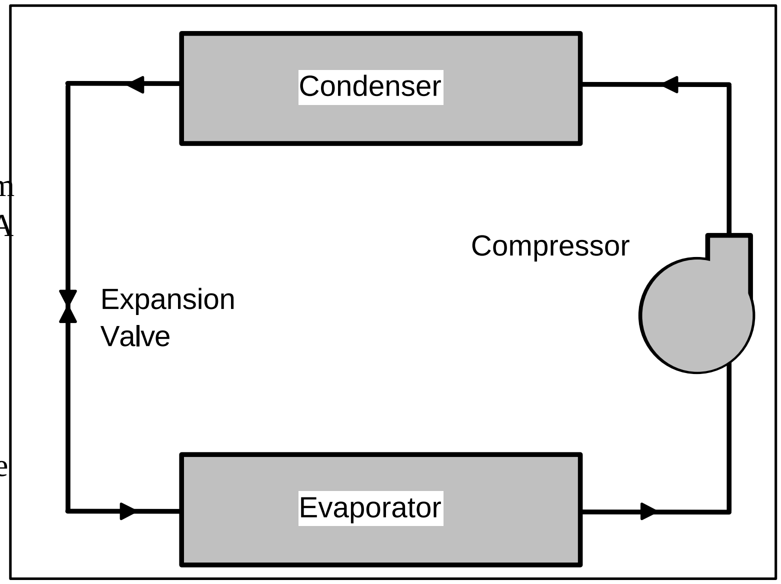

Fig. 6. Schematic diagram for reverse Rankine cycle heat pump.

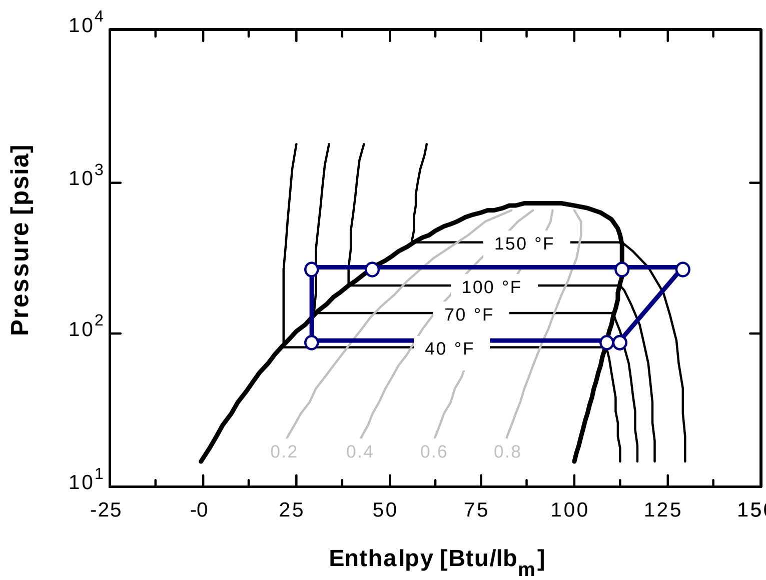

Fig. 7. Pressure - enthalpy (P-H) diagram for an idealized reverse Rankine cycle heat pump.

Background Information

Rankine cycle heat pumps grew out of the development of refrigeration systems for ice making and food preservation dating back to the 1830s. Reductions in size and improvements in reliability and safety led to the adaptation of refrigeration equipment to provide space comfort conditioning. Air conditioning was a novelty in the

1950s and 60s, becoming common in much of the country in the 1970s, and ubiquitous in the 1990s. A strong manufacturing base and sales and service organization exists for vapor compression heating and air-conditioning industry. R-22 has been used exclusively for residential and commercial unitary equipment since these systems became popular, but system and component manufacturers are currently redesigning their equipment to use new refrigerants because manufacturing and use of R-22 will be phased out under the Montreal Protocol. Future refrigerants in unitary systems could be blends of fluorocarbons, either azeotropic or zeotropic mixtures, hydrocarbons, or carbon dioxide; no single refrigerant has yet been determined as the preferred replacement for R-22.

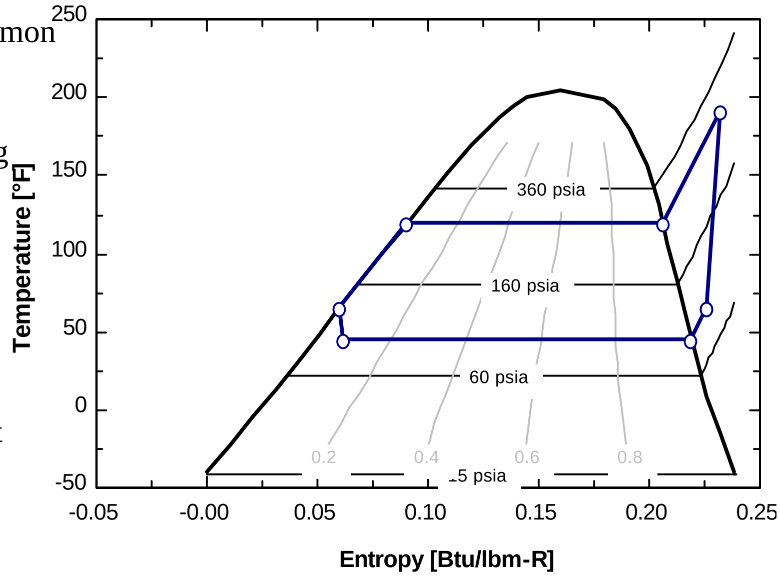

Fig. 8. Temperature-entropy (T-S) diagram for an idealized reverse Rankine cycle heat pump.

Secondary System Requirements

No secondary systems are required in “standard” air-to-air system. Secondary heat transfer loops are required in water source or ground loop systems and they could be used as a safety feature if the working fluid is flammable.

Efficiency Data

Cycle efficiencies are computed using the state points defined in Table 3 with R-22 as the working fluid. The combined motor/compressor efficiency is assumed to be 70%. The calculated steady-state COPs are listed in Table 4; separate entries are given for compressor only COPs

Table 3. State Point Temperatures for Rankine Cycle Calculations

State Point Temperatures	Ambient Temperatures			
	47EF	17EF	82EF	95EF
condensing	108EF	95EF	110EF	120EF
evaporating	32EF	8EF	47EF	49EF
superheat	10EF	0EF	20EF	10EF
subcooling	30EF	5EF	20EF	15EF

Table 4. Calculated and Observed Efficiencies for Rankine Cycle Heat Pumps with R-22.

	Heating			Cooling		
Cycle Efficiency	47EF	17EF	Seasonal (Btu/Wh)	82EF	95EF	Seasonal (Btu/Wh)
Compressor only COP						
theoretical	4.98	3.08		5.30	3.97	
observed						
System COP						
theoretical	3.90	2.60	9.0	4.02	3.20	11.9
observed	3.84	2.60	8.3		2.66	12.0

notes: blank entries denote absence of calculated or measured information, calculated and observed cycle efficiencies do not apply for the shaded seasonal boxes

and system COPs. System efficiencies are computed assuming 140 W per ton of cooling capacity for the indoor blower and 70 W per ton for the outdoor fan. Outdoor fan power is adjusted for the alternative technologies evaluated in this report based on the heat rejection requirement relative to the R-22 Rankine cycle baseline; the lower the cooling COP, the greater heat rejection is, and the large the fan motor power requirement.

A computer program from NIST using algorithms for computing HSPF and SEER is used to compute seasonal performance factors. The results in Table 4 are from an Excel spreadsheet that duplicates the calculations based on the Fortran program from NIST. Both heating and cooling seasonal performance factors are computed using a cycling Cd of 0.25. These results show a theoretical heating season performance factor 10% higher than the rated performance and a cooling SEER the same as the rated performance.

Technical Advantages/Benefits

These systems have been developed to the point where they are highly efficient, relatively inexpensive, and very dependable. There is an established network of sales and service personnel.

Technical Disadvantages

The fluorocarbon refrigerants that have been used traditionally, and all fluorocarbon alternatives to R-22, have appreciable global warming potentials (GWPs). Use of these refrigerants may be regulated or phased out under future international agreements to reduce emissions of greenhouse gases.

Top of the line, Rankine cycle heat pumps are also approaching the limits of efficiency for this technology, although the efficiency of the "average" system in use is much lower.

Technical Barriers

None.

Economic Analysis

The estimated installed cost of a three ton electric air-to-air heat pump (SEER 12) was $4660 to $5200 in 1995 (E Source 1995), or $1553 to $1733 per ton. A second source reported installed costs of $3850 to $4810 depending on climate (EPA 1993), or $1285 to $1600 per ton. Adjusting for inflation these numbers range from $1430 to $1830 per ton. Maintenance cost is estimated to be $100 per year.

Contacts and Sources of Information

Product literature.

EPA 1993. "Space Conditioning: The Next Frontier," EPA 430-R-93-004.

E Source 1995. "Product Profile: The York Triathalon," November.

Obvious Holes in Knowledge, Understanding, Information

None.

RANKINE CYCLE: HYDROCARBONS

Basic Concept Description

Fundamentally, the cycle is the same as the reverse Rankine cycle described on page 7 for fluorocarbon refrigerants. System redesign is necessary to use a flammable/explosive refrigerant safely.

Background Information

Hydrocarbons are excellent refrigerants and can be used in conventional reverse Rankine cycle electric-driven heat pumps. They have not been used in the U.S. because they are flammable and have not offered any compelling advantage over R-22 in unitary equipment. Some researchers, primarily in Europe, are promoting the use of hydrocarbons as refrigerants in commercial refrigeration and space conditioning because of the negligible GWPs of hydrocarbons. Use of hydrocarbons in these applications in the U.S. would necessitate changes in design to achieve levels of safety comparable to those achieved with non-flammable fluorocarbon refrigerants.

Secondary System Requirements

Secondary heat transfer loops can be used in unitary equipment designed with the entire mechanical package outside. This would isolate the flammable refrigerant from the occupied space, reducing fire hazards, and decrease the possibility of refrigerant leaks resulting in explosive concentrations. While improving safety, a secondary loop imposes thermodynamic losses and increased electrical parasitic power consumption.

Alternatively, lower life cycle costs may be possible for this system by modifying the design of a split system to use the flammable refrigerant safely. The analysis presented in this study assumes direct expansion heat exchangers with enhanced design to reduce the risks as listed by Keller (1997). These include:

- brazed tube joints isolated within the air handling section of the heat pump,
- pumping the refrigerant charge into a receiver in the outdoor unit during the off-cycle,
- totally enclosing the fan and blower motors and protecting the capacitor so it cannot serve as an ignition source,
- using thicker walled refrigerant tubing and providing additional external guards to protect the refrigerant circuit from accidental damage,
- use an explosion proof cover for the compressor terminals.

These, and additional safety features, are expected to increase unit costs by about 35% relative to R-22 (Keller 1997), but they will not have a significant effect on system efficiency.

Efficiency Data

The state point temperatures used to calculate cycle efficiencies for Rankine cycle heat pumps using a hydrocarbon as the refrigerant are listed in Table 3 on page 8. Calculated cycle and system efficiencies for a Rankine cycle heat pump using propane (R-290) are listed in Table 5. These values are based on an assumed motor/compressor efficiency of 70%. System COPs are computed using fan and blower powers as described on page 8 (70 W/ton and 140 W/ton).

Table 5. Calculated and Observed Efficiencies for Reverse Rankine Cycle Using Propane.

	Heating			Cooling		
Cycle Efficiency	47EF	17EF	Seasonal (Btu/Wh)	82EF	95EF	Seasonal (Btu/Wh)
Cycle COP theoretical observed	4.99	3.05		5.27	3.93	
System COP theoretical observed	3.84	2.57	8.1	4.00	3.18	11.8

notes: blank entries denote absence of calculated or measured information, calculated and observed cycle efficiencies do not apply for the shaded seasonal boxes

Technical Advantages/Benefits

Hydrocarbons have excellent thermodynamic and thermophysical properties that result in high COPs *if additional losses are not imposed on the cycle due to safety considerations*. Hydrocarbons can be used with mineral oils, unlike the chlorine-free fluorocarbon refrigerants that require new lubricants.

Technical Disadvantages

The flammability of the refrigerant.

Technical Barriers

Safe design.

Economic Analysis

There is essentially no difference in efficiency between a heat pump using propane and the baseline electric heat pump using R-22. The economic consequence of this is shown clearly in Table 6 where the system using propane cannot support any increase in first costs in much of the U.S. and in fact must be slightly less expensive in the heavy load regions of the northeast and southwest. This is in stark contrast with estimates of up to 35% higher costs to accommodate design changes necessary for safe use of a flammable refrigerant in unitary equipment (Keller 1997). Applying Keller's estimate to the cost data for the baseline heat pump listed on page 10 gives a likely increase in installed cost of $500 to $640 per ton.

Table 6. Installed Cost Premiums Possible Relative to an Electric heat pump for a Rankine Cycle Heat Pumps Using Propane.

	Installed Cost Premium ($/ton)		
Region	3 Year Payback	5 Year Payback	Equal Life Cycle Cost
Northeast	-$5	-$10	-$25
Southeast	$0	$0	$0
South Central	$0	$0	$0
Southwest	$0	$0	$0
Midwest	-$5	-$10	-$25
Northern Plains	-$5	$0	-$25
Rocky Mountain	$0	$0	$0
Pacific Northwest	$0	$0	$0
California	$0	$0	$0

Contacts and Sources of Information

Keller, F. et al., 1997. "Assessment of Propane as a Refrigerant in Residential Air-Conditioning and Heat Pump Applications," *Proceedings of Refrigerants for the 21st Century*, ASHRAE/NIST Conference, October 6 and 7, pp. 57-65.

Obvious Holes in Knowledge, Understanding, Information

None.

RANKINE CYCLE: TRANSCRITICAL CO_2

Basic Concept Description

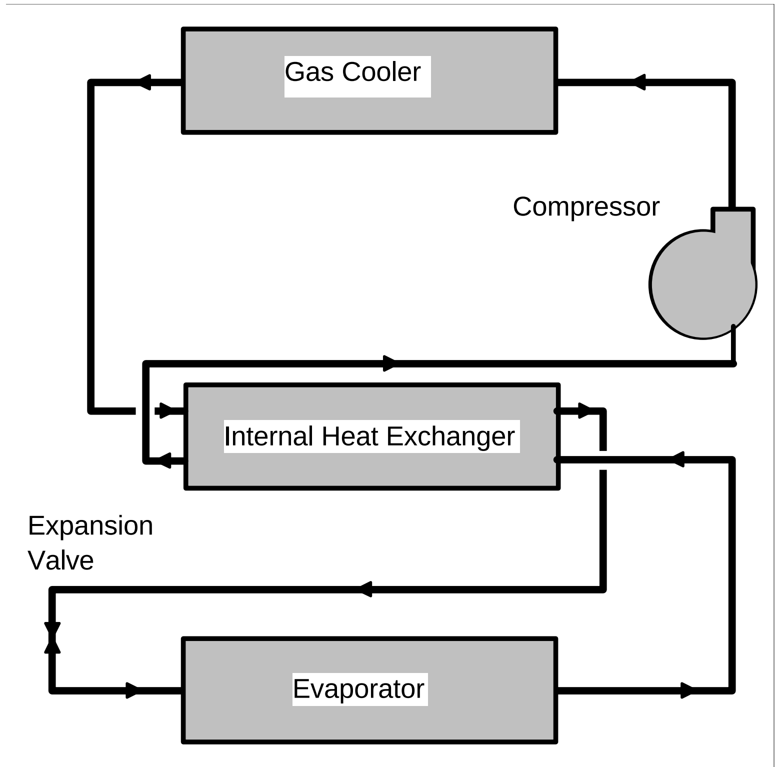

Fig. 9. Schematic diagram for transcritical CO_2 heat pump with internal heat exchange.

compression system to use CO_2 as the refrigerant; this alternative can be attractive because of the benign environmental effects of CO_2 but it requires special considerations because of the low critical point of CO_2. A schematic of the basic equipment is shown in Fig. 9. The pressure-enthalpy diagram in Fig. 10 shows that the high-side operating pressure is above the critical point. A positive displacement compressor is used to compress the refrigerant above its critical point where it rejects heat to the ambient air through a gas cooler. The refrigerant is expanded to a pressure below the critical point and absorbs heat through an evaporator much like a conventional cycle. High-side heat transfer occurs at a fixed pressure but across a wide temperature glide so there is an efficiency advantage in applications using counter-flow heat exchangers. Furthermore, there is a degree of freedom available in selecting the high-side pressure that is not available in conventional compression systems which can be used to maximize COP. It should be noted in Fig. 10 that the internal heat exchanger adds evaporator capacity by transferring heat between points “D” and “E” on the high side to the region between points “A” and “B” on the low side. This heat transfer boosts cooling capacity and air conditioning COP.

Background Information

Carbon dioxide was used in very early refrigeration equipment dating back to the mid-1800s. It dominated shipboard refrigeration systems until the early 1950s (a period when ammonia dominated stationary equipment) because it is non-toxic and non-flammable. There was a decline in the use of CO_2 after 1950 for a couple of reasons. First, the shipboard systems typically used seawater as the heat sink, and there was a rapid loss of capacity at the high cooling water temperatures they crossed in the tropics. Second, development of compressors for CO_2 did not keep pace with the development of high speed, high efficiency compressors for fluorocarbon refrigerants. Shipboard CO_2 systems were rapidly replaced by refrigeration systems using CFC-12 and R-502. The last shipboard CO_2 system was taken out of service in 1972.

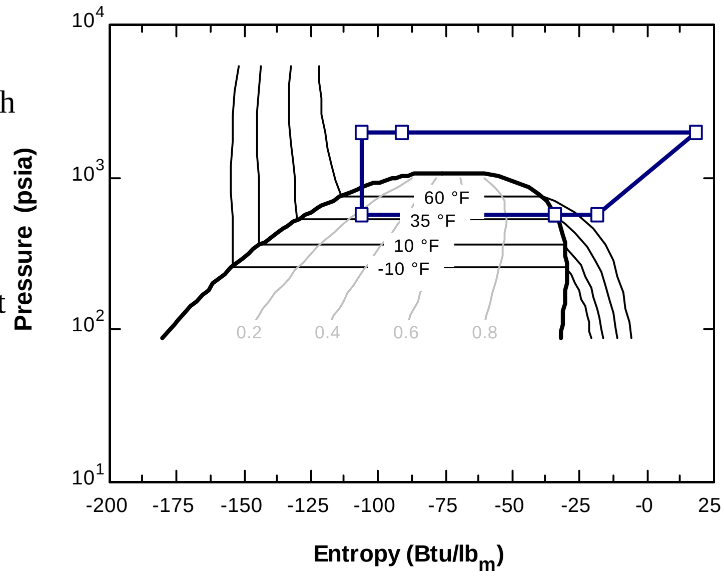

Fig. 10. Pressure-enthalpy diagram for transcritical CO_2 heat pump.

The phase-out of CFCs that began in the late 1980s caused researchers, primarily in Norway, to reassess the potential of using CO_2 as a refrigerant. SINTEF, a quasi-private corporation at the Norwegian Technical University (NTH) in Trondheim, did a significant amount of work on using the transcritical cycle in vehicle air-conditioning systems (primarily automobiles but also buses and trains) with some analysis in heat pumping applications. The early work at SINTEF relied on compressors built in their own machine shop which had low efficiencies and massive compressor shells. Later work at SINTEF, Denso, and elsewhere have produced compressors “comparable” to fluorocarbon compressors in size, weight, and efficiency (Quack 1994, Pettersen 1993, Lorentzen 1994, Nekså 1994, Nekså 1992, Lorentzen 1993).

Transcritical CO_2 compression is currently being examined for application in automobile air conditioning, air conditioners and heat pumps with integrated water heating, and district heating. There is some problem inherent in CO_2 that requires special consideration when applying the system to an application like automobile air conditioning where there is a wide range of compressor shaft speeds. CO_2 experiences changes in density and volumetric capacity that causes the cooling capacity to drop off much more rapidly as the compressor speed drops than is experienced by fluorocarbon or hydrocarbon refrigeration systems. If the system is sized for highway speed operation, there is inadequate capacity under idle conditions; if it is sized for idle conditions there is far too much capacity at highway speeds and loads. Variable capacity compressors are being considered in efforts to address this loss of capacity.

Bullock presented a paper at the 1997 NIST/ASHRAE meeting on theoretical performance of an air-to-air heat pump using CO_2. His analysis probably answers a lot of the questions surrounding this technology, but shows that significantly better heat exchangers and internal heat transfer are necessary to achieve the same efficiencies possible with less sophisticated R-22 heat pumps. Pettersen also published an analysis of a Japanese split-system heat pump.

Secondary System Requirements

No secondary loop requirements.

Efficiency Data

Cycle calculations were performed for a transcritical CO_2 cycle with internal heat exchange. Assumptions are consistent with those used in analysis of transcritical CO_2 cycles by SINTEF (1995). The gas cooler effectiveness was specified at 0.95 which results in approach temperatures below 10EF in heating and 5EF in cooling. Evaporating temperatures were specified as listed in Table 7 to be 5EF above the temperatures for the Rankine cycle heat pump because of the improved thermodynamics of CO_2. The compressor efficiency is 75% (lower pressure ratio), internal heat exchange was computed using a heat exchanger UA of 10 (units to be determined). High-side operating pressures were determined to give the maximum COP. The calculated COPs and seasonal performance factors are listed in Table 8. The cooling COP at 95EF is about 30% below that for the baseline R-22 heat pump and the SEER is about 20% lower. There is about a 6% reduction in heating seasonal efficiency. The system COP at 95EF compares favorably with the value calculated by Bullock (2.26 vs. 2.27) while the COP at 47EF is about 50% higher (3.74 vs. 2.49) (Bullock 1997). The results in Table 8 are based on a higher isentropic efficiency (75% vs. 66%) and more optimistic assumptions about heat exchanger performance; Bullock's calculations employ detailed heat exchanger models but do not achieve the low gas cooler approach temperatures reported elsewhere (SINTEF 1995, Pettersen 1997a).

Table 7. State Point Temperatures for Transcritical CO_2 Cycle Calculations

State Point Conditions	Ambient Temperatures			
	47EF	17EF	82EF	95EF
gas cooler exit temperature	73EF	78EF	85EF	100EF
evaporating temperature	33EF	-10EF	49EF	49EF
high-side pressure (psia)	1160	1250	1240	1540

Note: gas cooler effectiveness 95%, compressor efficiency 75%, internal heat exchanger UA 10.

Technical Advantages/Benefits

There are advantages to the concept because it uses an environmentally benign, non-flammable refrigerant, operates with a low pressure ratio, and has a low volume requirement. The large high-side temperature glide is also advantageous in water heating applications.

Technical Disadvantages

Table 8. Calculated and Observed Efficiencies for Transcritical CO_2 Cycle.

	Heating			Cooling		
Cycle Efficiency	47EF	17EF	Seasonal (Btu/Wh)	82EF	95EF	Seasonal (Btu/Wh)
Cycle COP theoretical observed	4.88	2.70		4.02	2.63	
System COP theoretical observed	3.78	2.32	7.8	3.21	2.26	9.5

notes: blank entries denote absence of calculated or measured information, calculated and observed cycle efficiencies do not apply for the shaded seasonal boxes

The inherent disadvantages of CO_2 compression cycles include the high operating pressure, the fact that conventional oils have low miscibility in transcritical fluids, and the low efficiency of the basic cycle. The inherently low efficiency can be compensated for by reducing expansion losses, reducing gas cooler approach temperature, and increasing compressor efficiency (Bullock 1997). High operating pressures may exacerbate problems with leaks; ASME pressure vessel requirements (multiple of highest pressure) are very high.

Technical Barriers

Heat transfer correlations have not been available and the transcritical cycle has not been treated in textbooks or classrooms. Recent activities are helping to overcome the lack of information and experience. Compressors need to be designed specifically for high efficiency space conditioning applications.

Economic Analysis

The COPs in Table 8 result in calculated operating costs that would require medium to high reductions in installed costs for a transcritical CO_2 heat pump relative to the baseline electric heat pump. These results are summarized in Table 9. The assumptions used to estimate these COPs, however, presume high heat exchanger effectivenesses and component efficiencies that have not yet been demonstrated in hardware.

In actuality, however, the installed costs of the CO_2 heat pump are likely to be similar to those for a conventional heat pump; small differences are possible because of design changes with smaller tubing and stronger welds and fittings and compressor size, but large reductions are unlikely.

Contacts and Sources of Information

Table 9. Installed Cost Premiums Possible Relative to an Electric Heat Pump for a Transcritical CO_2 Heat Pump.

Region	Installed Cost Premium ($/ton)		
	3 Year Payback	5 Year Payback	Equal Life Cycle Cost
Northeast	-$110	-$170	-$500
Southeast	-$75	-$120	-$350
South Central	-$90	-$140	-$400
Southwest	-$130	-$200	-$600
Midwest	-$80	-$130	-$375
Northern Plains	-$65	-$100	-$300
Rocky Mountain	-$65	-$100	-$300
Pacific Northwest	-$25	-$50	-$150
California	-$65	-$100	-$300

Bullock, C. 1997, "Theoretical Performance of Carbon Dioxide in Subcritical and Transcritical Cycles," *Proceedings of Refrigerants for the 21st Century*, ASHRAE/NIST Conference, October 6 and 7, pp. 20-26.

Lorentzen, G. 1993, "Application of 'Natural' Refrigerants: New System Concepts for the Use of CO_2," NTH-SINTEF, *Proceedings of the 1993 Non-Fluorocarbon Insulation, Refrigeration, and Air-Conditioning Technology Workshop*, pp. 251-261, Wiesbaden Germany, September 27-29, 1993.

Lorentzen, G. 1994, "Use of CO_2 in Commercial Refrigeration: An Energy Efficient Solution," NTH-SINTEF. *Proceedings of New Applications of Natural Working Fluids in Refrigeration and Air Conditioning*, pp. 703-708, May 10-13, 1994, Hannover, Germany.

Nekså, P. 1992, "The Transcritical Vapour Compression Cycle: Its Potential in Heat Pump Processes,"NTH-SINTEF, *Proceedings from the International*

Symposium on Refrigeration, Energy, and Environment, pp. 273-289, June 22-24, 1992, Trondheim, Norway.

Nekså, P. 1994, "Transcritical Vapor Compression Heat Pumps," NTH-SINTEF, *Proceedings of New Applications of Natural Working Fluids in Refrigeration and Air Conditioning*, pp. 395-404, May 10-13, 1994, Hannover, Germany.

Pettersen, J. 1993, "A New, Efficient, and Environmentally Benign System for Automobile Air Conditioning,"Jostein Pettersen, SINTEF, SAE 1993 Annual Meeting, Paper #931129

Pettersen, J. 1997, "Experimental Results of Carbon Dioxide in Compression Systems," *Proceedings of Refrigerants for the 21st Century*, ASHRAE/NIST Conference, October 6 and 7, pp. 27-37.

Pettersen, J. 1997a. Personal communication on gas cooler approach temperatures.

Quack, H. 1994, "Carbon Dioxide As A Refrigerant for Railway Refrigeration and Air Conditioning," H Quack and W. Kraus, Technische Universität Dresden *Proceedings of New Applications of Natural Working Fluids in Refrigeration and Air Conditioning*, pp. 489-494, May 10-13, 1994, Hannover, Germany.

SINTEF 1995. <u>CO_2 in Residential Air Conditioning and Heat Pumps: A First Assessment</u>, SINTEF Refrigeration and Air Conditioning, The Norwegian Institute of Technology, N-7034 Trondheim, Norway, March.

Obvious Holes in Knowledge, Understanding, Information

Actual hardware testing and design optimization are necessary to support the assumed component efficiencies and calculated COPs.

BRAYTON (AIR) CYCLE

Basic Concept Description

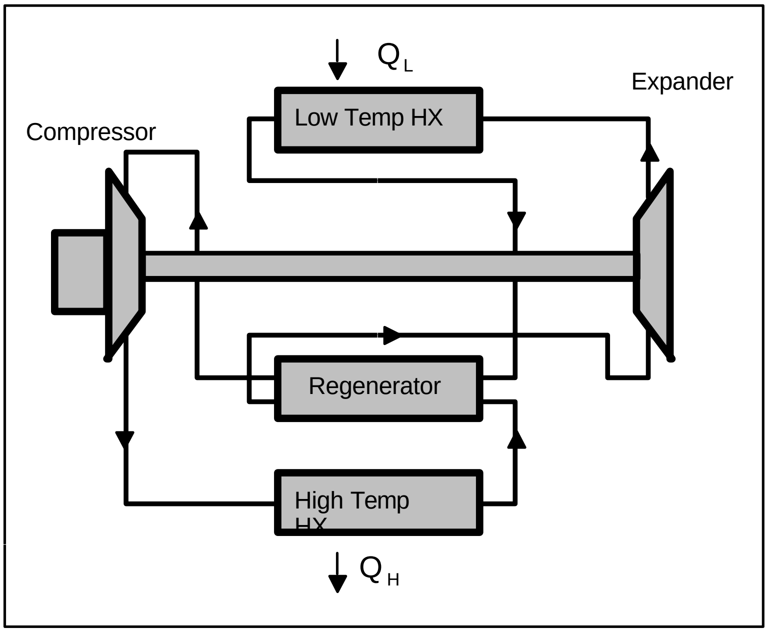

Fig. 11. Schematic diagram of a Brayton cycle heat pump.

cycle consists of a compressor, a heat exchanger to reject heat, a turbine or expansion machine, and a second heat exchanger withdrawing heat from the conditioned space, as illustrated in Fig. 11. The fundamental principle is that when air is compressed, it is heated and that heat can be used for space conditioning; when the compressed air is expanded, it is cooled significantly and the cold air can be used for space conditioning. Expansion losses are recovered through a turbine sharing a common shaft with the compressor to reduce input power and boost COP. The Brayton cycle is one of a group of thermodynamic processes referred to as "gas cycles" because the refrigerant or operating fluid is always in a gaseous state. This is illustrated in Fig. 12 showing the cycle superimposed on a temperature-entropy diagram above and to the right of the refrigerant vapor dome. The heat flows, Q_H and Q_L, and constant pressure lines of a cycle with a regenerator are shown in Fig. 13.

Unlike vapor compression equipment, the pressures on both sides are not dependent on the source and sink temperatures, but are determined by the desired temperature difference between high and low pressure sides as well as the pressure ratio. Thus, one of the pressures can be chosen independent of the temperatures.

Selecting one of the pressures to be ambient pressure allows the use of open cycles, eliminating one of the heat exchangers. If the high pressure side heat exchanger is eliminated, a low pressure cycle is built, expanding outside air, rejecting heat from the conditioned space, and compressing the air to ambient pressure before it is discharged. High pressure systems use air from the conditioned space, which is compressed, the heat is rejected to the ambient before the air is expanded back into the conditioned space. Internal heat exchangers or regenerators can be used to enhance open or closed cycles, high or low pressure cycles.

Background Information

Brayton cycle equipment has been used for air conditioning on commercial and military aircraft for many years. It has been investigated for applications in commercial water heating, automobile air conditioning, air conditioning on passenger trains, and transport refrigeration. Rovac Inc. tried to develop air-cycle equipment for automobile air conditioning, but finally gave up; it isn’t clear whether they failed for technical reasons or failure to demonstrate any advantage over the established compression technology.

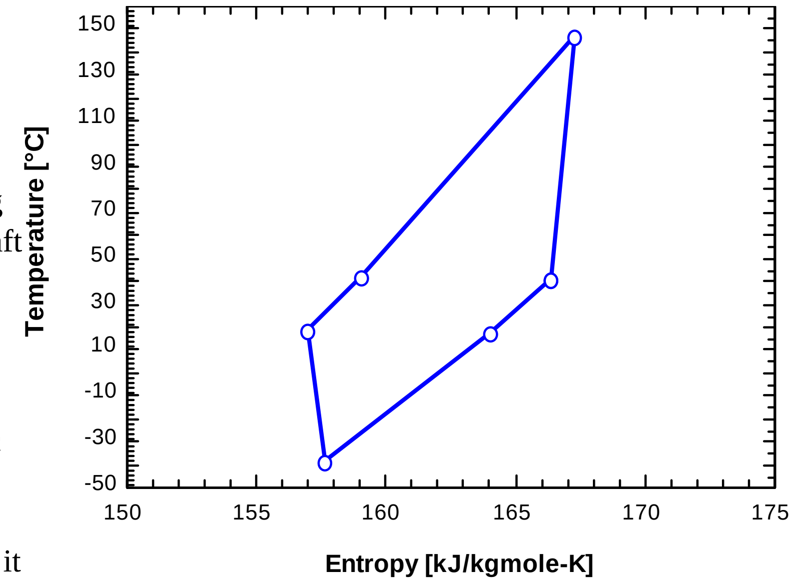

Fig. 12. T-S diagram for Brayton cycle showing refrigerant outside vapor dome.

DOE/ORNL funded Foster Miller to design and build a prototype residential air-cycle heat pump water heater and to do a marketing study. The payback period was favorable based on the project design goal COP of 1.7, but unit testing produced a COP of only 1.26. Significant valve losses were experienced in the expander.

Murphy (1994) looked at 18 potential applications of air-cycle equipment and identified both recommended applications and promising applications. The three recommended applications are freeze drying of foods, refrigerated containers for transport refrigeration, and fabric drying. Promising applications included heating only heat pumps, automobile air conditioning, and applications requiring concurrent heating and cooling. Murphy’s evaluation included comparisons of first cost and maintenance; this

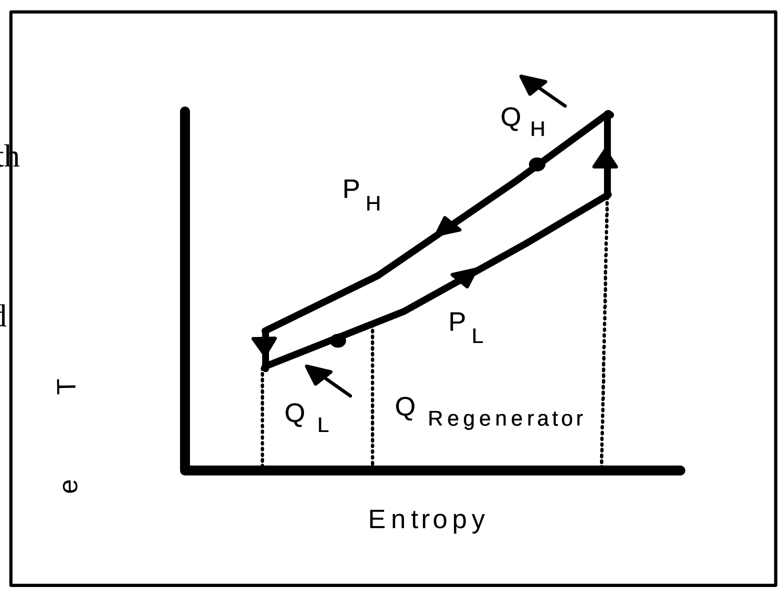

Fig. 13. T-S diagram for Brayton cycle with regenerative heat transfer.

assessment may be suspect because the paper stated specifically that automobile air conditioners require servicing every 50 to 100 hours of operation. That is approximately a third of the annual operating hours for auto a/c in the U.S. (Murphy 1994, Hannover 1994a, Sicars, Hannover 1994b, FMA 1979, Hannover 1994c)

General Electric was under contract to DOE with a task to evaluate gas cycle refrigeration for domestic applications (refrigerator/freezers). Their analysis concluded “[t]he efficiency of Brayton open air cycle is higher than that of the closed cycle. With compressor and expander efficiencies lower than 0.9, the system COP will generally be lower than the targeted COP of 1.5. Because of the unrealistically high efficiency requirements of Brayton cycle components in order to achieve parity with today’s Rankine COP’s, Brayton coolers are not practical for household refrigeration.” This conclusion should be examined to see if it is relevant to space conditioning applications.

Secondary System Requirements

No secondary systems are required.

Efficiency Data

Cycle calculations were performed for a simple closed Brayton cycle with a recuperator using dry air as the working fluid. The state points were defined by the data in Table 10. Calculations were performed using assumptions for component efficiencies based on the best currently available and the best efficiencies possible. The current technology steady-state COPs listed in Table 11 are computed using; compressor efficiency 0.88, expander efficiency 0.92, regenerator effectiveness 0.85, heat exchanger)T’s 9E and 17EC for the low and high temperature hx’ers (.0.85 effectiveness), pressure ratio 2.5. The best possible technology COPs are computed using; compressor efficiency 0.88, expander efficiency 0.92, regenerator effectiveness 0.95, heat exchanger)T’s 3E and 5EC for the low and high temperature hx’ers (.0.95 effectiveness), pressure ratio 2.5.

Table 10. State Point Temperatures for Brayton Cycle Calculations.

State Point Temperatures	Ambient Temperatures			
	47EF	17EF	82EF	95EF
hot heat exchanger	100	85	105	120
cold heat exchanger	29	10	49	49

Technical Advantages/Benefits

The principal advantages of this cycle are its compact size and weight requirements, the fact that it uses a totally benign refrigerant, and it has a temperature glide in the heat exchanger.

Technical Disadvantages

The disadvantages of the air cycle are the low efficiency (open cycle is more efficient than the closed cycle), the high volume flow rates necessary which require very high speeds (i.e. turbo compressors), the poor heat transfer, and the fact that the COP is strongly affected by pressure drop in the heat exchanger.

Table 11. Calculated and Observed Efficiencies for Closed Regenerative Brayton Cycle.

	Heating			Cooling		
Cycle Efficiency	47EF	17EF	Seasonal (Btu/Wh)	82EF	95EF	Seasonal (Btu/Wh)
Cycle COP						
theoretical						
current technology	1.98	1.95		1.05	0.99	
best possible	2.11	2.02		1.20	1.13	
System COP						
theoretical						
current technology	1.77	1.75	5.0	0.99	0.93	2.9
best possible	1.87	1.80	5.2	1.12	1.06	3.3
measured						

notes: blank entries denote absence of calculated or measured information, calculated and observed cycle efficiencies do not apply for the shaded seasonal boxes

Technical Barriers

Some of the technical problems facing successful commercial development of air cycle equipment applications other than aircraft air conditioning are:

- the expander efficiency (58% in Foster Miller project vs. required 85%),
- condensation in an open cycle, reducing COP and possibly obstructing air flow,
- possible turbine damage from water droplets, and
- lubrication of open cycle machines must avoid oil contamination of supply air and limit oil lost to environment

Economic Analysis

The Brayton cycle was modeled using two sets of assumptions for component efficiencies; (1) those for equipment that is commercially available in 1998 and (2) estimates for highest possible component efficiencies. The economic analysis is reported only for the second case; it doesn't get any better than that. Equipment costs would need to be $3,000 to $7,000 per ton less than for a conventional electric heat pump for the two systems to have comparable life cycle costs.

Contacts and Sources of Information

H. Kruse, University of Hannover, Germany

U. Hesse, Robert Bosch GmbH, Stuttgart, Germany

McGovern, J. et al., 1994, *"Environmentally Benign Air Cycle Heat Pumps and Refrigeration Systems, Part 1: Potential Applications for Air Cycles*," *Proceedings of New Applications of Natural Working Fluids in Refrigeration and Air Conditioning,* Hannover, Germany, May 10-13 pp. 169-177.

Henatsch A., et al., 1994, "Cooling, Heating, and Electrical Power Cogeneration With Air as a Working Fluid," A. Henatsch, et al., Hochschule für Technik und Wirtschaft, Dresden, Germany *Proceedings of New Applications of Natural Working Fluids in Refrigeration and Air Conditioning*, Hannover, Germany, May 10-13 1994, pp. 519-530.

Sicars, S., 1994, *"Air Cycle Systems for Transport Refrigeration"*, *Proceedings of New Applications of Natural Working Fluids in Refrigeration and Air Conditioning*, Hannover, Germany, May 10-13, pp. 507-518.

FMA 1979, *"Research and Development of an Air-Cycle Heat-Pump Water Heater,"* ORNL/Sub-7226/1 Foster-Miller Associates

Murphy, S. 1994, et al, "Environmentally Benign Air Cycle Heat Pumps and Refrigeration Systems," University of Dublin, and Netherlands Organization of Applied Technical Research, TNO

Obvious Holes in Knowledge, Understanding, Information

It is important to get corroborating information on the COPs for this cycle.

ELECTRICALLY-DRIVEN STIRLING CYCLE

Basic Concept Description

constant volume processes with two constant temperature processes as illustrated in the pressure-volume (P-V) and T-S diagrams in Figs. 14 and 15. Basic operation is illustrated in Fig. 16. A system of pistons and displacers is used to move the working fluid, commonly hydrogen or helium, between volume spaces with a regenerator storing heat between steps of the cycle. Like the Brayton cycle, the Stirling cycle is a gas cycle and the working fluid does not change phase in the heat exchangers. System capacity, hence, is the product of the mass flow rate, specific heat, and)T in the heat exchanger. Large flow rates are needed to produce large capacities.

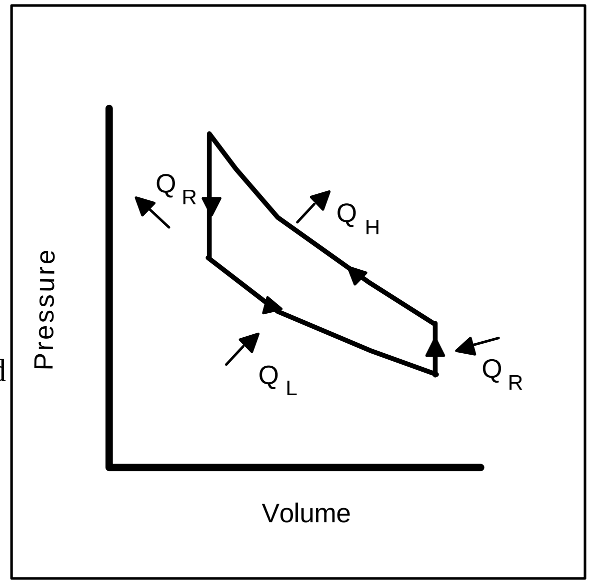

Fig. 14. P-V diagram for Stirling cycle.

Background Information

The Stirling cycle was first developed as a power cycle in the 1800s and in the past 100 years numerous attempts have been made to build refrigeration or power systems based on it. Developments include Stirling engines for automobiles and military generator sets and Stirling coolers for domestic, commercial, and transport refrigeration, heat pumps, and cryocoolers. Stirling cycle cryocoolers have been commercially successful in land-based and space-based systems.

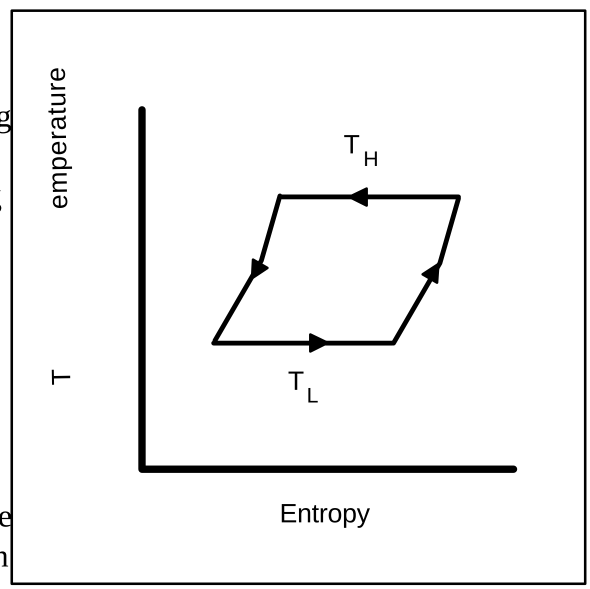

Fig. 15. T-S diagram for Stirling cycle.

Secondary System Requirements

Heat pipes or secondary heat transfer loops will be necessary to provide useful heating or cooling with a Stirling device. The working volume of gas in the Stirling cooler is a fundamental design property of the machine and the internal volume cannot be adjusted to circulate the gas through either an indoor or outdoor heat exchanger.

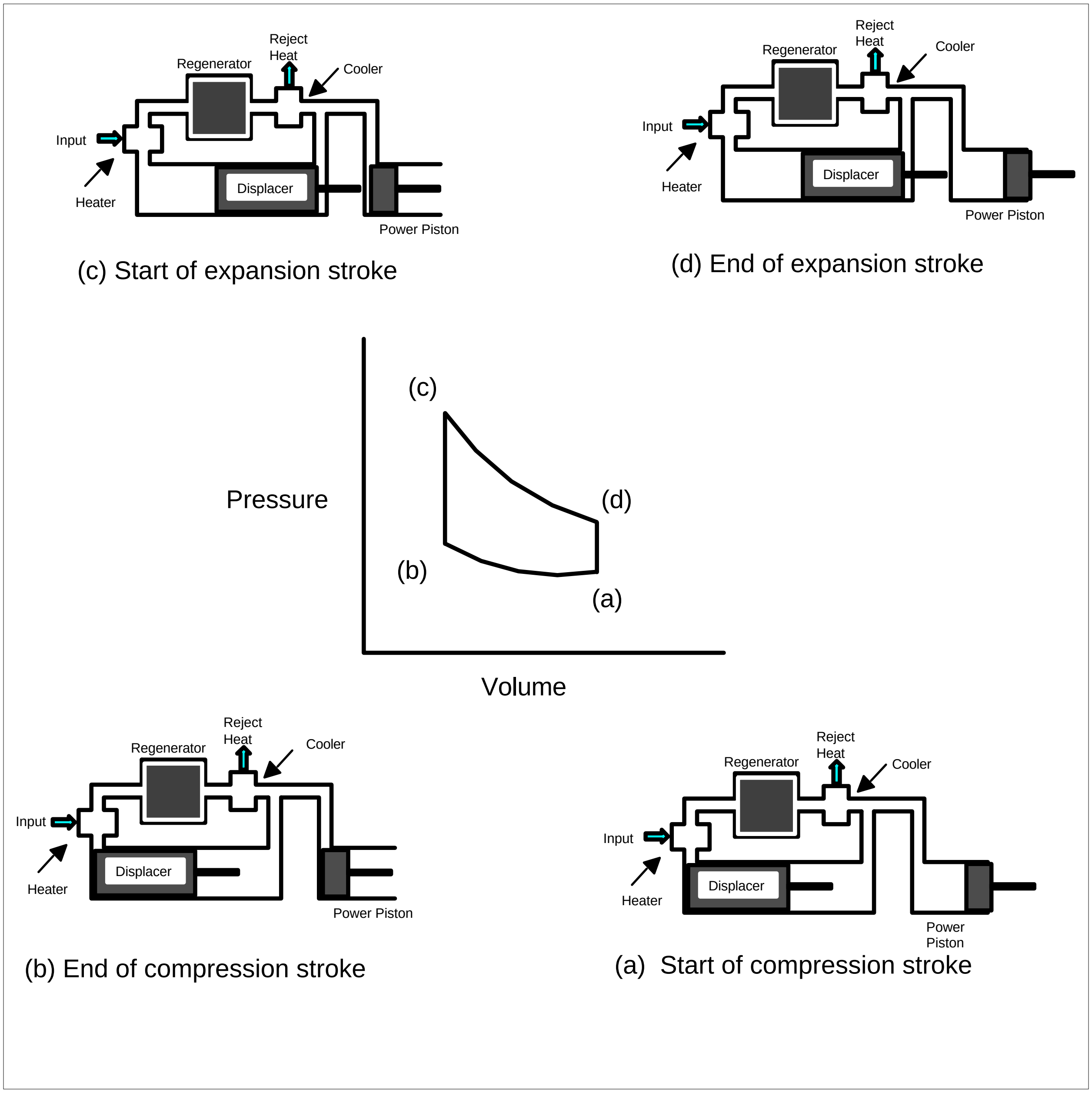

Fig. 16. Schematics of Stirling cycle refrigeration system showing movement of power piston and displacer.

Efficiency Data

The Stirling cycle was modeled using helium as the working fluid with a pressure ratio of 1.5 (low-side pressure of 1 atmosphere). The principal assumptions included component efficiencies, and gas pressure drops:

- ! compression efficiency (90%), regenerator efficiency (85%), motor efficiency (97.5%), and transmission efficiency (85%), and
- ! no pressure drops in the heat exchangers.

The heat exchanger temperatures are listed in Table 10 on page 25. The calculated COPs are listed in Table 12. These efficiencies are extremely low and probably are not an accurate representation of this cycle. Additional data were located (ADL 1993) and included in Table 12. System, as opposed to cycle, efficiencies were computed that correspond to the ADL data by adding fan and blower power comparable to the power requirements for the reverse Rankine cycle heat pump and 100 W/ton pumping power for a secondary loop.

Table 12. Calculated and Observed Efficiencies for a Stirling Cycle Heat Pumps.

	Heating			Cooling		
Cycle Efficiency	47EF	17EF	Seasonal (Btu/Wh)	82EF	95EF	Seasonal (Btu/Wh)
Cycle COP theoretical ADL (1993) observed	 1.91 2.6	 1.69 2.5		 0.99 	 0.92 2.5	
System COP theoretical ADL observed	 1.67 2.10	 1.50 2.04	 4.7 5.8	 0.93 2.04	 0.86 2.04	 2.7 6.0

notes: blank entries denote absence of calculated or measured information, calculated and observed cycle efficiencies do not apply for the shaded seasonal boxes

Technical Advantages/Benefits

Very few moving parts, theoretically long product lifetime. Environmentally benign refrigerant. Theoretically high efficiency.

Technical Disadvantages

Relatively low COP in low lift applications.

Technical Barriers

ADL (1993, p. 2-12) identified several research needs for Stirling cycle refrigeration in general:

- ! accurate cycle modeling capability,

- improved regenerator performance to achieve higher effectiveness, lower pressure drop, lower void volume, lower cost, and less susceptibility to contaminant plugging.
- reduction in log mean temperature difference for the hot and cold heat exchangers where high density heat transfer is required, and
- improvement of secondary heat transfer loops.

Economic Analysis

The economic analysis for the Stirling cycle heat pump was performed using the efficiencies given by ADL (1993, p. A-47) and listed in Table 12. The maintenance costs assumed to be the same as those for the electric baseline ($100 per year). Stirling cycle heat pumps are most favorable in the South Central states where their installed cost would need to be nearly $2000 per ton below the comparable costs for the baseline electric heat pump.

Contacts and Sources of Information

ADL 1993. Energy Efficient Alternatives to Chlorofluorocarbons (CFCs): A Research Needs Assessment Final Report, U.S. Department of Energy, Office of Energy Research, DOE/ER/30115-H1, June.

Berchowitz, D. And Bessler, W. 1993. “Progress on Free-Piston Stirling Coolers,” Sixth International Stirling Engine Conference and Exhibition, The Netherlands, May 26-28.

D.M.Berchowitz
Sunpower
Athens, OH 45701

Wurm, J., et al. 1990. *Stirling and Vuilleumier Heat Pumps: Design and Application*, McGraw-Hill, New York, NY.

Obvious Holes in Knowledge, Understanding, Information

It is important to get corroborating information on the COPs for this cycle.

VORTEX TUBE COOLING

Basic Concept Description

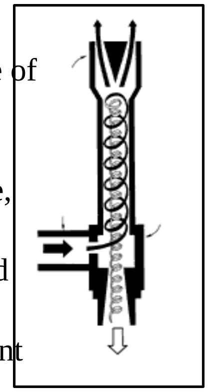

Fig. 17. Vortex tube.

Thompson effect and the Hilsch effect. Joule-Thompson is the cooling of a gas through adiabatic expansion across a restriction, the Hilsch effect refers to the use of a forced vortex in the gas stream causing the separation of gas and liquid and a temperature gradient across the vortex. As shown in Fig. 17, compressed gas in a vortex tube is fed through a tangential inlet nozzle. This gas spirals down the tube, producing two distinct flows, one hot and one cold. The temperature difference is due to the radial pressure gradient in any vortex and the viscosity of the air (Wood 1969). Due to the temperature gradient the expansion process in a vortex tube moves away from the adiabatic Joule-Thompson expansion toward a more efficient isentropic expansion.

Background Information

The vortex tube phenomenon was discovered in 1930 by French physicist Georges Ranque. In 1961 ITW Vortec was the first company to develop the process into practical and effective cooling equipment for industrial applications. Spot cooling equipment is commercially available that can provide refrigeration up to 6000 Btu/h or temperatures down to -40EF (FILTRAN, Newman, Cockerill). Vortex tube cooling is currently applied toward gas dehydration; removal of water vapor and droplets from natural gas streams, gas dewpointing, and process and spot cooling for industrial processes with cold air guns.

Secondary System Requirements

Supply of compressed air.

Efficiency Data

Commercial products for spot cooling appear to be rated on capacity and inlet-to-outlet air)T without any reported efficiency or input power. Cockerill reports a COP of 0.08 for a vortex tube household refrigerator. COPs were also calculated using product specification data from ITW Vortec and Air Compressor Products, Inc. using a motor efficiency of 85%. These calculations also showed a COP of 0.08 for the ITW products independent of capacity and inlet to outlet)T.

Technical Advantages/Benefits

The major advantage of vortex tubes are the innate simplicity of the systems (no moving parts), and their compact size and light weight.

Table 13. Calculated and Observed Efficiencies for a Vortex Tube Cooler.

	Heating			Cooling		
Cycle Efficiency	47EF	17EF	Seasonal (Btu/Wh)	82EF	95EF	Seasonal (Btu/Wh)
Cycle COP						
theoretical						
observed						
System COP						
theoretical				0.08	0.08	0.3
observed	0.08	0.08	0.3	0.08	0.08	

notes: blank entries denote absence of calculated or measured information, calculated and observed cycle efficiencies do not apply for the shaded seasonal boxes

Technical Disadvantages

The disadvantages are very low efficiency: 0.08 in cooling and domestic refrigeration (Cockerill) and low capacity: *maximum* 6,000 Btu/h (Cockerill and Newman Tools). The technology scales very poorly with performance dropping off substantially as the diameter of the vortex tube increases.

Technical Barriers

Limited capacity; Cockerill summarizes his conclusions that " 'normalized' performance vortex tubes declines as their radius increases. Thus while increasing the size of a tube increases the maximum throughput of air, it also tends to reduce the maximum temperature difference achievable and hence there seems to be an overall physical limit on the thermal power that can be obtained from tubes of 'conventional' design." He goes further to discuss the possibility of cascading vortex tubes to achieve greater overall)T's (he's funded to look at technologies for air liquefaction), but does not mention multiple tubes in parallel to increase capacity.

Economic Analysis

Vortex tubes are not considered a viable alternative to electric air-source heat pumps because of their low efficiency and limited capacity. The economic analysis was not performed for this technology.

Contacts and Sources of Information

Wood, B. 1969. *Applications of Thermodynamics*, Addison-Wesley Publishing Company.

Cockerill, T., es0tco@environment.sunderland.ac.uk

FILTAN Web Sites: http://www.internetdienste.de/filtan/vortex.html

Newman Tools Web Site: http://www.newmantools.com/vortex.htm#vortex

Newman Tools, Inc.
151 New Park Avenue
Hartford, CT 06106
1-800-465-1384
tom@newmantools.com

Keith Thomas
Falk & Thomas Engineering GmbH
Rodheimer Strasse 4a
D-35435 Wettenberg 1
Germany
49 641 980 187
fteng@t-online.de

FILTAN Filteranlagenbau GmbH
Gänsgasse 9
D-63505 Langenselbold
Germany
49 6184 7081
ml.filtan@internetdienste.de

Obvious Holes in Knowledge, Understanding, Information

None.

THERMOELECTRIC COOLING

Basic Concept Description

Thermoelectric refrigeration is based on the observation first made by Peltier in 1834 that a direct electric current passing through a circuit formed by two dissimilar conductors or semiconductors will cause a temperature difference to develop at the junctions of the two conductors. A refrigeration effect develops at the cold junction, and heat is rejected at the hot junction.

Background Information

There are several thermoelectric phenomena associated with joining two dissimilar materials. Perhaps the most familiar is the Seebeck effect; if a temperature difference is maintained between the two junctions, an open circuit electrical potential difference ΔV develops which is proportional to the temperature difference ΔT between the junctions, or:

$$\Delta V = \alpha \times \Delta T \tag{1}$$

The relationship in (1) is the basis for the widely used measurement of temperature using thermocouples. The constant of proportionality, α, is termed the Seebeck coefficient after the scientist who first described this process in 1822. The absolute Seebeck coefficient for a material is determined by using this material as one leg of a junction and lead as the reference leg. The α for the reference leg is taken to be zero. Therefore, for any material A the absolute Seebeck coefficient, α_A, is a property of that material and can be positive or negative.

If a direct electrical current is made to flow through a junction of two dissimilar materials, A and B, then the heat energy which is produced or absorbed at the junction is proportional to the current and to the absolute Seebeck coefficients by the relation:

$$Q = (\alpha_A - \alpha_B) \times i \times T \tag{2}$$

where T is the absolute temperature of the junction and I is the direct electrical current. This relation was developed by Peltier. Whether this heat is absorbed or produced depends on the direction of current flow.

The magnitude of heat flow at a junction depends on the values of the absolute Seebeck coefficient for the individual materials. In the case of metals, this coefficient does not exceed 50µV per °C (ASHRAE 1981). However, in semiconductors, α can be much higher. Some materials with the highest α (≈250μV per °C) are alloys of tellurium (Te) doped with antimony tri-iodide (SbI_3) to produce an "n-type" semiconductor and with excess Te to make a "p-type" material (Houst 1982).

The relation between the cooling delivered by a thermoelectric couple and its material properties and configuration can be used to determine the efficiency of thermoelectric cooling. A simple thermoelectric cooling device consisting two semiconductors and electrical connectors, which also serve as heat exchangers, is shown in Fig. 18. A direct electric current passes through the n-type semiconductor on the left, through the finned copper or aluminum conducting strap at the top, and then through the p-type material on the right. At the cold junction at the top, heat Q_C is removed from the ambient (the cooling effect), and at the hot junction, heat Q_H is rejected.

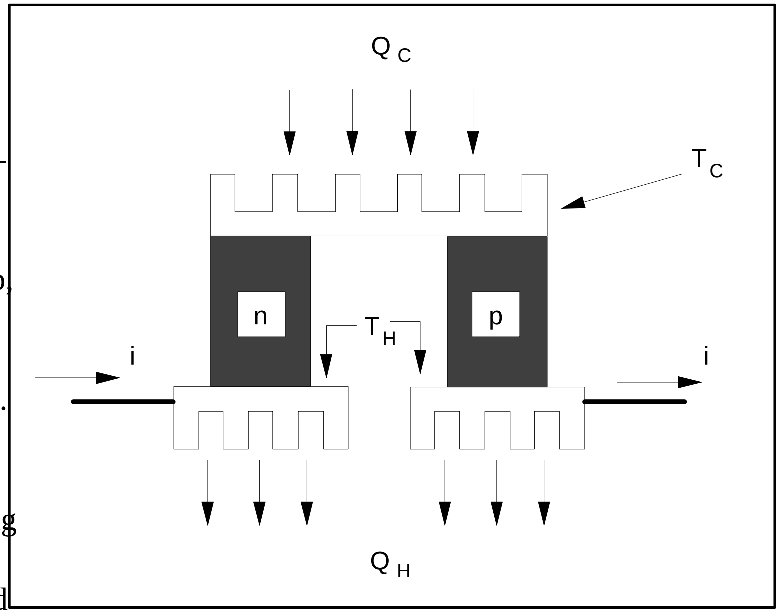

Fig. 18. Schematic for a simple thermoelectric couple.

Theoretically the maximum efficiency is given by Eq. 3 where the variable "Z" is defined according to (4), and T_H and T_C are the absolute temperatures at the hot and cold junctions. The relations in (4) show that the maximum COP of a thermoelectric refrigerator depends simply on the Seebeck coefficients α, thermal conductivity K, and semiconductor resistivity ρ of each leg, and on the operating temperatures. The expression Z is called the figure of merit for the couple. Selecting materials with high difference in α's, low K, and low ρ raises the figure of merit and improves the maximum COP. At an average temperature T=25°C (77°F) for space cooling applications, typical off the shelf thermoelectric modules produce a value of Z=0.0026 (Mei 1992).

$$COP_{max} = \frac{T_C}{T_H - T_C} \times \frac{\left[1 + Z \times \frac{T_H + T_C}{2}\right]^{1/2} - \frac{T_H}{T_C}}{\left[1 + Z \times \frac{T_H + T_C}{2}\right]^{1/2} + 1} \qquad (3)$$

$$Z = \frac{\left[\alpha_p - \alpha_n\right]^2}{\left[\sqrt{K_n \rho_n} + \sqrt{K_p \rho_p}\right]^2} \qquad (4)$$

Thermoelectric modules are now being mass produced with Z=0.003/K (Mei 1998).

"The materials used in today's [thermoelectric] modules have a ZT [T is the mean operating temperature, the average of T_H and T_C] of about 1.0, which is not enough. A ZT value of 3 and above is required to produce energy efficient cooling units (Mathiprikasam 1993)." At an absolute temperature of 300 K (27°C or 80°F), ZT = 1 would correspond to a figure of merit Z = 0.0033; Z = 0.0035 is the highest figure of merit attained under laboratory conditions (Mei 1994).

Researchers have developed theories on the thermoelectric processes and projected limits on what values for the figure of merit may be possible with ideal materials. In developing his ideas Mahan found "the maximum value of ZT to be about one to two. This value is close to experimental reality, where it is hard to find values of ZT greater than one (1989)." Such an analysis adds emphasis to the difficulty in making the material breakthrough necessary to achieve the ZT = 3 that is cited by Mathiprikasam as necessary to produce energy efficient cooling systems.

The literature on thermoelectric cooling can be confusing because three different terms are frequently used to measure or report the efficiency of semiconductor pairs; (1) the relative Seebeck coefficient α, (2) the figure of merit Z, and (3) the relative figure of merit ZT. Discussions or comparisons can become confused because of the similarity in the absolute "values" of these quantities while they differ substantially in orders of magnitude (e.g. α = 250 to 300x10^{-6} V/K in Labinov's paper, Z = 0.00274 /K in Gauger's dissertation, ZT=0.25 in Mahan's graphs). The following definitions might help:

α relative Seebeck coefficient (µV/K); the difference between the Seebeck coefficients for the two materials in the thermoelectric cell:

$$\alpha = \alpha_p - \alpha_n \qquad (5)$$

Z figure of merit (/K), the best commercially available thermoelectric couples have Z=0.00274 /K with laboratory couples a little higher at Z=0.0030 /K

$$Z = \frac{\alpha^2}{\left(\sqrt{\rho_n k_n} + \sqrt{\rho_p k_p}\right)^2} \qquad (6)$$

ZT dimensionless figure of merit (no units), T is the average of the hot and cold heat exchanger temperatures (K); ZT generally ranges between 0.4 and 1.3 for current thermoelectric materials (Mahan 1997)

The maximum refrigeration COP for a thermoelectric pair is given by:

$$\Phi = \frac{\sqrt{1 + Z \cdot T_m} - \frac{T_h}{T_c}}{\sqrt{1 + Z \cdot T_m} + 1} \times \frac{T_c}{T_h - T_c} \qquad (7)$$

Increasing α and the dimensionless figure of merit, ZT, increases COP. Traditionally, research has focused on increasing α and Z through the selection of increasingly exotic materials for the thermoelectric couple. Aspden and Strachan and Thermodyne, Inc. have worked independently to use A/C electric fields to increase the Seebeck coefficient α. Their work has not been accepted by the scientific community.

Aspden and Strachan constructed a device as part of a project on power generation. Their unit essentially consisted of 500 planar capacitors with a film of polyvinylidene fluoride (PVFD) as the dielectric with nickel substrates on both sides covered with aluminum foil (Labinov 1998). The nickel and aluminum were joined in such a manner as to form a classic nickel-aluminum thermocouple; these were connected to form 20 parallel blocks, each with 25 thermocouples in series. An external, alternating current circuit was added, and tuned in some manner that achieved a significant increase in the thermoelectric effect between the nickel and aluminum couples.

Aspden and Strachan claimed to have observed a relative Seebeck coefficient for their device of α = 250 - 300 µV/K, which is said to be the maximum theoretically possible for this pair and 15 times greater than previously reported for nickel-aluminum (Labinov 1998). There is no fundamental explanation of why the A/C field boosts α to the vicinity of its theoretical maximum. Their test lasted only 73 seconds before the device failed; efforts to repeat the test have failed. Labinov concluded that natural convection was inadequate to provide the cooling required by this device and that it overheated after 73 seconds causing its own failure. Aspden and Strachan’s work is held in low regard by some of the best people in solid state electronics and their reported results are not accepted.

Thermodyne, Inc. is pursuing a device similar to that constructed by Aspden and Strachan, although they are using a ceramic layer instead of polyvinylidene fluoride. Thermodyne’s initial interest is also for power generation instead of cooling. They are seeking funds ($30,000 to $50,000) from an electronics manufacturer to produce a single “chip” using a 60 to 70°C ΔT to drive a fractional wattage motor. Thermodyne is unwilling to discuss details of their work at this time, although they would be interested in getting assistance from national laboratories on material related problems. Their patented process uses lead scandium tantalate ceramics (Jaeger 1997). The primary interest at this time is the extremely high power densities claimed in the Thermodyne patent (hundreds of W/cm^2, Jaeger 1997).

Secondary System Requirements

No secondary systems are required.

Efficiency Data

Steady-state cycle efficiencies are computed using the heat exchanger temperatures listed in Table 10 on page 23. The figure of merit is assumed to be 0.00274 /K which is representative of the best commercially available thermoelectric couples in 1998. Seasonal COPs are computed using a cycling Cd of 0.0. COPs for the thermoelectric cells and system COPs are shown in Table 14.

Table 14. Calculated and Observed Efficiencies for Thermoelectric Cooling.

	Heating			Cooling		
Cycle Efficiency	47EF	17EF	Seasonal (Btu/Wh)	82EF	95EF	Seasonal (Btu/Wh)
Cycle COP						
best possible (1998)	1.58	1.20		0.92	0.65	
maximum possible ZT	2.69	1.94		3.38	2.82	
System COP						
best possible (1998)	1.40	1.09	3.9	0.86	0.62	2.5
maximum possible ZT	2.30	1.73	5.8	2.79	2.40	8.3

notes: blank entries denote absence of calculated or measured information, calculated and observed cycle efficiencies do not apply for the shaded seasonal boxes

Technical Disadvantages

Inherently low efficiency. A relative figure of merit ZT of approximately 3 is needed to achieve efficiencies comparable to vapor compression equipment.

Technical Barriers

Low figure of merit requires significant breakthroughs in materials. Also, the limited supply of thermoelectric materials would limit production to a maximum of 100,000 to 200,000 units per year.

Economic Analysis

The inherently low efficiencies of thermoelectric cells results in very unfavorable economic comparisons. COPs derived from the maximum figure of merit currently achievable (Z=0.00274) results in operating costs that would require reductions in installed costs in excess of $4000 per ton; the installed cost of either the electric or gas furnace baseline systems are less than $2000 per ton. A comparison of the performance using the theoretical maximum efficiency, however, (ZT=3) results in operating costs that would require reductions in installed costs of only $300 to $600 per ton (20% to 25%) to have the same life cycle cost as the electric baseline heat pump. These results are discussed more thoroughly on page 43 for thermionic heat pumps.

Contacts and Sources of Information

ASHRAE 1981. ASHRAE Handbook: Fundamentals

Gerald Mahan
Oak Ridge National Laboratory
Solid State Division
P.O. Box 2008
Building 3025, MS 6032
Oak Ridge, TN 37831
(423) 576-8675

Obvious Holes in Knowledge, Understanding, Information

None at this time.

THERMIONIC COOLING

Basic Concept Description

There is a fine distinction between thermionic and thermoelectric cooling. Thermoelectric uses a flow of electrons through a pair of semiconductors in intimate physical contact. Thermionic cooling uses the flow of electrons between two separated electrodes. Consider the old vacuum tube diodes, a negatively charged surface emits electrons that traverse an evacuated space to a positively charged surface. Thermionic cooling is the solid state equivalent with extremely small gaps separating the electrodes (on the order of microns). Theoretically, under an applied electrical potential, the electrons emitted by the electrode are at a higher energy level than those that are left behind which reduces the average energy level (temperature) of the emitting electrode. The electrons being absorbed on the other side of the gap are at a higher energy level than those in the electrode, the average energy level is increased, and the electrode is heated.

Background Information

Knowledge of thermionic converters goes back to Edison's study in 1885 that established experimentally that if two plane electrodes were placed in a vacuum an electrical current developed between them if one was heated to a temperature higher than the other. Most of the subsequent developments related to the direct conversion of heat energy into electricity. A number of experimental studies in 1957 established quite reliably that the efficiency of heat energy conversion to electricity is 5 to 10% with specific power of 3 to 10 W/cm^2. According to theory, a thermionic converter should operate in direct mode as a power generator and also in reverse mode as a heat pump. Little work was done until recently in applying thermionic converters as cooling devices.

Applying thermionic converters to cooling devices is limited, first of all, by the presence of materials capable of active electron emission in the temperature range of 250 to 300 K (-10E to 80EF). The first tangible results of a 30 year long search for suitable materials brought results in the 1990's. Edelson and Cox received patents in 1995 and 1997 for two possible ways of providing cooling with thermionic converters and Mahan published a paper in 1997 on a third method. Edelson proposed using an evacuated space between two electrodes allowing free electron movement (ballistic electron motion). Mahan proposes a thin semiconductor between the electrodes employing the tunnel effect for electron movement. Cox proposed an ionized gas evaporating at one electrode and condensing on the other.

While each of these approaches has its own specific features, they all use one common idea. Each of proposed devices uses materials with high electrical conductivity because of free electrons. At a given temperature, the electrons move at various speeds and in various directions, and have various energy distributions that can be found using Fermi-Dirac statistics (Moelwyn-Hughes 1961). The portion of the electrons at energy levels sufficient to overcome the potential barrier, escape the boundary of the metal surface; this is called thermionic emission.

If two parallel flat electrodes are placed in a vacuum, then the electrons have energy sufficient to overcome the potential barrier and be released from the surface of one electrode will move in a direction normal to the electrode surface until they reach the opposing electrode where they are absorbed. This free motion of electrons is called “ballistic” to differentiate it from “diffusion motion” which experiences the resistance of the medium where electron motion takes place. A similar effect is observed when the electrons move in a medium that has structural effects allowing a “tunneling effect” permitting free movement through the medium.

Secondary System Requirements

There are problems associated with heat transfer to and from the very small electrode surfaces which may require, or work best, using a secondary system like a heat pipe.

Efficiency Data

Mahan is working on a demonstration of solid-state thermionic converters; his primary interest is in using heat to generate electricity although he acknowledges that the reverse process has valuable applications. Mahan speaks of theoretical efficiencies equivalent to ZT between 3 and 4 for conventional thermoelectric cooling. Mahan has applied for patents on his ideas, but prefers not to discuss them in detail until after proof of concept testing has been successful. COPs assuming ZT of 3 are also listed in Table 14 for thermoelectric cooling on page 37.

Thermionic refrigerators will be competitive with thermoelectric cooling devices as they are developed for higher efficiencies. At the current stage of their development they are unable to compete with alternative cooling technologies because of significantly lower operating efficiencies. The greatest potential for thermionic cooling may be for very low and micro-power applications.

Technical Advantages/Benefits

There are no moving parts outside of the air handling equipment, no refrigerants, and the possibility of low manufacturing costs as exhibited by sectors of the electronics industry.

Technical Disadvantages

There are several disadvantages or problems with thermionic converters in space conditioning applications:

! electrodes must be made of materials with low work functions to provide sufficient electrical current at low temperatures, but this results in decreased capacity,

! an interelectrode space of 1 ton 5 μm is necessary to decrease the power requirement of the converter which will be difficult to achieve or maintain in vacuum thermionic devices,

! the temperature difference between the electrodes must be kept small to decrease the radiant and conductivity heat losses, Mahan recommended 1 to 2EC. Reducing radiant and conductive losses, thus, requires multilayer construction to achieve a useful)T in this application with an increase in electrical resistance and additional energy losses,

! thermionic devices with a thin layer of a semiconductor between the electrodes need to be tested experimentally to determine their efficiencies under real values of the layer heat conductivity loss, and

! even with the heat transfer density of 1 W/cm^2, thermionic devices will need to overcome common problems associated with heat removal from very small surface areas; this task probably requires a cooling system with an actively pumped working fluid.

Technical Barriers

The greatest barrier to developing more efficient thermionic devices is probably the manufacturing technologies for achieving extremely small interelectrode spacing. Mahan speaks of using advanced technologies to build prototype systems essentially building the semiconductor divider in the interelectrode space an atom at a time. Developers of vacuum electrode gaps have not commented on manufacturing techniques.

Economic Analysis

The inherently low efficiencies of thermionic converters are compensated for in part by the absence of cycling losses and low maintenance costs. Comparisons were made for the theoretical maximum efficiencies using C_d=0 for the thermoelectric heating and cooling and maintenance costs of $25 per year. Installed costs would need to be $325 to $600 per ton below the cost of the electric baseline heat pump for the systems to have comparable life cycle costs in the southeastern, south central, and southwestern states assuming the maximum theoretically possible cell efficiencies (ZT=3).

Contacts and Sources of Information

Gerald Mahan
Oak Ridge National Laboratory
Solid State Division
P.O. Box 2008
Building 3025, MS 6032
Oak Ridge, TN 37831
(423) 576-8675

Moelwyn-Hughes, E.A. 1961. Physical Chemistry, Pergamon Press.

Hafsopoulos, G. N., et al. 1973, Thermionic Energy Conversion, The Massachusetts Institute of Technology

Rowe, D. M. 1994. Proceedings of the 13th International Conference of Thermoelectrics.

Bogomolov, V. N., 1995. Proceedings of the 14th International Conference of Thermoelectrics.

Moyrhes, B., 1996. Proceedings of the 15th International Conference of Thermoelectrics.

Mahan, G. D. 1994. Journal of Applied Physics, 76 (7), p. 4362, October 1.

Mahan, G. D. 1998. Journal of Applied Physics, 83 (9).

Obvious Holes in Knowledge, Understanding, Information

No measured performance data, either capacity or efficiency, are available at any conditions. Mahan's proof of principal testing at ORNL in August 1998 may prove whether or not the phenomenon of thermionic exists for power generation, although further work would be needed to provide any information on efficiency.

THERMOACOUSTIC COOLING

Basic Concept Description

Thermoacoustic cooling relies on a high energy standing sound wave to generate a temperature gradient across a stationary element called the stack; heat exchangers at the ends of the stack are used to transfer heat in and out of the system. This cycle is illustrated in Fig. 19; it consists of four principal components:

1. a "stack" of porous material, parallel plates, or sheets of a thin material rolled into a spiral
2. hot and cold heat exchangers consisting of finned tubes, parallel plates, screens, or metallic wool,
3. a rigid and sealed tube that may incorporate a Helmholz resonator to shorten the device and minimize losses, and
4. an acoustic energy source, referred to as an electroacoustic transducer (i.e. a loud speaker or a piston).

The working fluid is usually a mixture of perfect gases, such as xenon and helium. The driver operates at the resonance frequency of the system to produce fairly large pressure fluctuations that alternately compress and expand the working fluid adiabatically and cause the fluid to oscillate back and forth within the stack and heat exchangers. The stack serves as a regenerator as the working fluid oscillates back and forth, absorbing heat during the compression phase of the acoustic wave in the working fluid and rejecting heat back to the gas during the expansion phase. The complete cycle, then, resembles a series of Brayton cycles grouped together as illustrated in Figs. 20 and 21. The stack is typically fairly short, on the order of inches, and there can be hot and cold heat exchangers at each end of the stack to get heat in and out of the system (several different techniques are being investigated to get useful heating and cooling from the stack).

Background Information

Development of thermoacoustic cooling has been promoted in large part by the U.S. Department of Energy at Los Alamos National Laboratory for liquefaction of natural gas and by the U.S. Navy for shipboard applications such as cooling electronic equipment or crew spaces, although there have been commercially funded prototypes built in the U.S. by Cryenco, Tectronix, and Ford Motor Company. Greg Swift and his colleagues at LANL recently demonstrated a device which generated sound thermoacoustically by burning natural gas and used that sound to liquefy 140 gal/day of natural gas in a pulse-tube refrigerator. A 500 gal/day unit is currently under development. A related heat-driven device the size of a soft drink can was designed for cooling of "down hole" instrumentation in well drilling applications.

Steven Garrett (formerly of the Naval Postgraduate school, now at Penn State) and his colleagues designed and built two space-qualified prototypes which cooled below -60EC and provided a few watts of cooling power. One was flown on the space shuttle Discovery (STS42) in 19922. This was followed by a larger unit which cooled to a minimum temperature of -20EC. It consumed 216

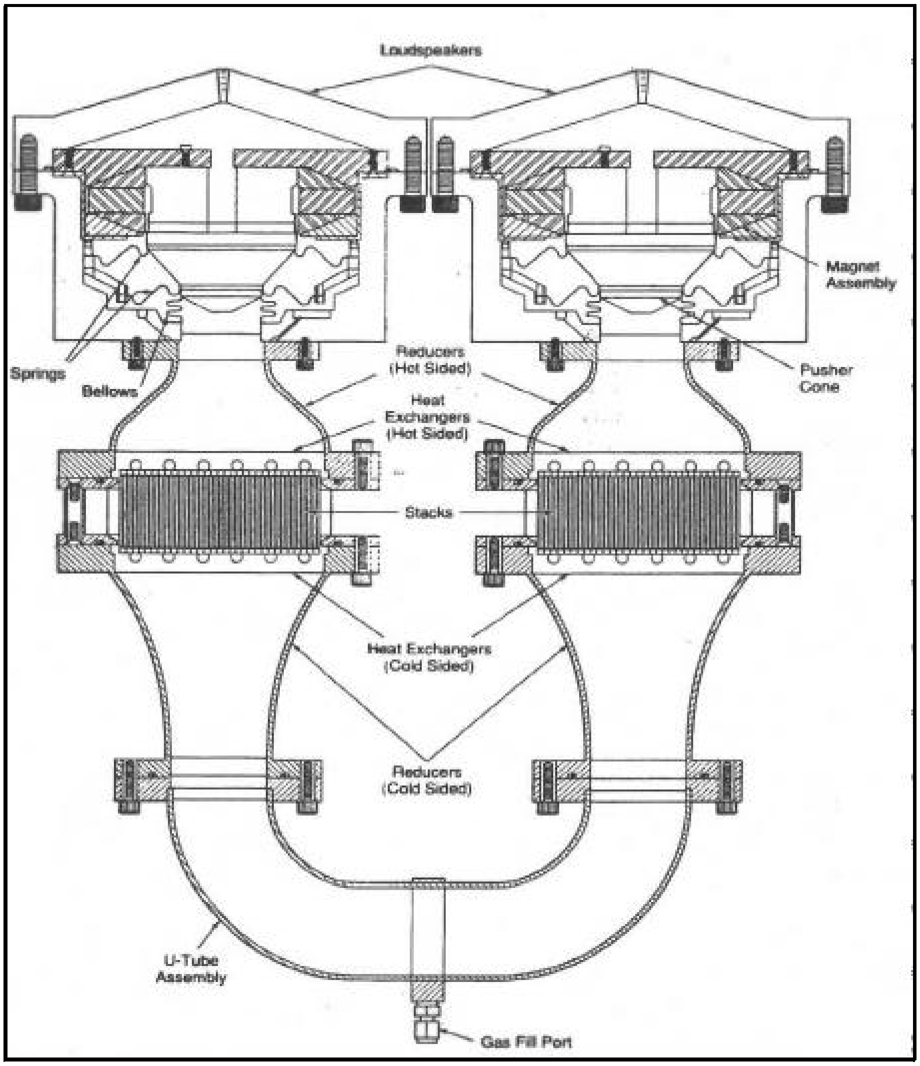

Fig. 19. Schematic of a thermoacoustic refrigerator (Source: NASA Tech Briefs, Vol. 21, No. 11, November 1997).

watts of acoustical power to produce 419 watts of useful cooling for a shipboard radar unit on board the USS Deyo (DD-989), a Spruance-class destroyer, in 1995. The loudspeakers used to produce the acoustical power had an electroacoustic efficiency of only 52%. This resulted in about one watt of cooling for each watt of electrical input power. Garrett and his colleagues are currently working on a three ton shipboard air conditioning unit that uses 85% efficient loudspeakers and is due for sea trials in early 2000.

Minner and colleagues at Purdue University used the DELTAE thermoacoustic refrigerator computer model, developed by Greg Swift and Bill Ward at Los Alamos, and combined it with a simplex numerical optimization program to tweak the design of a prototype cooler to maximize COP. “Tweaking” in ther case means altering operating parameters such as mean pressure, inert gas mixture ratios, heat exchanger designs, and geometric parameters (e.g. stack position) for the resonation tube in a systematic way to reduce losses. Minner showed that systematic optimization could improve the COP significantly. Minner's analysis was based on a 200 W cooler with hot and cold heat exchanger temperatures of 260 K (8.3EF) and 310 K (98EF); parasitic energy requirements associated with heat transfer across the heat exchangers using the secondary fluids and air were not included.

Secondary System Requirements

To date, most systems have required a secondary heat transfer loop, but recent designs have cooled the process fluid (air) directly with improved efficiency.

Efficiency Data

The effort necessary to model a thermoacoustic cooler or heat pump was beyond the funding and time limitations of this project and beyond the expertise of its authors. Data reported in Table 15 are from Garrett and Swift. Both sources reported electroacoustic driver efficiencies between 75 and 90%. Garrett is constructing a 10 kW air conditioner for the Navy with a COP at 95EF between 2.3 and 2.5. Swift predicts a COP 1.7 to 2.0 using a secondary loop and less optimistic assumptions.

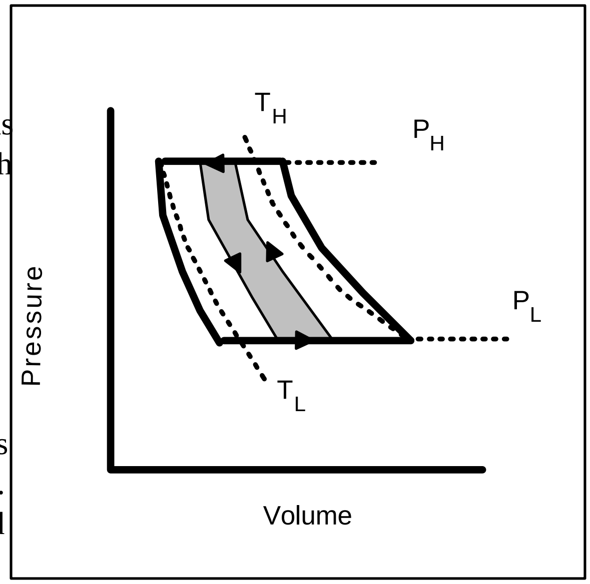

Fig. 20. P-V diagram for a thermoacoustic refrigerator.

Technical Advantages/Benefits

Thermoacoustic systems should have low cost and high reliability since there are no parts in contact with working fluid that require lubrication. With gas as the working fluid the system operates as well in near zero gravity conditions in space bound equipment as it does in terrestrial applications.

Technical Disadvantages

Thermoacoustic systems have had lower efficiency than conventional vapor compression systems in room temperature applications, but the rate of developments in this field have been

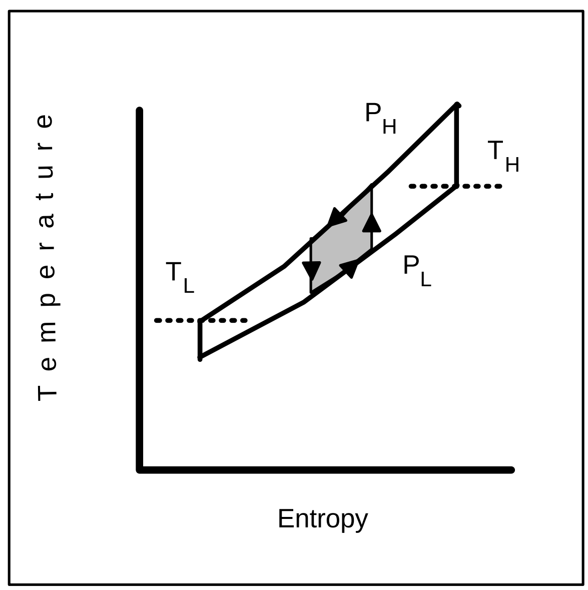

Fig. 21. T-S diagram for a thermoacoustic refrigerator.

Table 15. Calculated and Reported Efficiencies for Thermoacoustic Cooling.

Cycle Efficiency	Heating			Cooling		
	47EF	17EF	Seasonal (Btu/Wh)	82EF	95EF	Seasonal (Btu/Wh)
Cycle COP reported	3.49	2.16		3.71	2.79	
System COP reported - electric reported - gas	2.87 1.15	1.90	6.6	3.02	2.38 0.50	8.9

notes: "reported" efficiencies are from Garrett and Swift. Blank entries denote absence of calculated or measured information, calculated and observed cycle efficiencies do not apply for the shaded seasonal boxes

very rapid. The thermoacoustic systems are also relatively large in size for the power levels they achieve and may require secondary heat transfer loops. Noise was a problem in some test bench prototypes, not from the internal sound, but from vibration of the whole vessel. This has been largely solved and should not be a problem if thermoacoustic heat pumps are ever mass produced.

Technical Barriers

Developments are needed in the design of compact heat exchangers in oscillating flow. Cost and availability of acoustic drivers could be a problem. Major impediment to further development is a talent bottleneck with extremely few people trained to work in thermoacoustics.

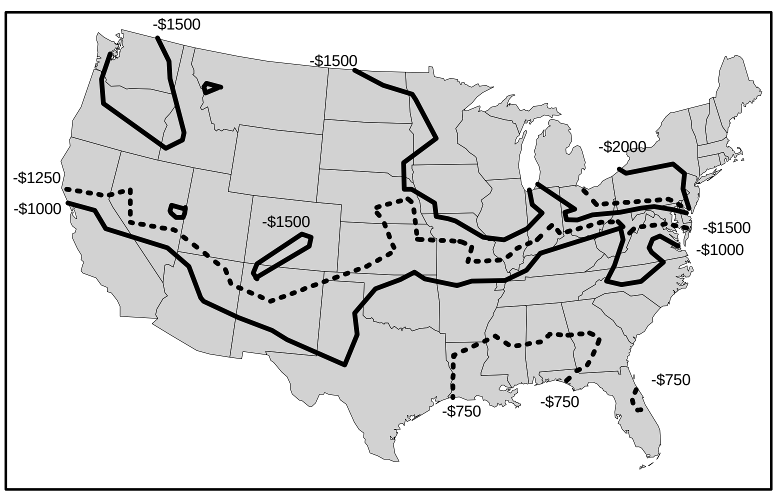

Fig. 22. Allowable installed cost price differential for a thermoacoustic heat pump relative to the electric baseline.

Economic Analysis

An economic comparison was performed using an annual maintenance costs of equal to that for the baseline electric heat pump, cycling C_d=0.10, and 100 W/ton for secondary fluid pumps with Garrett's optimistic estimate of COP's 30%

below those of R-22 heat pumps. The results are shown in Fig. 22. Under those assumptions the thermoacoustic heat pump would have to have an installed cost of $600 to $1000 per ton below the baseline electric heat pump to have equivalent life cycle costs; essentially a 35% to 60% price reduction. The installed cost reductions indicated in Table 16 reflect the low cycle efficiencies; the longer it is in use the greater the economic losses. Significant efficiency improvements are necessary for thermoacoustic heat pumps to be cost effective relative to conventional electric heat pumps.

These results necessarily depend on the assumptions for secondary loop pumping power and annual maintenance costs. Lower pumping power for the secondary loop or maintenance costs significantly lower than those of the baseline heat pump would allow installed costs closer to those of the baseline system.

The thermoacoustic system eliminates the conventional electric motor and compressor at the expense of adding an acoustic generator, resonating chamber, and secondary fluid system. Although some cost reductions may be possible, it is unclear if the relative cost of the thermoacoustic system can be that much lower than the baseline system.

Table 16. Installed Cost Premiums Possible for a Thermoacoustic Heat Pump Relative to an Electric Heat Pump.

Region	Installed Cost Premium ($/ton)		
	3 Year Payback	5 Year Payback	Equal Life Cycle Cost
Northeast	-$541	-$858	-$2465
Southeast	-$188	-$297	-$855
South Central	-$214	-$339	-$982
Southwest	-$233	-$380	-$1133
Midwest	-$366	-$584	-$1705
Northern Plains	-$283	-$452	-$1320
Rocky Mountain	-$278	-$443	-$1322
Pacific Northwest	-$192	-$303	-$903
California	-$225	-$358	-$1067

Contacts and Sources of Information

Gregory Swift
Condensed Matter and Thermal Physics Group
Mail Stop K764
Los Alamos National Laboratory
Los Alamos, New Mexico 87545
ph: (505) 665-0640
fax: (505) 665-7652
e-mail: swift@lanl.gov

Steve Garrett
Pennsylvania State University
P.O. Box 30
State College, PA 16804
ph: (814) 863-6373
fax: (814) 865-3119
e-mail: garrett@sabine.acs.psu.edu

Jim Braun
Purdue University
West Lafayette, IN
e-mail: jbraun@ecn.purdue.edu

Appliance Manufacturer 1998. “Sound Idea: Acoustic Compressor to Power Residential Refrigerator,” June, pp. 63-64.

Obvious Holes in Knowledge, Understanding, Information

Rigorous modeling using DELTAE is required evaluate the performance of thermoacoustic systems at standard HVAC rating conditions; the required effort is beyond the scope of this study.

PULSE-TUBE REFRIGERATION

Basic Concept Description

A pulse tube refrigerator is a device for cooling to low temperatures operating at frequencies well below the resonance frequencies used in thermoacoustic devices. Two alternative configurations for a pulse tube cooler are shown in Fig. 23. These are closed systems that use an oscillating pressure at one end (typically produced by a compressor) to generate an oscillating gas flow in the rest of the system. This gas flow (usually helium) can carry heat away from a low temperature point (cold heat exchanger) if the conditions are right. An orifice controlling the flow at the other end of the cooler can provide the right condition for cooling to occur. The cycle is similar to thermoacoustic refrigeration thermodynamically where the tube walls act as a regenerator instead of the stack (see Figs. 20 and 21).

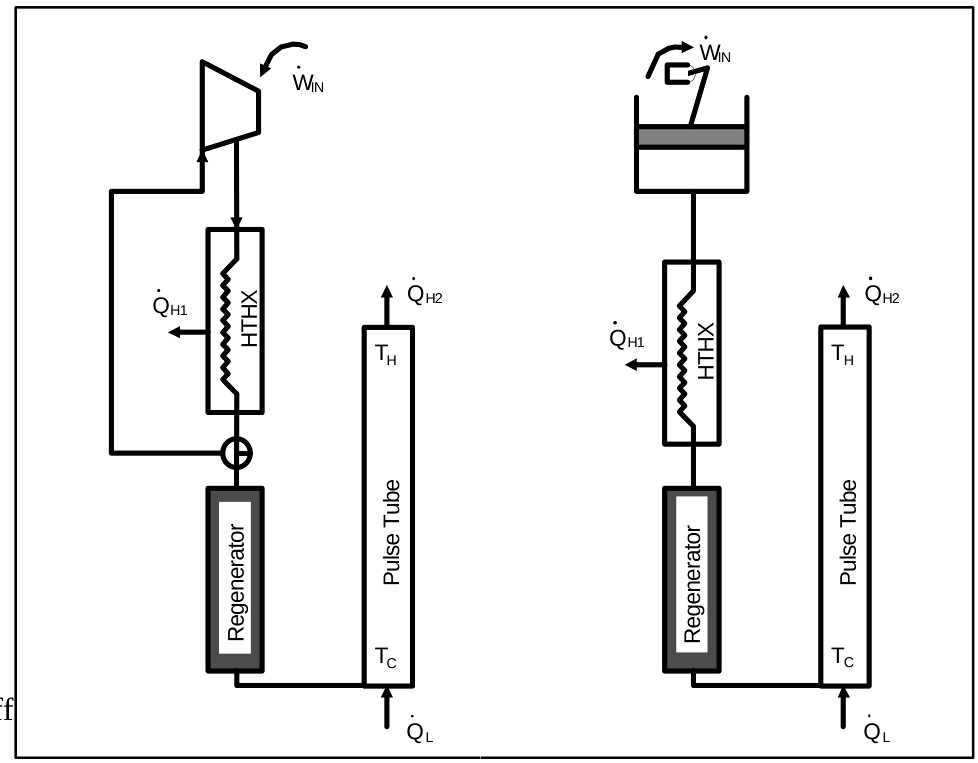

Fig. 23. Pulse tube refrigeration systems.

Background Information

Pulse tube coolers are a recent discovery. They were first reported by W. Gifford of Syracuse University in 1963 from his observation of heating in blanked off plumbing lines attached to gas compressors. NASA and DOE have sponsored work in pulse tube refrigeration for cryocoolers. Pulse-tube refrigeration systems were developed for cryogenic applications. A single cooler can cool from room temperature to 70-80 K and multi-stage systems can cool much lower. The amount of heat they can remove is only limited by their size and the power used to drive them. Their efficiency as cryocoolers is comparable to other systems such as Stirling coolers.

Pulse tube refrigeration systems were developed for infrared sensors used in atmospheric monitoring, night vision, missile guidance. They are also used in gamma ray sensors (monitoring nuclear activity), cryogenic catheters and cryosurgery, and the liquefaction of gases. This equipment has a high reliability for cryogenic refrigeration; no moving parts at the cold end of cryocoolers. The efficiency is very low with COPs ranging from 0.005 to “comparable to Stirling coolers” for cryogenic applications. Scaling to high capacities may be a problem because current development appears to be for sensors at low capacities; more information is needed.

The following description is taken verbatim from the doctoral dissertation by Don Gauger (1993):

“The pulse-tube concept was developed by Gifford and Longsworth in the mid-1960s. Mikulin and Radebaugh improved the COP of the pulse tube by adding an orifice and an expansion chamber to the high-temperature end of the tube.

“An ideal pulse tube system is composed of a compressor, regenerator, high temperature heat exchanger, and the tube. Figure 23 depicts two pulse-tube schematics illustrating different methods of periodically compressing the working gas. Periodic compression can be accomplished by a steady flow compressor and rotary control valve, as shown on the left side of the figure or by a reciprocating compressor, as shown on the right. The heat generated due to compression of the gas is rejected by a high temperature heat exchanger; the gas then passes through a regenerator. The tube wall is constructed of a material with a low thermal conductivity, commonly stainless steel. The ends of the tube are capped with a highly conductive material like copper. The heat is accepted by the low temperature heat exchanger located at the entrance end of the tube, and rejected by the high temperature heat exchanger at the opposite end.

“The principal of operation of the ideal cycle may be understood by considering a thin cylindrical control mass segment as shown in Fig. 24. The following assumptions are made:

1. Invicid flow,

both step functions with respect to time as shown in Fig 24,

3. Perfect regeneration,
4. The heat is transferred to and from the mass segment through the tube wall,
5. Ideal gas,
6. Isentropic compression, and
7. All ducts are adiabatic.

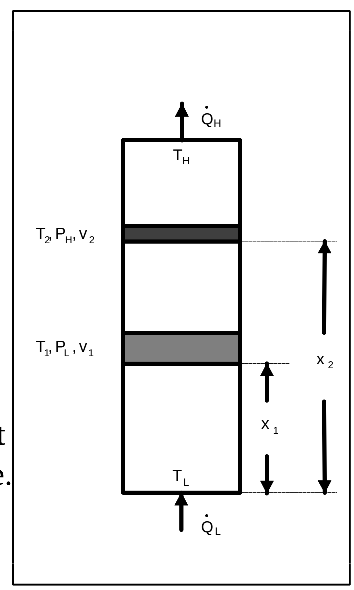

Fig. 24. Control volume for pulse tube refrigeration.

“The mass is initially contained in volume V_1 of tube inside diameter and thickness h_1. As the pressure and temperature of the gas in the element are changed during the cycle, the volume will also change. Since the tube wall is rigid the diameter of the element will not change, however, the thickness of the element must change. The gas is at a thermodynamic state having properties P_L and T_1, and an initial height in the tube x_1. When the pressure in the tube is increased to P_H, the volume is compressed to V_2, elevated to position x_2, and the temperature raised to T_2. A temperature gradient ranging from T_L to T_H exists along the length of the tube. The local temperature of the tube wall at position x_2 is lower than the temperature of the mass segment, T_2. Therefore, heat will be transferred from the mass segment to the wall, and the thermodynamic properties will be: T_3, P_H, and v_3. When the pressure is lowered to P_L, the mass segment undergoes an isentropic expansion to state 4 with properties T_4, v_4, and P_L, at a slightly higher elevation than the original position. As the gas is re-heated, it will be returned to the original thermodynamic state (state 1) and position in the tube; the cycle has been completed.

"Ideally, the control mass of gas in the tube undergoes an isentropic compression from states 1 to 2, isobaric cooling from states 2 to 3, an isentropic expansion from states 3 to 4, and isobaric heating from 4 to 1. The ideal cycle formed by the series of processes undergone by the control mass is the reversed Brayton cycle. Furthermore, the cycle for the entire mass of gas in the tube is an interconnected series of Brayton cycles as shown in Figs. 25 and 26. The tube wall acts as a continuous regenerator."

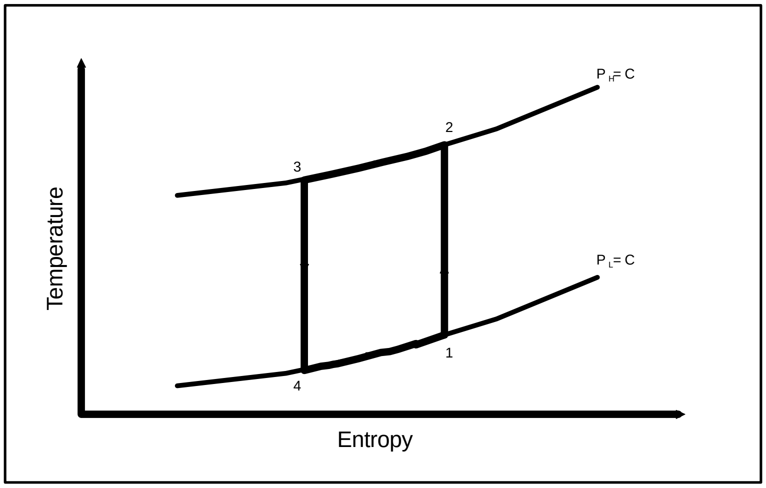

Fig. 25. Temperature - entropy diagram for pulse tube control volume.

Secondary System Requirements

A secondary heat transfer loop is required.

Efficiency Data

No information has been located relevant to applying pulse tubes at space conditioning temperatures, particularly for operating efficiencies. NASA Web sites have a reasonably large amount of measured performance data on-line giving tube dimensions, operating pressure, capacity, etc. but nothing on efficiency. Capacities are typically a few Watts. The highest cold heat exchanger temperature is in the neighborhood of 80 K.

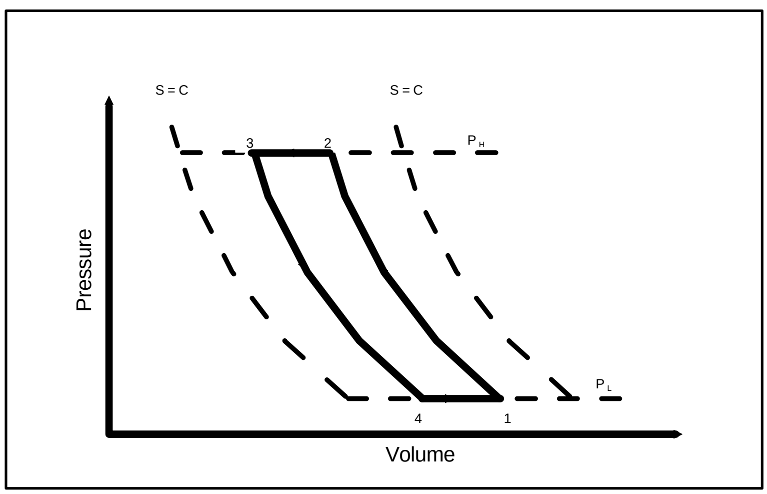

Fig. 26. Pressure - volume diagram for pulse tube refrigeration.

- 1 Watt output / 200 Watt input at 35 K
- 1.5 Watt output / 100 Watt input at 55 K
- 5 Watts output / 3 kW input at 120 K

The theoretical calculations for the pulse tube system are in Table 17 are based on a computer model by Gauger.

Table 17. Calculated and Observed Efficiencies for Pulse Tube Cooling.

	Heating			Cooling		
Cycle Efficiency	47EF	17EF	Seasonal (Btu/Wh)	82EF	95EF	Seasonal (Btu/Wh)
Cycle COP theoretical observed	0.96	0.96		0.40	0.39	
System COP theoretical observed	0.88	0.88	3.4	0.39	0.39	1.1

notes: blank entries denote absence of calculated or measured information, calculated and observed cycle efficiencies do not apply for the shaded seasonal boxes

Technical Advantages/Benefits

Pulse-tube systems are well suited for cryogenic applications because there are no moving parts at the low temperatures.

Technical Disadvantages

Low efficiency at space conditioning lifts.

Technical Barriers

A single pulse-tube cannot be enlarged beyond an optimum surface-to-volume ratio, which depends on the cycle frequency and the desired temperature range. The capacity is increased by the operation of several tubes in parallel from the same source of compressed gas (Wood 1969).

Economic Analysis

The modeled COPs for this system are extremely low and there is no independent corroboration of these values so calculated energy use data are highly questionable. Installed costs would need to be thousands of dollars per ton less than conventional heat pumps to have comparable life cycle costs. There are two configurations for pulse tube cooling, one using acompressor and the other a pump and valve. The compressor configuration is unlikely to have any significant equipment cost savings relative to conventional electric heat pumps; the pump and valve system may have smaller equipment costs but not thousands of dollars below a motor driven compressor driven system.

Contacts and Sources of Information

Swift, G., Gardner, D., and Backhaus, S. 1999. "Acoustic Recovery of Lost Power in Pulse Tube Refrigerators," Journal of the Acoustic Society of America, Vol. 105, pp. 7110724.

NASA Web, http://ranier.oact.hq.nasa.gov/Sensors_page/Cryo/CryoPT/CryoPTHist.html

NASA Ames Research Center: http://irtek.arc.nasa.gov/WhatisOPT.html

Wood, B. 1969. *Applications of Thermodynamics*, Addison-Wesley Publishing Company, p. 281.

http://irtek.arc.nasa.gov/CryoGroup/PTDatabase/PTData-Basic.-html (data)

http://irtek.arc.nasa.gov/WhatisOPT.html

http://ranier.oact.hq.nasa.gov/Sensors_page/Cryo/CryoPTHist.html

Gordon.Johnston@hq.nasa.gov

Greg Swift
Physics Division
Los Alamos National Laboratory
K764
Los Alamos, NM 87545
phone: (505) 665-0640
fax: (505) 665-7652
e-mail: swift@lanl.gov

P. Kittel, NASA Ames Research Center
Dr. E. Mikulin, Moscow Bauman State Technical University, Russia,
Dr. R. Radebaugh, NIST.

Obvious Holes in Knowledge, Understanding, Information

Refined efficiency calculations or corroboration of COPs at rating conditions from other sources.

MALONE CYCLE REFRIGERATION

Basic Concept Description

The Malone "cycle" is perhaps a misnomer. Malone engines and refrigeration devices are really the application of liquids as the working fluid in a Brayton or Stirling cycle configuration. Liquids have attracted very little attention as operating fluids because "ideal" liquids are not appropriate for refrigeration cycles and "ideal" gases are. The working fluid in a heat pump must cool as the fluid is depressurized in order to absorb heat from the conditioned space. The cooling on depressurization (and thermal expansion for a heat engine) is proportional to the coefficient of thermal expansion. The thermal expansion coefficients for gases are large, essentially infinite for boiling and condensation. It is generally small for any liquid with "nearly ideal" behavior, but it can be large for liquids close to their critical points.

Background Information

Malone refrigeration exists primarily as a theoretical concept with little, if any, hardware development or proof of concept demonstration. John Malone built a liquid-based 50 hp engine in 1925 that burned coal and used high pressure liquid water as the working medium. Malone's idea was largely ignored for 50 years, when John Wheatley developed in interest in innovative cooling and refrigeration technologies in the 1970's. The effort on Malone refrigeration has been done almost exclusively at Los Alamos National Laboratory with theoretical studies of liquids in both Stirling and Brayton cycle machines. Laboratory prototype cooling devices have been built at Los Alamos National Laboratory (LANL) to demonstrate the concept.

The staff at LANL examined several fluids, including hydrocarbons, CFCs, and inorganic fluids before selecting liquid propylene as the working fluid for a demonstration Malone/Stirling refrigerator. This machine was designed for ease of instrumentation and study rather than for high performance and it had a COP about half of that achieved by CFC based Rankine cycle equipment of the time. In 1993, the LANL staff began looking at using liquid CO_2 in a free-piston Stirling machine to reach higher efficiencies with 2 kW cooling capacity. A 40 kW Brayton cycle, liquid CO_2, system was under development at the Naval Surface Warfare Center at Annapolis, Maryland in 1993 (Swift 1993a). No further information has been found on the follow-on work at LANL.

Secondary System Requirements

A secondary heat transfer loop is probably necessary to minimize dead space in the operating volume.

Efficiency Data

No performance data, at any conditions, have been located in the literature for Malone cycle refrigeration. Calculations cannot be performed without accurate thermodynamic properties of liquids (CO_2, propylene) near their critical points. Heat exchanger pressure drops are significant factors for a Malone machine, and viscosity data are also needed near the critical point in order to estimate cycle efficiency. No cycle calculations were performed as part of this project.

Technical Advantages/Benefits

The equations in Appendix I show several advantages of using a liquid working fluid near its critical point instead of a gas:

! the power requirements for compressing the working fluid are basically determined by the coefficient of isothermic compression, K_p, and these decrease as K_p increases,

! the quantity of heat transferred and absorbed, Q, depends on β_T and this increases abruptly near the critical point,

! the quantity of heat transferred and absorbed depends on C_V, and C_V is significantly larger for a liquid than it is for a gas, and

! the heat transfer coefficient for the regenerator is a couple of orders of magnitude higher for a liquid than it is for a gas which allows for a smaller surface for convective heat transfer.

The low compressibility of liquids means that a larger pressure change is generated than with a gas for a given change in volume. Swift states that heat transfer is proportional to the pressure change, so either smaller compressors can be used to meet a specified load, or greater heat transfer can be accomplished for a given compressor size (Swift 1993). Liquids also have heat capacities per unit volume that are orders of magnitude larger than those of gases at pressures generally encountered in refrigeration equipment. Thus, far less fluid needs to be circulated than with a gas cycle system and less work is required. The pressurization of a liquid without transferring heat, however, results in a small temperature change because of the large heat capacity; refrigeration requires that the working fluid undergo a large temperature change in order to move heat from source to sink. Regenerators are required in the Malone cycle in order to achieve acceptable ΔT's.

Technical Disadvantages

There are several problems associated with using liquid working fluids that have not been resolved:

! the operating pressures can be extremely high with associated problems with mechanical stresses and operating safety,

! a refrigeration device using a liquid would have a significant mass of working fluid and there are associated lag times at starting, stopping, and changing modes of operation,

- the operating controls need to be extremely accurate because proper operation is limited to a small region near the critical point; moving past the critical point to gaseous region results in sudden temperature drops and “water hammer” that could destroy the equipment,
- there are high pressure drops in the heat exchangers, particularly for the Stirling cycle Malone machine because of the pulsating nature of the working fluid flow in the Stirling cycle. The heat exchanger pressure drops will be high for space conditioning application and offset possible efficiency gains from low compression power.

Technical Barriers

The principal barriers in development of applications of the Brayton/Malone cycle are in funding and trained engineers. Development of Stirling/Malone is more difficult because of the spatially distributed oscillating flows.

Economic Analysis

An economic comparison is not performed due to the absence of modeled and reported efficiencies.

Contacts and Sources of Information

Malone, J. F. J. 1931. Journal of the Royal Society of Arts, Vol. 179, p. 679.

Allen, P. C. Et al. 1980. Proceedings of the National Academy of Science, Vol. 177, p. 39.

Swift, G. 1989. Journal of Applied Physics, Vol. 65, p. 4157.

Swift, G. 1990. “*Malone Refrigeration*,” ASHRAE Journal, November, pp. 28-34.

Swift, G., 1993, “*Malone Refrigeration: An Old Solution to a New Problem,*” Los Alamos Science, Number 21, 1993, pp. 112-123.

Swift, G., 1993a, *“Malone Refrigeration,”* Proceedings of the 1993 Non-Fluorocarbon Refrigeration and Air Conditioning Technology Workshop, Breckenridge, Colorado June 23-25, 1993, ORNL-6797.

Greg Swift
Physics Division
Los Alamos National Laboratory
K764
Los Alamos, NM 87545
phone: (505) 665-0640
fax: (505) 665-7652
e-mail: swift@lanl.gov

Obvious Holes in Knowledge, Understanding, Information

Steady-state data at the ARI test conditions or seasonal performance factors, costs

MAGNETIC REFRIGERATION

Basic Concept Description

magnetic materials, there is a decrease in entropy within the material related to an increase in the ordering of the electron spin state. This is illustrated in Fig. 27. The decreased entropy is associated with a decrease in internal energy and an increase in temperature of the material for an adiabatic process. If the process occurs isothermally, heat must be rejected to the surroundings through a secondary loop. The process is nearly reversible with very small internal losses, at least for small temperature rises, and can be used in a heat pump. The maximum temperature rise is proportional to the magnetic field; for gadolinium the maximum)T is 25EF at 68EF. In actual practice the temperature rise is on the order of 10E to 15EF so regenerative heat transfer is necessary to employ the magneto-caloric effect in practical applications.

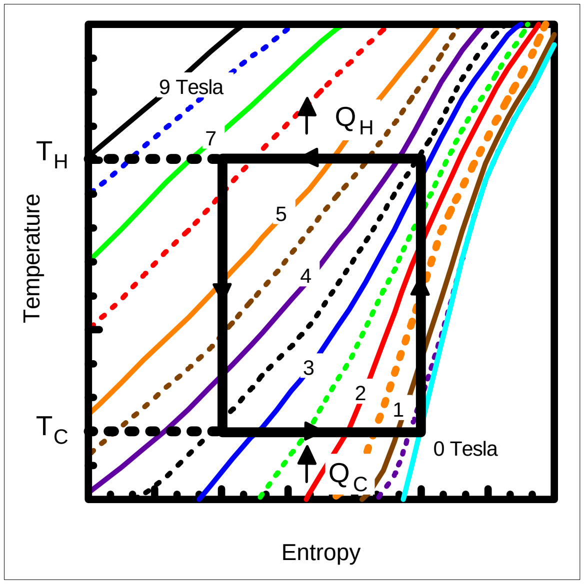

Fig. 27. Temperature-entropy variation for paramagnetic materials..

Background Information

Magnetic refrigeration systems are applied perhaps exclusively to cryogenic coolers because they have no moving parts or working fluids at temperatures near absolute zero. The design of a new type of near-room temperature magnetic refrigerator and the demonstration of its technical feasibility as an alternative refrigeration technology for energy-intensive industrial and commercial refrigeration systems is under development at Iowa State University. The magnetic refrigeration cycle has a very high intrinsic efficiency; the efficiency appears to be limited by factors susceptible to control, such as non-ideal materials properties, parasitic heat transfer, and flow losses. Replacement of vapor cycle refrigerators with magnetic refrigerators offers a significant potential energy savings.

DOE is supporting a $1 million project at Iowa State to investigate magnetic refrigeration for room temperature applications. Astronautics Corp. is under contract to Ames Laboratory (ISU) to develop a magnetic refrigerator; one of their working prototypes is depicted in Fig. 28. Some of their results were published at a Cryogenic Engineering Conference in Portland, Oregon in July 1997 (Zimm). These results show a strong dependence of COP on the temperature lift with a maximum COP of 8 with an 8 K lift falling to just above 1 with a 23 K lift. The experimental rig is using a hydronic loop as a heat transfer medium; the data is massaged to provide efficiency as a fraction of Carnot COP across the range of)T's including all the losses <u>except</u> heat added to the water from the pump seal friction (they used a very inefficient pump). The coefficient of performance of the Astronautics device has also set a record for magnetic refrigerators, suggesting that recent design innovations can make magnetic refrigeration competitive with conventional gas compression technology.

Magnetic refrigeration could be applied to gas liquefaction (low temperatures for separating gases), large scale refrigeration, and supermarket refrigeration. There are claimed high efficiencies; although it is not clear what is meant by “high” and whether that is for cryogenic conditions or near-room temperature conditions.

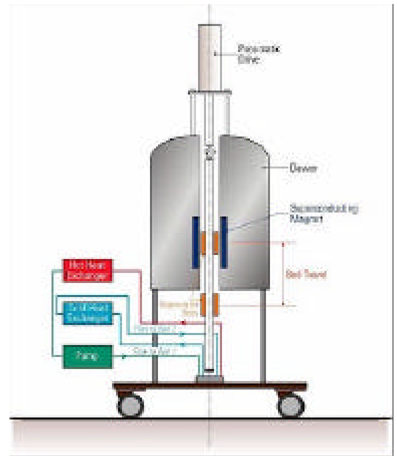

Fig. 28. Test stand for prototype magnetic refrigeration device (*Source:* http://www.external.ameslab.gov/news/Inquiry/fall97/bigchill.html).

Secondary System Requirements

Super-conducting magnets and regenerative and secondary heat transfer loops.

Efficiency Data

A computer program developed at Iowa State University (Gauger 1993) was used to calculate cycle COPs for a magnetic heat pump with field strength varying between 0 and 7 Tesla. Hot and cold heat exchanger temperatures used in these calculations are listed in Table 18. The cycle COPs listed in Table 19 exclude *all* electrical peripheral energy; the device under development at Astronautics uses an electrically-driven device to move canisters of gadolinium pellets into and out of the superconducting magnetic field. This is a high loss for their system because they use a secondary heat transfer loop with complicated circuitry and valving that circulates brine through the gadolinium pellets. Consequently the electrical drive system is working against high friction losses from the seals required by the secondary loop. The secondary loop pumping power and electrical requirements for the superconducting magnets are also unknown. The system COPs in Table 19 are based on 200 W/ton for the secondary loop pump, superconducting magnets, and drive

Table 18. State Point Temperatures for Magnetic Refrigeration Calculations

State Point Temperatures	Ambient Temperatures			
	47EF	17EF	82EF	95EF
hot heat exchanger	105EF	90EF	110EF	125EF
cold heat exchanger	29EF	5EF	44EF	44EF

mechanism. Results are also included in Table 19 for a magnetic heat pump operating between 0 and 5 Tesla, which is achievable without superconducting magnets.

Table 19. Calculated and Observed Efficiencies for Magnetic Refrigeration.

	Heating			Cooling		
Cycle Efficiency	47EF	17EF	Seasonal (Btu/Wh)	82EF	95EF	Seasonal (Btu/Wh)
Cycle COP						
theoretical - 7 Tesla	5.58	5.76		5.78	3.89	
- 5 Tesla	4.66	5.00		4.59	2.34	
- observed						
System COP						
theoretical - 7 Tesla	4.18	4.28	9.9	4.29	3.15	13.7
-5 Tesla	3.60	3.80	9.1	3.56	2.04	11.3
- 7 Tesla w/ ¼ hp pump	3.90	3.99	9.5	3.99	2.99	12.8

notes: system COPs do not include pumping power for the secondary circulating pump except in the very last line. Blank entries denote absence of calculated or measured information, calculated and observed cycle efficiencies do not apply for the shaded seasonal boxes

Technical Advantages/Benefits

Some of the major losses present in conventional gas-compression systems are absent in magnetic refrigerators, and thus it is expected that cooling systems based on this new technology can attain substantially higher efficiency than conventional gas-compression coolers.

Technical Disadvantages

Requires superconducting magnets and regenerative heat transfer. Very high regenerator effectiveness and very low parasitic power consumption for the secondary loop are required to approach system efficiencies competitive with conventional vapor compression.

Technical Barriers

Breakthroughs needed in magnetic materials and high temperature super-conducting materials in order to reduce both equipment and maintenance costs. Major developments are required in the regenerator to improve effectiveness, reduce pressure drop, while decreasing size and cost.

Economic Analysis

The economic evaluation of magnetic heat pumps is somewhat open ended because of unknown parasitic energy consumption and cost of peripheral equipment. As mentioned earlier, current configurations of magnetic refrigeration use an electric pump to circulate water or a brine solution through canisters packed with gadolinium pellets. They also use a linear motor or pneumatic device to move the canisters in and out of the magnetic field. Finally, the systems require superconducting magnets. Four sets of results are shown for the economic evaluation:

- contours of installed cost price differential relative to the electric heat pump baseline excluding all peripheral energy use by the magnetic heat pump,
- contours of installed cost price differential relative to the gas furnace baseline excluding magnetic system peripherals,
- a bar chart showing approximate increases in life cycle cost for the magnetic system using a ¼ hp pump in the secondary loop, and
- tabulated installed cost price differentials under three payback scenarios for a magnetic system with a ¼ hp pump and 60 W/ton for a linear motor.

The first two cases show the highest possible values for the differential in installed costs between magnetic heat pumps and both baselines; the second two cases provide some insights into how the system economics are affected by parasitic energy use.

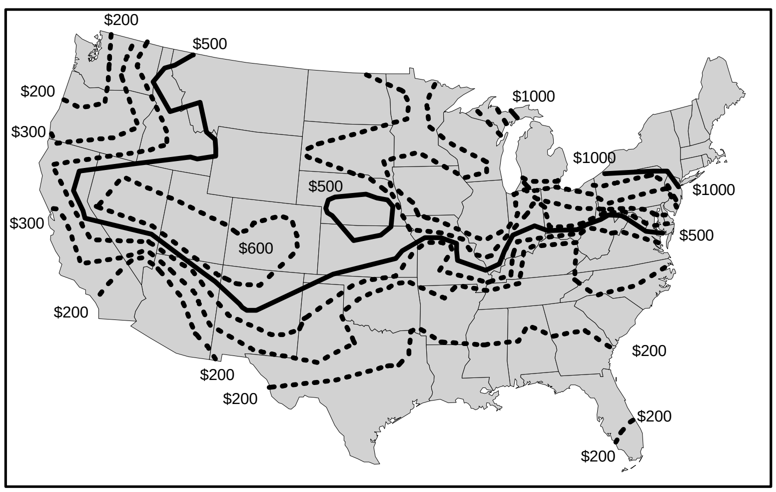

Fig. 29. Allowable installed cost price differential for a magnetic heat pump relative to the electric baseline exclusive of pumping power.

The results presented here assume that there would be low cycling losses (C_d=0.10) because the system does not need to build a high pressure differential each time it cycles on. The results for a 7 Tesla superconducting magnetic heat pump exclusive of pumping power are shown in Figs. 29 and 30 (assuming a $30 per year differential in maintenance costs).. The curves in Fig. 29 indicate that the system requires a lower installed costs than the baseline electric heat pump in order to have the same life cycle cost; $200 to

$500 per ton in the southern tier of the country ranging to more than $1000 per ton in the northeast. The results relative to the gas furnace and electric air conditioner baseline in Fig. 30 show that substantial cost reductions ($500 to $1000 per ton and more) would be needed outside of the southeast and desert southwest. In both sets of comparisons, though, the increase in life cycle cost for the power required to circulate the heat transfer fluid is not included. Approximate values for the life cycle cost of pumping power are shown in Fig. 31 for a system using a ¼ hp pump. The $200 per ton allowable first cost premium in the southeast and southwest of Fig. 29 is reduced to only about $50 per ton because of the increase in life cycle cost from pumping power; the extra $1000 per ton that could be spent on the magnetic heat pump in the northeast is nearly cut in half due to the pumping power.

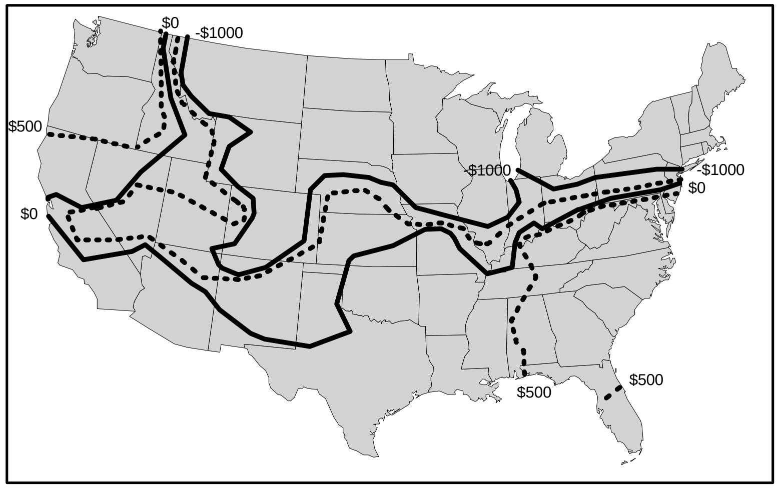

Fig. 30. Allowable installed cost price differential for a magnetic heat pump relative to the gas baseline exclusive of pumping power.

The addition of energy to move the gadolinium canisters in and out of the magnetic field reduces the allowable installed cost premiums even further. Again, the energy necessary to do this is not well defined; results are listed in Table 20 assuming 185 W for a three-ton heat pump (125 W/ton, or 375 W, for pump and linear motor). These data indicate that installed costs would need to be lower than the electric baseline system (described on page xiii) in the traditional heat pump markets in the southeast, south central, and southwestern states (Fig. 31

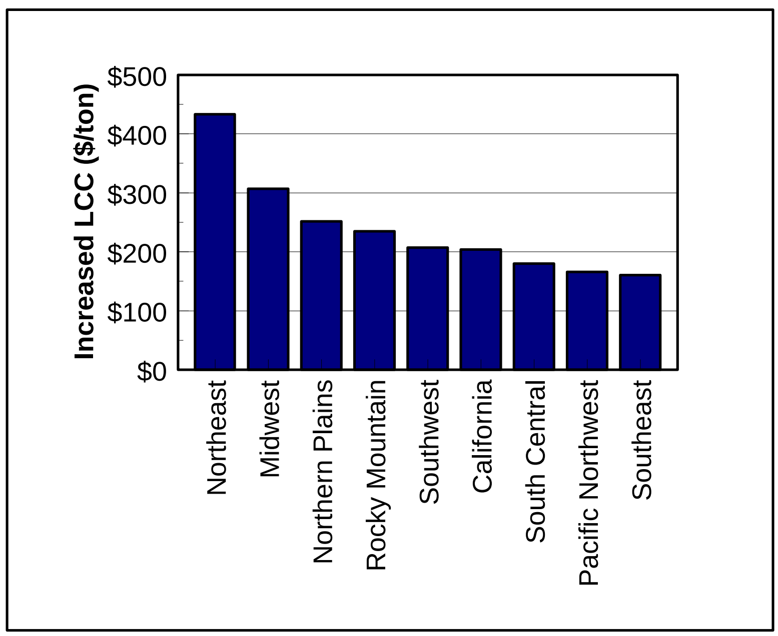

Fig. 31. Increase in life-cycle-cost of magnetic heat pump due to ¼ hp pump.

shows that magnetic heat pumps compare unfavorably with the gas baseline described on page xiii outside the traditional heat pump markets).

The economic results are also dependent on the assumed increase in annual maintenance costs. Current configurations of magnetic refrigeration devices (outside of cryogenic work) assume a secondary fluid with sliding seals. It is assumed that maintenance of such a system will be more expensive than for a conventional vapor compression heat pump or a gas furnace. This additional cost is arbitrarily assumed to be $30 per year, but it really is not known. Every $10 increment in annual maintenance costs for this system raises the life cycle cost by $65 to $90 per ton, depending on the area of the country (variation occurs because maintenance costs are specified in absolute figures and results are expressed in $/ton). Savings in maintenance costs would have corresponding decreases in life cycle costs. Any increase in life cycle costs due to higher maintenance costs would necessarily reduce the allowable first cost premium by an equal amount.

Considering the actual hardware for a magnetic heat pump, this system saves on the costs associated with a hermetic compressor in the baseline systems, but has additional costs associated with the pump and heat exchangers for a secondary heat transfer loop, gadolinium canisters, and superconducting magnets. The costs of magnets and gadolinium alone are very large and reductions of two orders of magnitude would be required for this technology to be competitive. Currently (1998) all superconducting magnets are custom made with costs around $30,000 apiece (dimensions unknown). Zimm reported measured cooling powers on the order of 400 to 600 W for 3.6 kg of gadolinium spheres fashioned from 13.6 kg of gadolinium purchased from China at $110 per kg. The price has since gone down to approximately $80 per kg. Consequently, the cost of gadolinium (excluding the extensive processing required) is approximately $6400 per ton of cooling capacity. Material costs and pumping power are likely to make magnetic heat pumps impractical relative to both the gas and electric baseline systems in spite of the high cycle efficiency possible with the magnetic system.

Table 20. Installed Cost Premiums Possible Relative to an Electric Heat Pump for a Magnetic Heat Pump.

	Installed Cost Premium ($/ton)		
Region	3 Year Payback	5 Year Payback	Equal Life Cycle Cost
Northeast	$92	$143	$349
Southeast	-$11	-$19	-$104
South Central	$4	$4	-$32
Southwest	$0	$5	-$23
Midwest	$55	$86	$199
Northern Plains	$37	$58	$121
Rocky Mountain	$33	$50	$102
Pacific Northwest	-$14	-$14	-$94
California	-$2	-$6	-$64

Contacts and Sources of Information

ADL 1993. Energy Efficient Alternatives to Chlorofluorocarbons (CFCs): A Research Needs Assessment Final Report, U.S. Department of Energy, Office of Energy Research, DOE/ER/30115-H1, June.

"Description and Performance of a Near-Room Temperature Magnetic Refrigerator," Zimm, C. Jastrab, A., Sternberg, A. Pecharsky, V., Gschneidner, K., Osborne, M. And Anderson, I., CEC July 1997.

MIT Website, http://lost.pfc.mit.edu/technology_engineering/mr.html

Ames Website, http://www.ameslab.gov/cool.html

Karl A. Gschneidner, Jr., Metallurgy and Ceramics Division, Iowa State University
Carl Zimm, Astronautics, Madison, WI (608-221-9001)
Steve Karsjen, Ames Lab (515-294-1856)

Obvious Holes in Knowledge, Understanding, Information

Magnitude of electrical parasitics and confirmation of modeled COPs.

COMPRESSOR-DRIVEN METAL HYDRIDE HEAT PUMP

Basic Concept Description

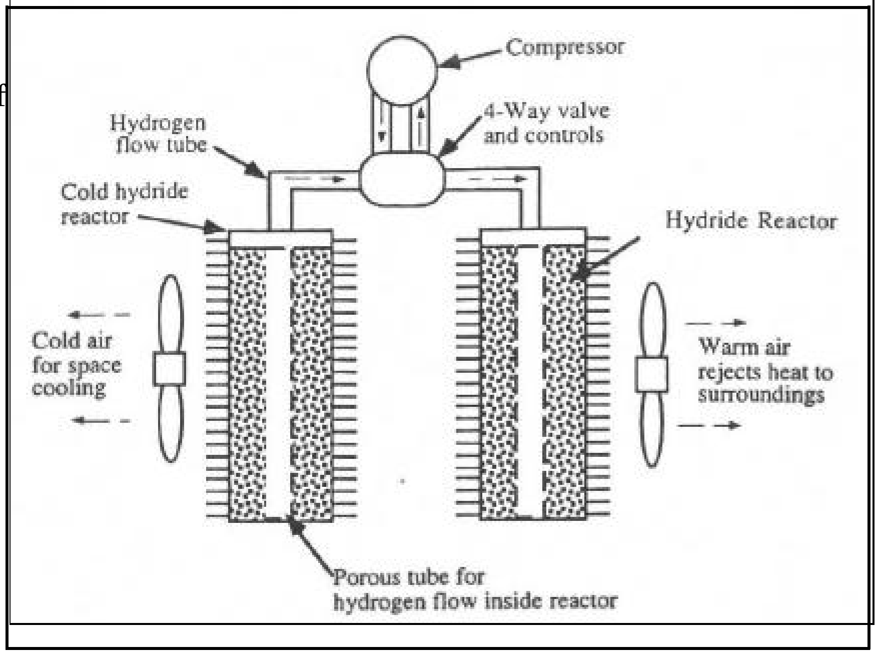

Fig. 32. Compressor driven metal hydride heat pump (source: Kim 1997).

The "traditional" adsorption heat pump design relies on the natural affinity of the adsorbent to provide the low pressure required to attract the refrigerant and a gas-fired burner to provide the energy necessary to desorb the refrigerant at high pressure. The refrigerant is circulated through a conventional configuration of condenser, evaporator, and expansion device. An adsorption cycle has been conceived, however, that uses an electrically-driven compressor to impose a pressure drop causing the gas, hydrogen in this case, to desorb from the metal hydride bed. The suction line of a conventional refrigeration compressor is connected to a bank of fully charged "reactors" of porous metal hydride "compacts." The discharge line is connected to a second discharged reactor. The refrigerant, hydrogen, is desorbed from the lanthanum pentanickle ($LaNi_5$) adsorbent at low pressure and temperature on the suction side and adsorbed on the $LaNi_5$ on the high pressure side. A three or four-way valve is used to cycle alternating hydrogen flow back and forth between the reactors. A schematic of this system is shown in Figs. 32 and 33.

Background Information

Work is being done under a DOE grant at the University of New Mexico on a compressor driven metal hydride heat pump. They have built and tested a laboratory prototype.

Secondary System Requirements

A secondary heat transfer loop would be required for safety reasons to avoid circulating pure hydrogen gas through a heat exchanger inside the occupied space.

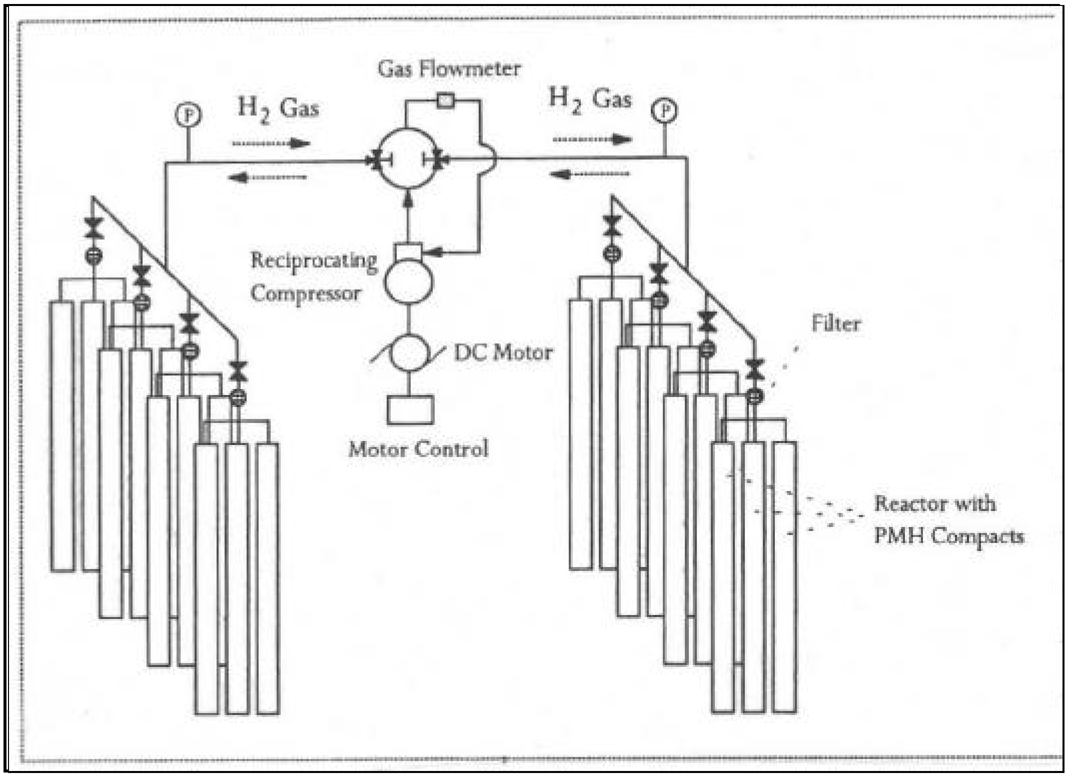

Fig. 33. Schematic of the experimental test stand for the prototype compressor driven metal hydride heat pump (source: Kim 1997).

Efficiency Data

Feldman et al. (1996) provide formulas for computing the theoretical COP for a metal hydride heat pump from the hot and cold heat exchanger absolute temperatures. They specify the useful cooling as:

$$q = -\Delta H - q \tag{8}$$

where q_{loss} is the energy required to cool the container and metal hydride to the cold heat exchanger temperature. The effective cooling can be rewritten as:

$$q = -\Delta H - \bar{m}\left(C + \frac{C`}{R}\right)(T - T) \tag{9}$$

$$q_c = 30 - 15.8 \cdot (0.1 + 0.1/2) \cdot (T_h - T_c) \qquad (10)$$

The ideal work of compression (cal/mole hydrogen) is given by:

$$W_{comp} = R \cdot T_c \left[e^{\frac{k-1}{k} \cdot \frac{\Delta H}{R} \cdot \left(\frac{1}{T_h} - \frac{1}{T_c} \right)} - 1 \right] \cdot \frac{k}{k-1} \qquad (11)$$

where k is C_p/C_v ; k=1.4 for hydrogen. Equations 9 and 11 are used to compute the COPs for a heat pump using $LaNi_5$ at the conditions listed in Table 10; the results are in Table 21. These results are based on a 70% compressor efficiency and cycling Cd factors of 0.25; the current laboratory test unit uses a secondary heat transfer loop so these results include 100 W of pumping power for the secondary loop (short brine loop with fluid pumped through tightly packed $LaNi_5$ heat exchanger bed).

Table 21. Calculated and Observed Efficiencies for Compressor-Driven Metal Hydride Heat Pumps.

	Heating			Cooling		
Cycle Efficiency	47°F	17°F	Seasonal (Btu/Wh)	82°F	95°F	Seasonal (Btu/Wh)
Cycle COP theoretical observed	3.64	1.65		5.16	3.85	
System COP theoretical observed	2.75	1.44	6.0	3.54	2.87	10.5

notes: blank entries denote absence of calculated or measured information, calculated and observed cycle efficiencies do not apply for the shaded seasonal boxes

Technical Advantages/Benefits

Working fluid without GWP or ODP.

Technical Disadvantages

Costs of the metal hydride and use of an explosive or highly flammable refrigerant are possible disadvantages.

Technical Barriers

Work needs to be done on effective heat and mass transfer in the metal hydride beds and efficient compressors need to be developed for use with hydrogen.

Economic Analysis

The economic analysis was performed assuming a secondary loop pumping power of 100 W/ton and an annual maintenance cost of $110. The installed cost of equipment for compressor driven metal hydride heat pumps would need to be at least $825 per ton below that of the electric heat pump baseline, or roughly half the installed cost, for this system to have the same life cycle cost as the electric baseline. The most competitive regions are the Southeast, South Central, and Southwest.

There are no apparent cost savings in this technology (since it employs a hermetic compressor) and cost increases associated with the hydriding material ($LaNi_5$), heat exchangers and pump for the secondary loop, and safety provisions necessary for using hydrogen as a refrigerant.

Contacts and Sources of Information

Kim, K. et al. 1997, *"Compressor-Driven Adsorption Heat Pump Development Employing Porous Metal Hydride Compacts,"* submitted for 1998 ASHRAE Absorption Symposium.

Kwang J. Kim, Ph.D.
Research Assistant Professor
Artificial Muscles Research Institute & Mechanical Engineering Department
University of New Mexico
Albuquerque, New Mexico 87131
Tel/Fax: (505) 277-1335
E-mail: kwangkim@slider.unm.edu

Obvious Holes in Knowledge, Understanding, Information

Cycle performance data at 82E, 47E, and 17EF.
Effects of air cooled heat exchangers.

ELECTRO-CHEMICAL HEAT PUMP

Basic Concept Description

The electro-chemical heat pump uses a conventional reverse Rankine cycle with an electro-chemical pump in place of the motor driven compressor. In the two systems proposed for cooling applications, hydrogen is ionized in either water or ammonia forming a “solvated” positive ion. An electrical field will then cause the ions to move through a semipermeable membrane, against a pressure gradient, from a positive electrode to a negative electrode. The two components are returned to neutral states at the positive electrode, the liquid and vapor are separated at high pressure, and the vapor is condensed and evaporated to provide heating and cooling.

Background Information

Electro-chemical pumps are based on the electrophoresis effect. This principle was first applied by the Swedish scientist Arne Tiselius in 1930 to separate molecules that differed in sizes. Since then various applications have been successfully developed with the majority of the work being in analytical chemistry and chemical technology. Most projects currently proposed are to develop electro-chemical pumps for use as artificial hearts; they are able to pump blood without the damage to red blood corpuscles caused by mechanical pumps. Several proposals to use electro-chemical pumps for refrigeration applications were made in the 1960s; only one company appears to have a current interest in the field.

Several special chemical and physical processes occur in the operation of an electro-chemical pump which do not have analogies for existing gas and liquid compression. For a system using hydrogen as the refrigerant and water as the solvent, the thermophysical properties of the solvated ion, $(2H+8H_2O)^+$ differ from those of the initial neutral substances of hydrogen and water. The equivalent “molecular weight” is 148, which is several times that of the mixture of neutral hydrogen and water. Also, the fluid of charged particles will be much less compressible than the neutral mixture because of the repulsive forces between like charges.

The COP for an electro-chemical heat pump can be derived from basic thermodynamics. The first and second laws state that:

$$T\,dS = dU + dL \qquad (12)$$

where T is the temperature of the process, S is the entropy, U is the internal energy, and L is the work. For an adiabatic process, dS=0, so:

$$\begin{gathered} -dL = dU \quad \text{and} \quad -(L_d + L_c + L_r) = U \\ \text{or} \\ L_d = U + -L_c + L_r \end{gathered} \qquad (13)$$

where L_{el} is the work of the electrical current driving the electro-chemical compressor, L_c is the work consumed to compress the working fluid, and L_r is the work consumed to overcome the internal electrical resistance of the compressor. Equation 13 can be expanded as:

$$-\varepsilon \cdot Z = C_v\left(T_1 - T_2\right) + \zeta \cdot R \cdot \frac{T_1 + T_2}{2A} \cdot \ln\left(\frac{p_1}{p_2}\right) + \rho \cdot I \tag{14}$$

where A, C_v and ζ are the molecular weight, constant volume specific heat and compressibility factor of the solvated ions, R is the universal gas constant (per mole), ρ is the electrical resistance of the membrane, I is the current flow, and the temperatures and pressures are T and p. The applied voltage is ε and Z is the total charge moving through the membrane. A little manipulation yields:

$$\dot{Q} = G \cdot C_v\left(T_1 - T_2\right) + \zeta \cdot R \cdot G \cdot \frac{T_1 + T_2}{2A} \cdot \ln\left(\frac{p_1}{p_2}\right) + \rho \cdot I \quad \text{and} \quad \dot{Q} = G \cdot r \tag{15}$$

with G being the flow rate of the working fluid (mole/sec) and r the heat of vaporization of the mixture (J/gmole). Thus the COP for an electro-chemical pump is:

$$COP = \frac{r}{C_v \cdot (T_1 - T_2) + \zeta \cdot R \cdot \left(\frac{T_1 + T_2}{2A}\right) \cdot \ln\left(\frac{p_1}{p_2}\right) + k \cdot \sigma \cdot I} \tag{16}$$

where $\rho = k\sigma$, k is the membrane resistance coefficient (ohm/cm^2), and $\sigma = \mathsf{A}/G$ is the specific transparency of the membrane (cm^2/mole, A is the membrane area, cm^2). Equation 16 gives the efficiency in terms of the operating temperatures and pressures, four mixture properties (r, Cv, ζ, and A), two membrane properties (k and σ), and the current (I).

Secondary System Requirements

None.

Efficiency Data

The only known efficiency data for an electro-chemical heat pump are for a system using hydrogen with ammonia as the refrigerant and solvent. Analytical Power Corporation provided measured and calculated efficiencies in a short technical memo. They cited a cooling capacity of 500 W with 413 W of electrical input for a COP of 1.21 at pressures of 2.1 and 19 atm and temperatures of 0°F, 85°F, and 110°F at the compressor inlet, condenser (average), and compressor outlet and a membrane resistance coefficient, k, of 0.2 ohms/cm^2 (best available). This is approximately 22% of Carnot efficiency. Calculated COPs of 0.68 and 1.92 were also reported for membrane resistance coefficients of 0.4 (commercially available) and 0.05 (not available), respectively (13% and 35% of Carnot), at the operating conditions previously mentioned.

ORNL has not been able to perform independent calculations of COP for this cycle because of the strong dependence on the unknown properties of the solvated ions. The memo from Analytic Power Corporation tabulates COPs for a matrix of cell, condenser, and evaporator exit temperatures, membrane resistivities, current densities, and membrane areas (see Table 22). Unfortunately Analytic Power did not provide the fluid or membrane properties needed to compute COPs using Eq. 16 so ORNL was unable to derive corresponding efficiencies at different conditions. Efforts to estimate these parameters using the data in Table 22 were not successful. Generally, the efficiencies from ACP are small fractions of the Carnot COP, as shown in the last column of Table 22, reaching 36% for membranes with resistivities that are significantly better than the best available membranes (α=0.05 vs α=0.20) and 33% for very low current densities (which would require multiple units to achieve the same capacity as the higher current densities, hence higher costs); the theoretical COPs for compression systems at the operating conditions used in this analysis are above 50% of Carnot efficiency. A membrane resistance of approximately 0.01 ohms/cm^2 would be necessary to reach COPs comparable to conventional compression systems (personal communication, Solomon Labinov).

Technical Advantages/Benefits

There are a number of advantages that support the development of electro-chemical pumps for some applications:

- there are no moveable parts or mechanical systems to transfer energy,
- silent operation,
- simple control of the flow rate and operating pressures of the working fluid, and
- the ability to mixtures of liquids and gases as well as single-phase working fluids.

Technical Disadvantages

The major disadvantage of electro-chemical heat pumps appears to be their low efficiencies. There could be additional losses associated with mixtures of gases (i.e. water vapor/hydrogen and hydrogen/ammonia) in the heat exchangers further reducing capacity and efficiency.

Technical Barriers

Knowledge of the properties of the solvated ions for hydrogen in water or hydrogen in ammonia needed to calculate COPs at the rating points..

Table 22. Theoretical Efficiency of Electro-Chemical Heat Pumps (Analytic Power Corporation).

Test Case	Temperatures (EF)			Resistivity (ohm/cm^2)	Current Density ($amps/ft^2$)	Membrane Area (in^2)	Efficiency	
	Cell	Condenser Exit	Evaporator Exit				COP	% Carnot
1.	110	85	0	0.20	500	9.35	1.21	22%
2.	100	85	0	0.20	500	11.86	1.00	18%
3.	90	85	0	0.20	500	43.06	0.29	5%
4.	100	95	0	0.20	500	13.23	0.85	18%
5.	100	75	0	0.20	500	7.85	1.44	24%
6.	100	85	40	0.20	500	7.88	1.85	17%
7.	100	85	-40	0.20	500	11.62	0.79	24%
8.	100	85	0	0.40	500	12.44	0.68	13%
9.	100	85	0	0.05	500	7.88	1.92	35%
10.	100	85	0	0.20	500	15.12	0.87	16%
11.	100	85	0	0.20	500	35.51	0.44	8%
12.	100	85	0	0.20	1000	6.73	0.59	11%
13.	100	85	0	0.20	250	16.21	1.76	33%

Economic Analysis

The economic analysis has not been performed for electro-chemical Rankine cycle heat pumps because of the absence of reported or modeled efficiency data.

Contacts and Sources of Information

Analytic Power Corporation
P.O. Box 1189
Boston, MA 02117
(617) 542-6352

Obvious Holes in Knowledge, Understanding, Information

Calculated COPs at the ARI rating conditions.

GAS FURNACE / ELECTRIC AIR CONDITIONER

Basic Concept Description

The baseline technology for unitary residential and commercial gas-fired equipment is a high efficiency, non-condensing gas furnace (AFUE 0.80) and an SEER-12 electric reverse Rankine cycle air conditioner. Both products are commercially available and established technologies. The baseline applied commercial system is a gas boiler and centrifugal chiller.

Background Information

This is a conventional gas furnace and electric air conditioner; albeit not the least efficient on the market, but not the most efficient either. The installed cost of the baseline system is approximately the same as that of the baseline electric heat pump (E-Source); see page 10.

Secondary System Requirements

None are required.

Efficiency Data

The theoretical heating energy consumption is based on 80% combustion efficiency and a blower power of 420 W (140 W/ton design cooling load); the air conditioner requires an additional 210 W (70 W/ton) for the outdoor fan. The theoretical (calculated) compressor only air-conditioner COPs are 5.59 and 4.37 at 82E and 95EF respectively with steady-state system (including blower and fan power at 210 W/ton) COPs of 4.19 and 3.47 at 82E and 95EF with a calculated SEER of 12.4. This is slightly higher than the rated SEER 12.

Technical Advantages/Benefits

High efficiency systems with established base of sales and service organizations.

Technical Disadvantages

Possible regulation of fluorocarbon refrigerants.

Technical Barriers

None

Contacts and Sources of Information

Product Literature

Obvious Holes in Knowledge, Understanding, Information

None

ENGINE-DRIVEN COMPRESSION HEAT PUMPS

Basic Concept Description

The refrigeration circuit of the engine-driven heat pumps is similar to that discussed elsewhere for electric driven systems with the addition of engine waste heat recovery to augment the system heating capacity. Multiple engine types are grouped together in this section of the report rather than repeating much of the discussion separately for Otto, Diesel, Stirling, Brayton, and Rankine engines.

Background Information

Diesel engine driven heat pumps: Yanmar manufactures and sells a diesel-engine driven heat pump in Japan. The product guide contains a table with capacity and gas input for heating and cooling at two rating points (one heating, one cooling). The products appear to span 7500 - 60,000 kW capacity (2½ to 20 tons cooling @ 95EF). The rated COPs are 1.3 heating and 0.9 cooling. Some products appear to have an additional electrical load while the large capacity systems appear to include generators and may not require external electrical connections.

Otto engine driven heat pumps: papers were located reporting on several different field tests, including the York Triathalon and an R&D project involving Tokyo Gas. The Triathalon is now a commercial product in the U.S. and there is a reasonably sized market for 1½ to 5 ton units in Japan. Miyairi (1989) describes some of the government and utility incentives in marketing engine driven heat pumps Japan.

Efficiency data for IC engine-driven Rankine cycle heat pumps are published in Nowakowski (1992), Nowakowski (1995), Taira (1992), Miyairi (1989), Kazuta (1989), and Kaneko (1992). Kazuta's (1989) paper includes graphs of capacity, COP, and power input as functions of engine speed. He also gives electrical data of 78 W for the 1.3 ton heat pump. Steady-state data are reported for the Triathalon at the 47E and 95EF rating points and also seasonal values from field tests.

Stirling engine driven heat pumps: the free-piston Stirling engine was an attractive power source for a reverse-Rankine cycle heat pump system because of the potential long life/low maintenance of the Stirling engine. DOE funded several contractors to develop and test prototype Stirling engine driven systems. GRI participated in these activities through their funding of Stirling engine development. Stirling engine driven heat pumps did not appear to offer any clear cost advantage to the consumer, they were projected to be too expensive, and there was no strong support or efforts at commercialization by the gas industry.

Aisin Seiki developed a Stirling engine-driven heat pump for the commercial space conditioning market in Japan. Their 20 ton machine had a target cooling COP of 1.09 without exhaust heat recovery and 1.57 with 70% heat recovery. Limited testing showed a cooling COP of 0.91 (apparently at the 95EF condition). Maximum engine efficiency with auxiliaries was approximately 34% (ADL 1987).

Stirling Power Systems (SPS) developed a 10 ton heat pump system with performance targets of 1.1 COP cooling and 1.8 heating. Environmental and reliability testing was conducted in 1987. This project was under development for more than 10 years and was planned for commercialization in the late 1980s. Engine efficiency with auxiliaries was approximately 25% (ADL 1987).

General Electric was under contract to DOE to develop a Stirling engine driven heat pump for residential applications. Two prototype systems were to be built and tested based on an inertial compressor concept. Testing of the Phase I prototype verified the 82-83% combustor efficiency (program goal) with a 76% isentropic efficiency for the free-piston linear compressor (exceeding the goal) with a 3 kW output. The Stirling engine efficiency was only 20 to 26%, below the 30% program goal. The Phase II performance goals were (1) Stirling engine efficiency of 35%, (2) a refrigeration loop COP of 3.5, and (3) overall combustion efficiency of 80%.

Phase II failed to meet its performance goals due to deficiencies in the performance of the free-piston Stirling engine and mismatching of the dynamic characteristics of the engine and compressor (GE 1982). A third phase of the contract examined problems revealed in the Phase II testing; test engine met the output power goals but the engine efficiency was found to be 25% instead of the required 27%, maximum brake efficiency was 21%. Reduction in efficiency from earlier testing was believed to be due to better measurements and data acquisition equipment in the second series of tests rather than poorer engine performance. Analysis showed the gas spring losses were too high resulting in lower efficiency.

Another effort at developing a Stirling engine driven heat pump included the participation of several contractors including MTI, Consolidated Natural Gas, Lennox, and John Deere with funding from DOE and GRI. GRI had primary responsibility for engine development and DOE was primarily responsible for “system” development. The engine / transmission / compressor assembly operated successfully and demonstrated many of the project goals, but it did not achieve the capacity goal of 3.0 tons cooling. GRI terminated their interest in engine development. DOE decided against further hardware development and sponsored a workshop on July 14-15, 1994 in Albany, NY to transfer the technology to the private sector. The workshop was eventually canceled because of lack of interest from manufacturers and the gas industry (BER 1991).

Sunpower developed and tested a magnetic coupling of a free-piston Stirling engine to a 3 ton heat pump module. The engine operated at an estimated 28% efficiency. The system assembly was tested and COPs of 0.42 and 1.0 were measured at 95E and 85EF cooling conditions and 1.36 and 1.08 at 47E and 15EF heating conditions, assuming 90% heat recovery. The major loss in the system was identified as the gas spring in the lower end.

Brayton engine driven heat pumps: a Brayton engine is used to drive a hermetic centrifugal compressor for a conventional Rankine cycle vapor compression heat pump. GRI and DOE/ORNL jointly supported a contract with AirResearch in the early 1980s to develop a 10 ton Brayton/Rankine heat pump for light commercial applications. A Brayton engine was to be used with a centrifugal compressor using R-12 in a subatmospheric system (GRI 1982, p. 1-1). The predicted overall engine efficiency was 27% with cooling COP of 1.0 at 95EF and heating COP of 1.2 to 1.4 at 47EF. Dunham Bush and Lennox Industries were both brought into the project to do marketing surveys. The project outcome is unknown (GRI 1982).

Rankine engine driven heat pumps: No background information was located relative to applying Rankine engines to general purpose space conditioning; one source was located in which a Rankine engine was used for a heat pump application in conjunction with a solar pond.

Secondary System Requirements

A “four pipe” system is required to recover engine waste heat for heating purposes which increases equipment and installation costs.

Engine Efficiency Data

The scope of this project limited the analysis of engine-driven systems to the combination of a single, “representative” engine efficiency with compressor-only COPs. The assumed engine efficiencies are:

! diesel engine: 35%
! IC (Otto) engine: 30%
! Stirling engine: 28%
! Brayton engine: 27%
! Rankine Engine: 24%

A more rigorous analysis would vary engine efficiency with speed and load.

Efficiency Data

Cycle COPs are computed using the state points listed in Table 23 with a compressor-only efficiency of 80%. The condensing temperature in cooling mode is assumed to be 15EF higher than the condensing temperature for the electric heat pump in cooling mode because in at least one commercial design the outdoor air flow is used to cool the engine compartment before it crosses the condenser. This)T was determined to give a COP for an IC engine driven heat pump of 0.90 at 95EF. The calculated cycle COPs are combined with a single fixed engine efficiency for each of the engine types.

The heating COPs include 50% waste heat recovery and a belt and pulley efficiency of 85%; seasonal COPs assume a cycling Cd of 0.10. The theoretical system gCOPs

Table 23. State Point Temperatures for Engine Driven Heat Pump Cycle Calculations

State Point Temperatures	Ambient Temperatures			
	47EF	17EF	82EF	95EF
condensing	100EF	85EF	120EF	135EF
evaporating	29EF	-14EF	49EF	49EF
superheat	18EF	18EF	11EF	11EF
subcooling	16EF	16EF	0EF	0EF

Table 24. Calculated and Observed Efficiencies for Engine-Driven Heat Pumps.

		Heating			Cooling		
Cycle Efficiency	engine efficiency	47EF	17EF	Seasonal gCOP	82EF	95EF	Seasonal gCOP
<u>Compressor COP</u>		5.78	3.98		4.54	3.52	
Diesel engine	35%	2.07	1.53	1.55	1.35	1.05	1.27
IC engine	30%	1.85	1.39	1.43	1.16	0.90	1.09
Stirling engine	28%	1.76	1.33	1.38	1.08	0.84	1.02
Brayton engine	27%	1.71	1.30	1.35	1.04	0.81	0.98
Rankine engine	24%	1.58	1.21	1.27	0.93	0.72	0.87
<u>Measured COP</u>							
Diesel engine							
IC engine				1.44		0.9	
Stirling engine		1.09				0.91	
Brayton engine							
Rankine engine							

notes: blank entries denote absence of calculated or measured information, calculated and observed cycle efficiencies do not apply for the shaded seasonal boxes

are listed in Table 24. Conditions were selected to obtain a cooling COP of 0.9 at 95EF for an IC engine-driven heat pump, but the calculated results at 82EF compare well with data measured by Domitrovic at ORNL. The steady-state COP of the IC engine-driven system at 47EF compares well with the specification of 1.8 for an engine-driven heat pump in Nowakowski (1992), as does the computed seasonal heating efficiency (1.43) and that reported by Nowakowski (1.44) three years later.

The gCOPs in Table 24 *do not* include peripheral energy use for fans or blowers; a combined COP including both gas and electrical input may be cited in some references, but usually without any acknowledgment that this has been done. Aisin Seiki reported Stirling engine-driven heat pump system gCOPs of 1.09 and 1.57 (70% heat recovery) at 47EF and 0.91 at 95EF. SPS report a gCOP of 1.80 at 47EF and 1.10 at 95EF. Sunpower reported heating COPs of 1.36 and 1.08 at 47EF and 15EF with 90% heat recovery and cooling gCOPs of 1.0 at 85EF and 0.42 at 95EF.

Technical Advantages/Benefits

Each of the engine-driven heat pumps has the advantages of (1) low energy costs for natural gas, (2) low CO_2 emissions from fuel combustion, and (3) high heating efficiencies attainable using waste heat recovery. The Stirling, Brayton, and Rankine engine-driven heat pumps also should have long engine life and low maintenance because of the low number of moving parts. Emissions for these engines should be lower than with an internal combustion and diesel engines.

Technical Disadvantages

The principal technical obstacle of engine-driven systems is the engine lifetime and the annual maintenance costs. Annual and lifetime operating hours are an order of magnitude higher than the operating hours for a motor vehicle engine. Long life, low maintenance engines are required for any of these technologies to be successful. The low efficiency of the Rankine engines makes them a poor choice for gas-fired systems, though they may be applicable to solar or waste heat driven systems.

First cost is the major non-technical disadvantage for engine-driven systems. A relatively high efficiency, low cost electric motor is being replaced by an internal or external combustion engine and more sophisticated controls.

Arthur D. Little (ADL) reviewed the recent experience in free-piston Stirling engine driven heat pumps to identify key technical and cost issues which should be the focus of future program efforts. ADL concluded that several key requirements for a successful HVAC system have been demonstrated (GE and MTI) including engine efficiencies approaching 30%.

Significant progress had also been made recently (1984, 1985) in demonstrating good life potential as a result of endurance testing for space power systems. Integrated free-piston Stirling engine heat pump systems have not demonstrated some of the essential requirements for a commercially viable product including high season performance factor, long life, and low maintenance. Outstanding issues that need to be resolved include:

- a reliable low cost means of coupling the free piston Stirling engine to a heat pump cycle,
- analytical models that can provide a reasonable level of accuracy for projecting the performance of current and future system configurations,
- accurate assessments of loss mechanisms associated with bearings, gas springs, gas flow through heat exchangers, and identification of design options for minimizing such losses, and
- development of seals, bearings, combustors, etc. which meet the stringent requirements of a gas fired heat pump system.

Furthermore, the potential for mechanical simplicity that could lead to long life has not been fully demonstrated in current (1984) designs (ADL 1986).

Several conclusions have been reached in analyses of Stirling engine driven heat pumps:

> “The kinematic Stirling engine should not be used in residential application because the small 5 hp (3.73 kW) engine model has relatively low efficiency; however, the 17 hp (12.7 kW) unit in commercial application is competitive with the alternative engine types.” (Fischer 1987).
>
> “Good performance potential of the free-piston unit [in residential application] (as indicated by reasonably good weighted engine and compressor efficiencies) may not result in attractive savings because of the high transmission loss (roughly 15%) and parasitic electrical power consumption of 300 W (in residential size) not needed in

other units." (Fischer 1987). The "other units" probably refers to the Otto and Wankel engine driven heat pumps and the conventional electric heat pump.

Technical Barriers

IC engine-driven heat pumps (Otto and Diesel) are commercially available products, so "barriers" may better be understood as impediments to increasing market share -- cost, inertia, etc. These products have been more successful in Japan than in North America and it may be informative to examine the underlying reasons for that.

There are several technical problems that would need to be resolved before Stirling engine driven heat pumps can be commercialized. These include matching the dynamic characteristics of the engine and compressor in a free-piston duplex Stirling configuration, the transmission efficiency for either a kinematic or free-piston configuration, and the gas spring in the lower end. These problems notwithstanding, Stirling engine-driven heat pumps would be very expensive. The inherent low efficiencies of the Brayton and Rankine engines are barriers to their development for this application.

Economic Analysis

Figure 34 shows the results of the economic calculations IC engine-driven heat pump assuming that the engine-driven system costs $25 per year more to maintain than the gas baseline furnace and air conditioner. The results show that installed costs could be $1000 per ton higher than the baseline system, or more, in the upper Midwest and northeastern states and $500 to $1000 per ton throughout the central regions of the country. Higher maintenance costs, of course, reduce the allowable installed cost premiums. A maintenance cost differential of $100 per year (instead of $25) reduces the installed cost premiums by $490 to $690 greatly restricting the regions of the country where engine-driven heat pumps compare favorably with traditional gas furnaces.

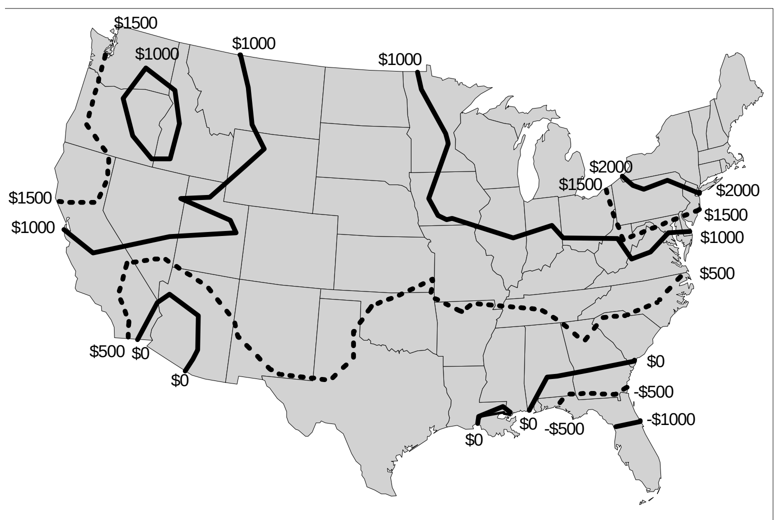

Fig. 34. Allowable installed cost premiums for IC engine-driven heat pumps.

Table 25 shows that three or five year paybacks can be achieved (with a $25/y higher maintenance costs) outside of the high cooling states with installed costs $200 to $500 per ton higher than a gas furnace and electric air conditioner. The costs could be as much as $700 per ton higher in the northeast and still achieve a five year payback.

The engine driven systems compare poorly against the *baseline electric heat pump* in Florida, southern Alabama, and extreme southeast Louisiana, but favorably in the southwest, south central states, Pacific Northwest and California where electric heat pumps may be used.

Tble 25. Installed Cost Premiums for an IC Engine-Driven Heat Pump for 3 and 5 Year Paybacks.

Region	3 Year Payback ($/ton)	5 Year Payback ($/ton)
Northeast	$440	$700
Midwest	$250	$400
Northern Plains	$170	$270
Rocky Mountain	$200	$330
Pacific Northwest	$350	$490
California	$210	$330

The hardware for an engine driven heat pump adds the relatively large cost of the engine, water pump, and installation of heat recovery loop while saving the relatively low cost of an electric motor. Maintenance costs are a significant factor and they are certainly going to be higher than they are for either baseline system.

While the economic analysis is only reported for IC engine driven heat pumps, it is clear that the results are somewhat more favorable for diesel engine driven systems because of the assumed higher engine efficiency and slightly less favorable for Stirling engine driven systems because of the slightly lower efficiency (absent a lower maintenance cost). A more rigorous analysis is necessary that incorporates differences in maintenance costs to obtain a definitive comparison of these three engine-driven heat pumps.

Contacts and Sources of Information

ADL 1986, "Status of Free Piston Stirling Engine Driven Heat Pumps - Development, Issues, and Options Final Report," ORNL/Sub/84-00205/1, Arthur D. Little, April 1986.

ADL 1987, "Technology Status of Components for Gas-Fired Cooling Systems," Arthur D. Little for GRI, April 1987, pp. 2-43 to 2-46.

Colosimo, D., 1987, *Introduction to Engine-Driven Heat Pumps - Concepts, Approach, and Economics,* ASHRAE Transactions, Volume 93, Part 2, pp. 987-996.

D'Aponte, F. et al., 1996, *Test Application of a Small Size Gas Engine Driven Heat Pump,* Proceedings of the 5th International Energy Agency Conference on Heat Pumping Technologies, Volume II, pp. 85-93.

E Source 1995, “Product Profile: The York Triathalon *Natural Gas-Fired, Engine-Driven Heat Pump,”* November 1995.

Fischer, R.D. et al, 1987. “*Engine-Driven Heat Pump Performance Analysis*,” ASHRAE Transactions, Vol. 93, pt 2, pp. 1046-1077.

Freedman, S., et al., 1992, *Unitary Gas Heat Pump Development Status in the USA*, IEA Heat Pump Centre Newsletter, Vol. 10, No. 4, pp. 4-8.

Fukuda, T. 1987, *Development of Gas-Engine Heat Pumps in Japan*, Proceedings of the 1987 International Energy Agency Heat Pump Conference: Prospects in Heat Pump Technology and Marketing, pp. 389-402, Lewis Publishers.

GE 1982, “Development and Demonstration of a Stirling/Rankine Heat Activated Heat Pump: Final Report Phase IIIB - Engine Technology Development Testing,” ORNL/Sub/82-17485/1, General Electric Co.

GRI 1982, *Phase II Brayton/Rankine 10-Ton Gas-Fired Space Conditioning System*, ORNL/Sub-80/24706/1, July 1982.

GRI, 1987, *“Technology Status of Components for Gas-Fired Cooling Systems,”* GRI-87/0023, pp. 2.70-2.81.

Kaneko, T., et al., 1992, *The Performance of a Four-Ton Gas-Engine-Driven Heat Pump*, ASHRAE Transactions, Volume 98, Part 1, pp., 989-993.

Kazuta, H., 1989, *“Development of Small Gas Engine Heat Pump,”* ASHRAE Transactions, Volume 95, Pt. 1, pp. 982-990.

Leslie, N. et al., 1991, *Gas Engine-Driven Air-Conditioner Performance in an Unoccupied Research House,* ASHRAE Transactions, Volume 97, Part 2, pp. 1054-1061.

Miyairi, T., 1989, “*Introduction to Small Gas Engine-Driven Heat Pumps in Japan - History and Marketing,”* ASHRAE Transactions Vol. 95, Pt. 1, pp. 975-981.

MTI 1986a, “Free-Piston Stirling Engine Diaphragm-Coupled Heat-Actuated Heat Pump Technology Program: Volume I Phase IIA and IIB Final Report: Technical Discussion,” ORNL/Sub/86-47985/2&V1.

MTI 1986b, “Free-Piston Stirling Engine Diaphragm-Coupled Heat-Actuated Heat Pump Technology Program: Volume II Phase IIA and IIB Final Report: Technical Discussion,” ORNL/Sub/86-47985/2&V2.

MTI 1986c, “Free-Piston Stirling Engine Diaphragm-Coupled Heat-Actuated Heat Pump Technology Program: Phase 1C Final Report” R. A. Ackerman, Mechanical Technology Inc.

MTI 1986d, “Free-Piston Stirling Engine Diaphragm-Coupled Heat-Actuated Heat Pump Technology Program: Phase 1B Final Report” R. A. Ackerman.

MTIe 1986, “Free-Piston Stirling Engine Diaphragm-Coupled Heat-Actuated Heat Pump Technology Program: Phase 1/1A Final Report” Mechanical Technology Inc.

Nowakowski, G. 1996, *An Introduction and Status Update on Unitary Engine-Driven Heat Pumps,* ASHRAE Journal, December, pp. 42-47.

Nowakowski, G., et al., 1992, *Development and Field Testing of a High-Efficiency Engine-Driven Gas Heat Pump for Light Commercial Applications,* ASHRAE Transactions, Volume 98, Part 1, pp. 994-1000.

Nowakowski, G., et al., 1995, *Field Performance of a 3-Ton Natural Gas Engine-Driven Heating and Cooling System*, ASHRAE Transactions, Volume 101, Part 2, pp. 1382-1388.

ORNL 1991, ORNL BER Program Monthly Progress Report, March 1991

Rusk, R. P., et al. 1990, *“Development and Use of a Mathematical Model of an Engine-Driven Heat Pump,”* ASHRAE Transactions, Vol. 96, Pt. 2, pp. 282-290.

Shelton, S., 1987, *Natural gas I.C. Engine-Driven Heat Pumps*, ASHRAE Transactions, Volume 93, Part 2, pp. 1034-1045.

Struck, W., et al. 1987, *Gas-Engine-Driven Heat Pumps - Design, Components, Experience, Layout, and Economic Feasibility*, Proceedings of the 1987 International Energy Agency Heat Pump Conference: Prospects in Heat Pump Technology and Marketing, pp. 403-414, Lewis Publishers.

Taira, K., 1992, *Development of a 2.5 RT Multiple-Indoor-Unit Gas Engine Heat Pump,* ASHRAE Transactions, Volume 98, Part 1, pp. 982-988.

The Triatholon System from York, http://www.york.com/newtri.html

Wurm, J., et al., 1987, *History and Status of Engine-Driven Heat Pump Developments in the U.S.*, ASHRAE Transactions, Volume 93, Part 2, pp. 997-1005.

Yamaha Motor Corporation
P.O. Box 6555 / 6555 Katella Avenue
Cypress, CA 90630

Yanmar Diesel Engine Co., Ltd.

Yokoyama, T., 1992, *Design Considerations for Gas-Engine Heat Pumps*, ASHRAE Transactions, Volume 98, Part 1, pp. 975-981.

Obvious Holes in Knowledge, Understanding, Information

Calculated COPs should be corroborated using detailed performance data on the York and Yanmar IC and diesel engine driven heat pumps. Cost analysis should be compared with economic evaluations from DOE projects on Stirling and Brayton engine driven heat pumps.

FUEL CELL POWERED RANKINE CYCLE

Basic Concept Description

A fuel cell could be used to convert natural gas to electricity (60 hz, A/C) to power a conventional Rankine cycle heat pump. The fuel cell itself consists of four major components: (1) a fuel processor ore reformer (which converts the fuel, natural gas or naphtha, into a hydrogen rich gas mixture), (2) a stack (which produces direct current electricity), (3) an inverter for converting DC to AC power, and (4) a heat recovery system, which removes surplus heat from the fuel cell stack and fuel processor for use in space conditioning and water heating. The fuel cell transforms the fuel directly to electricity without combustion. Electricity from a fuel cell can be used to power a conventional electrically driven heat pump with waste heat providing supplemental heating.

Background Information

The fuel-cell principle has been known for more than 150 years since it was described by Sir W. R. Grove in 1839. Some sporadic research was done during the 30s, but it was not until the 1950s that significant amounts of money were put into fuel-cell research. The first application of fuel cells was during the Gemini and Apollo space missions in the U.S. The principal components of a fuel cell are catalytically activated electrodes for the fuel (anode) and the oxidant (cathode) and an electrolyte to conduct ions between the two electrodes. The fuel is hydrogen, or a reformed hydrogen-rich hydrocarbon such as methanol or natural gas, and the oxidant is derived from air (i.e., oxygen). In a phosphoric acid or polymer electrolyte fuel cell, hydrogen is fed to the anode and then "split" into protons and electrons. The protons are transmitted through the electrolyte to the cathode where they combine with oxygen to form water. The remaining electrons, which cannot be transported by the electrolyte, then move through an electrical conductor.

There is a great deal of research and development underway on fuel cells. There are five different basic types of fuel cells which have fundamental differences in their design and operation:

! alkaline fuel cells,
! molten carbonate fuel cells (MCFC),
! solid oxide fuel cells (SOFC),
! phosphoric acid fuel cells (PAFC), and
! proton exchange membrane (PEM) fuel cells

Some of their properties are summarized in Table 26. Alkaline fuel cells are used on the space shuttle and have a relatively long history of development. They can have efficiencies as high as 70% but are not seeing much development for commercial applications becuase of their high costs. Both molten carbonate and solid oxide fuel cells attractive for large capacity applications because they have high conversion efficiencies (>60%). Their operating temperature are high (above 1200EF, 650EC) which may create disadvantages (e.g. response to startup and load changes, costs) that may make them inappropriate for building applications. The greatest amounts of fuel cell development activity are in phosphoric acid and proton exchange membrane fuel cells. Each of these technologies has conversion efficiencies from 40 to 50%, they each use platinum as a catalyst, and require an external reformer for preparing the fuel. Both the platinum and external reformer raise issues associated with high costs. PAFCs are commercially available in capacities above 100 kW, but prices are around $4000 per kW and have not changed significantly for several years. This is significantly higher than other electric generating technologies (e.g. engine-driven generators, microturbine generators). Operating temperatures for PAFCs are around 390EF which might make them very attractive for building applications where waste heat can be recovered and used. Many development activities for PAFCs center around reducing the cost by reducing the amount of platinum required for a given capacity. Much of the recent development of PEM fuel cells has been for use in automobiles and buses. This work has been primarily in the areas of permeable membranes and reduced platinum requirements. Operating temperatures are around 170EF, which may be too low to provide useful waste heat recovery.

Table 26. Fuel Cell Technologies (Lloyd 1999)

Fuel Cell Technology	Conversio n Efficiency	Operating Temperature	Status of Development
Proton Exchange Membrane (PEM)	40-50%	175EF (80EC)	demonstration systems up to 50 kW
Phosphoric Acid (PAFC)	40-50%	around 390EF (200EC)	commercial systems 100 kW and up; most in use are 200 kW
Molten Carbonate (MCFC)	> 60%	1200EF (650EC)	demonstration systems up to 2 MW
Solid Oxide (SOFC)	> 60%	1475-1800EF (800-1000EC)	demonstration units up to 100 kW

Secondary System Requirements

A waste heat recovery system is required.

Efficiency Data

COPs for a fuel cell powered heat pump are computed in the same manner as those for engine driven heat pumps using a conversion efficiency of 40% and a combined compressor and motor efficiency of 75%, the state point temperatures listed in Table 3 on page 8, and cycle COPs in Table 4. The results are listed in Table 27.

Table 27. Calculated and Observed Efficiencies for Fuel Cell Powered Heat Pumps.

Cycle Efficiency	conversion efficiency	Heating			Cooling		
		47EF	17EF	Seasonal gCOP	82EF	95EF	Seasonal gCOP
Compressor Only COP	40%	4.98	3.08		5.30	3.98	
theoretical gCOP observed		2.02	1.38	1.5	1.75	1.35	1.7

notes: theoretical gCOPs include gas consumption required to produce electricity for 140 W/ton fan power and 70 W/ton blower power.

Technical Advantages/Benefits

Fuel cell powered heat pumps have the advantages of high conversion efficiency of gas to electricity and the capability to supplement low ambient heating capacity with waste heat from the fuel cell. Fuel cell could be sized to provide electricity to power more than just the heat pump.

Technical Disadvantages

It is not clear whether fuel cells can be scaled down, economically or not, to the capacity required for single-residence space conditioning applications. The costs of certain components, such as the signal conditioning equipment, probably will not scale with the capacity. The fuel cell "package" includes both power conversion and also signal conditioning equipment to provide AC current at 60 Hz and 240 V; the signal conditioning adds a degree of electronic complexity that is not a factor in conventional single-speed electric heat pumps. The electronics package could also be vulnerable to lightning strikes and power surges if the fuel cell is not electrically isolated from the power grid.

Technical Barriers

Application of this technology is limited by the development of long lived, affordable fuel cells in relatively low capacities. Cost reductions associated with catalyists (reduced platinum requirement) and permeable membranes are necessary.

Economic Analysis

Results for a fuel cell powered electric heat pump are shown in Fig. 35 assuming an annual maintenance cost $100 higher than that for the baseline system. Installed cost premiums can be $500 to $1000 per ton outside the southern tier of states. Installed cost premiums higher than $1000 per ton are justified in the northeast under these assumptions. Average regional installed cost premiums are listed in Table 28 for three-year and five-year paybacks and for equal life cycle costs.

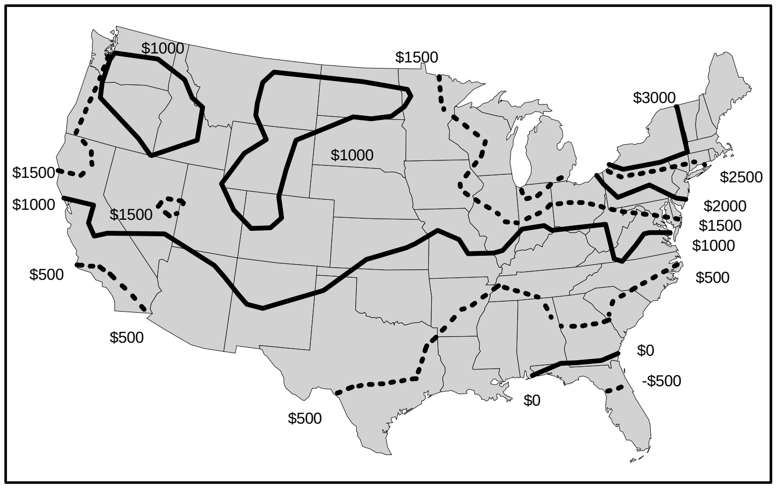

Fig. 35. Allowable installed cost premium for fuel cell powered heat pumps relative to the gas furnace baseline.

There is a great deal of uncertainty surrounding the installed cost, annual maintenance costs, and the functional lifetime of “small” fuel cells, all of which have strong impacts on the system economics. This is shown graphically in Fig. 36 where there are eight curves showing the allowable installed cost premium for a fuel cell powered heat pump compared to the gas furnace / electric air conditioner baseline. The horizontal axis in Fig. 36 is the difference in annual maintenance costs (or non-energy operating costs if the fuel cell is replaced during the lifetime of the heat pump) between the fuel cell powered system and the gas baseline.

Table 28. Installed Cost Premiums for a Fuel Cell Powered Electric Heat Pump Relative to the Gas Baseline.

Region	Installed Cost Premium ($/ton)		
	3 Year Payback	5 Year Payback	Equal Life Cycle Cost
Northeast	$627	$988	$2,646
Southeast	$147	$224	$478
South Central	$191	$296	$709
Southwest	$209	$341	$902
Midwest	$359	$566	$1,495
Northern Plains	$256	$402	$1,028
Rocky Mountain	$259	$404	$1,025
Pacific Northwest	$309	$438	$1,103
California	$248	$387	$982

Consider an example to illustrate the significance of these unknowns. Suppose that the difference in maintenance costs between the fuel cell powered and gas furnace baseline is $100 per year. Then Fig. 36 shows that installed costs could be $750 to $2500 per ton higher in the northeast, Pacific Northwest, Midwest, and California and the two systems would have the same life cycle costs. Collectively, those regions represent a reasonably large market. Those cost premiums are also in line with the fuel cell development cost targets discussed below. If the fuel cell must be completely replaced once during the lifetime of the heat pump (20 years), at the target cost of $1000 /kW ($1200 / ton) there is an additional $3600 in operating costs to be averaged over the lifetime of the heat pump or $180 per year. The total annual non-energy operating costs of the fuel cell system are thus $280 and the installed cost premium is the cost of the initial fuel cell or $1200 per ton. The point corresponding to these estimates falls above the line for the northeast in Fig. 36, consequently the life cycle costs of the fuel cell powered system is always higher than the gas baseline in every part of the country. Substantially longer fuel cell lifetimes and installed costs are necessary for this alternative to be competitive with the gas baseline.

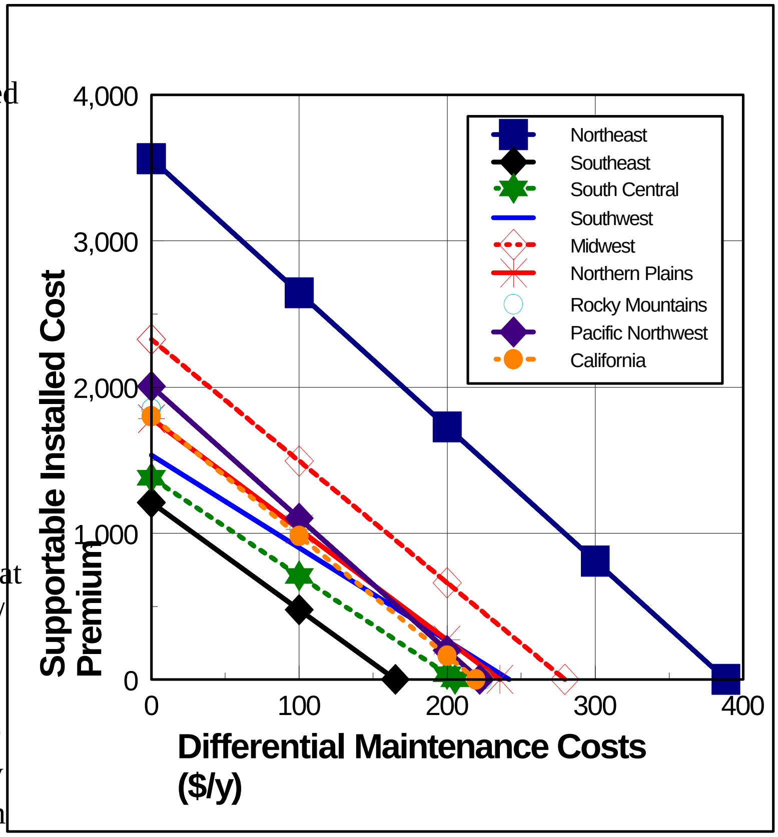

Fig. 36. Allowable installed cost premium and non-energy operating expenses for fuel cell powered heat pumps.

The equipment cost of this alternative technology is essentially that of an electric heat pump plus the cost of the fuel cell, installation costs will be higher than an electric heat pump. A fuel cell powered three ton heat pump would require a peak electrical capacity of approximately 3.6 kW[1] or 1.2 kW per ton of cooling capacity.

The cost and lifetime of the fuel cell are thus critical factors. Fuel cells fall into five different categories: (1) alkaline, (2) phosphoric acid, (3) molten carbonate, (4) solid oxide, and (5) proton exchange membrane fuel cells. Much of the development effort on fuel cells has been for mega-Watt applications for power plants and the costs will not scale with size to the capacities appropriate for single-family or business unitary equipment. Phosphoric acid fuel cells have been built in 12.5 kW capacity, but cost information is not known. In the late 1980s 200 kW PAFCs cost on the average $2000 to $3600/kW; SoCalGas projected that with mass production the costs could fall to $1000/kW (Hadder 1992). Avista Laboratories of Spokane, Washington is developing a 2 kW proton exchange

[1] Carrier 38AY(M)036-30 with FK4BNB005 indoor unit.

membrane fuel cell; costs are not known. *C*ost estimates in the Argonne (ORNL/CON-38) report were supplied by UTC and were probably pretty good at the time. Adjusting the costs simply based on the Consumer Price Index translates the 1979 numbers to $1055 /kW to $1315 /kW for 25 to 250 kW fuel cells (decreasing in price as capacity goes up). (Christian 1978).

Contacts and Sources of Information

ADL, 1994, *"Fuel Cells for Building Applications: Market Analysis, Technology Status, and Program Plan Overview,"* Draft Topical Report prepared for U.S. DOE Building Equipment Division, Office of Building Technologies, Volume II, Rev. 1, September.

Borys, S. And Marianowski, L. 1998. *"Fuel Cells* -- *Where They Are and Where They Are Going,"* Canadian Gas Association Operating and Technical Workshop and Conference, April 24, Institute of Gas Technology.

Hadder, G. 1992, *"Fuel Cells Background Information for Residential and Commercial Applications,"* Draft report prepared for U.S. Department of Energy, Office of Building Technologies, June.

Jacoby, M. 1999, *"Fuel Cells Heading for Sale,"* Chemical and Engineering News, June 14, pp. 31-37.

Lloyd, A. 1999, "*The Power Plant in Your Basement,*" Scientific American, July, pp. 80-86.

Mixon, W., et al, March 1979, "*Market Assessment of Fuel Cell Total Energy Systems, Summary Report"*, ORNL/CON-36.

G. Pine, et al, 1980, "*Development of an Energy Consumption and Cost Data Base for Fuel Cell Total Energy Systems and Conventional Building Energy Systems"*, ORNL/CON-38, July 1980.

Obvious Holes in Knowledge, Understanding, Information

Lifetime and maintenance costs for fuel cells. Pros and cons of alternative fuel cell technologies should be discussed with emphasis on which is most appropriate for stationary building application.

VUILLEUMIER CYCLE HEAT PUMPS

Basic Concept Description

Although the Vuilleumier cycle has been around since 1918, it is not taught in most thermodynamics classes or textbooks. First, the Vuilleumier cycle is by definition a combination of a heat engine and a refrigeration cycle. Two distinct features of the cycle are that it is a *thermocompression* cycle instead of a *mechanical compression* cycle and that the engine and refrigeration cycles share the same working fluid. The basic Vuilleumier machine is shown in Fig. 37. P-V and T-S diagrams are in Figs. 38 and 39. Heat is input at the high temperature heat exchanger to increase the pressure of the working fluid, normally helium. Heat is rejected, to the ambient in a cooling application or to the conditioned space for a heat pump, through the two intermediate heat exchangers. Cooling is performed for an air conditioner at the low temperature heat exchanger. The working fluid is moved between hot and cold volumes in the machine through the use of two displacers operated by a crank mechanism 90E out of phase (mechanical energy is input to rotate the crank and move the displacers). The displacers are operating only against the pressure drops across the heat exchangers and regenerators and friction along the tube walls so there is a low pressure ratio. The low pressure ratio results in a low specific volume for the basic Vuilleumier cycle.

While the basic cycle relies on thermal compression, compounded machines may use mechanical compression. These machines closely resemble duplex Stirling cycles, the primary difference being that the working fluid is shared between the engine and refrigerator segments in the Vuilleumier machine while the working fluid

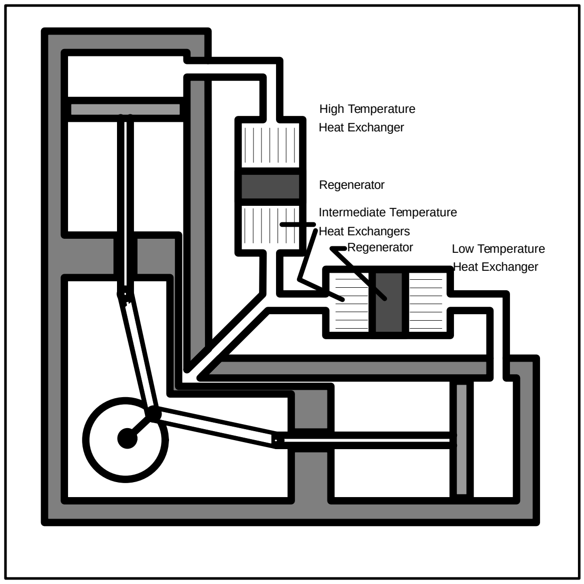

Fig. 37. Basic Vuilleumier cycle machine.

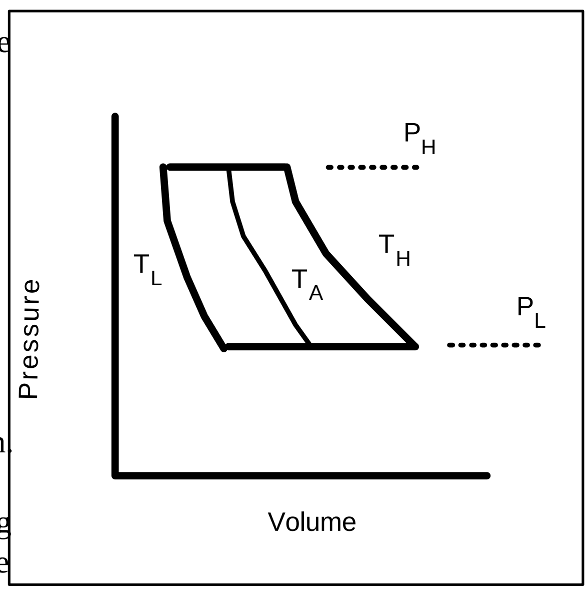

Fig. 38. P-V diagram for a Vuilleumier cycle machine.

in the engine-warm space of the duplex Stirling is separated from the working fluid in the refrigerator-warm space. The Vuilleumier cycle transfers work between components through transfers of the working fluid. The duplex Stirling cycle transfers work from the engine to the refrigerator segments through mechanical means (movement of the piston). A Vuilleumier cycle machine can be configured either as a kinematic or a free-piston machine; the free-piston Vuilleumier system is expected to have lower costs than kinematic version because of the reduction in equipment size and weight (Carlsen, Hannover 1994).

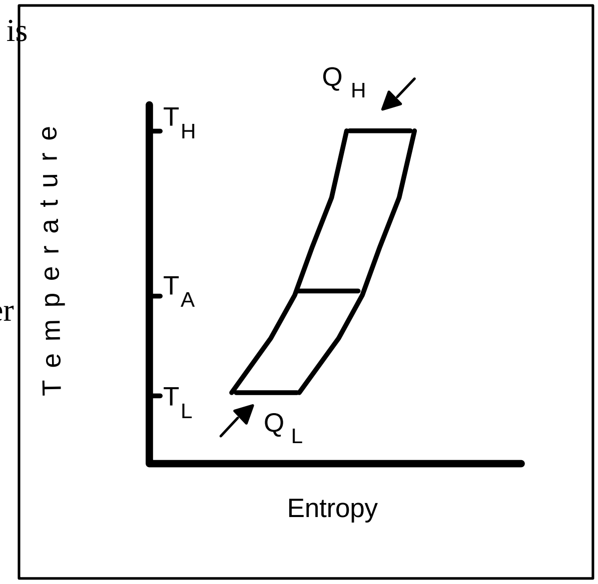

Fig. 39. T-S diagram for a Vuilleumier cycle machine.

Background Information

Carlsen et al. mention the existence of more than 10 prototype Vuilleumier machines, though it isn't clear whether this is worldwide or just represents their own work at the Universities of Denmark and Dortmund. They provide test results for a 20 kW (5.7 ton) kinematic heat pump which was converted to a free-piston prototype.

Development work has also occurred in Japan. Sanyo has worked in cooperation with the Japan Gas Association and four gas utilities to develop a Vuilleumier cycle heat pump for space conditioning applications. Sanyo gives data for measured steady-state COP and capacity at various hot space helium temperatures (as shown in Fig. 40). They also cite performance data for the outdoor unit (though not stated explicitly, this is probably a multiple indoor unit system so that overall performance is defined by the outdoor unit) with a cooling COP of 0.63 and a heating COP of 1.34. These numbers are stated in terms of the helium hot space temperature and not related to an ambient condition.

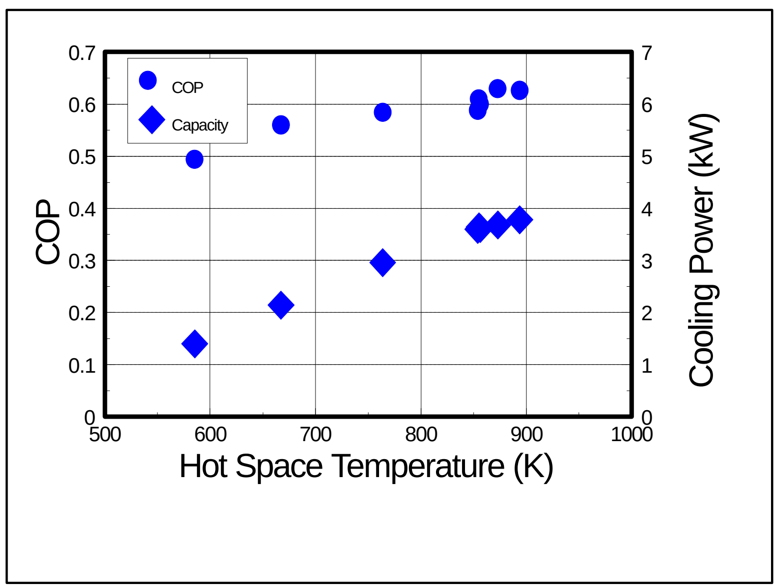

Fig. 40. Measured COPs and capacities for a Vuilleumier cycle heat pump.

Secondary System Requirements

The performance of this cycle is strongly dependent on the dead space volume, so the heat exchangers need to be located very close to the primary mechanical package. A secondary heat transfer loop is needed between the indoor and outdoor units.

Efficiency Data

Table 29. State Point Temperatures for Vuilleumier Cycle Calculations

State Point Temperatures	Ambient Temperatures			
	47EF	17EF	82EF	95EF
hot space	1000EF	1000EF	1000EF	1000EF
cold space	29EF	7EF	49EF	49EF
intermediate space	102EF	72EF	137EF	150EF

The computer model TCVLM.BAS (Wurm 1990) was used to compute steady-state COPs for a thermal-compression Vuilleumier cycle heat pump. Recommended data provided with the program were used for the regenerator efficiencies (95%), mean operating pressure, cycle speed (16.67 Hz), and fin specifications. Heat exchanger temperatures are specified at the values listed in Table 29. Calculated gCOPs are reported in Table 30 using a combustion efficiency of 80%. The cycling coefficient Cd was set at 0.10 to approximate variable speed operation. The resulting heating season gCOP of 1.0 is credible compared with the 1.3 measured in field testing by Sanyo at 47EF; the cooling COP of 0.20 is significantly below the 0.63 at 95EF reported by Sanyo. The difference, particularly in cooling, could be explained if the Sanyo machine is a mechanical-compression device rather than a thermal compression device.

Technical Advantages/Benefits

Gas-fired systems are expected to have lower emissions than internal combustion driven systems and they use a benign operating fluid (helium). There is a potentially high COP despite the disadvantages of Stirling/Vuilleumier as a cooling cycle (Carlsen) and potentially long equipment lifetimes and low maintenance requirements.

Technical Disadvantages

The disadvantage to the cycle is that the ideal efficiency is lower than Carnot cycle because the temperature of the gas in the cylinder volumes differs from the heat exchanger temperatures (Carlsen). There is also a low specific output so that an application requires larger, more expensive, equipment to meet a specified load.

Table 30. Calculated and Observed Efficiencies for Vuilleumier Heat Pumps.

Cycle Efficiency	conversion efficiency	Heating 47EF	Heating 17EF	Heating Seasonal gCOP	Cooling 82EF	Cooling 95EF	Cooling Seasonal gCOP
<u>Cycle COP</u>							
theoretical	80%	1.21	1.23	1.1	0.27	0.24	0.3
observed		1.30				0.63	
scaled observed		1.30	1.32	1.2	0.71	0.63	0.7

notes: blank entries denote absence of calculated or measured information, calculated and observed cycle efficiencies do not apply for the shaded seasonal boxes

Technical Barriers

A major technical problem relates to centering the displacer pistons in free-piston machine and reduced efficiency relative to kinematic version. There is also a low specific output requiring relatively large and expensive equipment

Economic Analysis

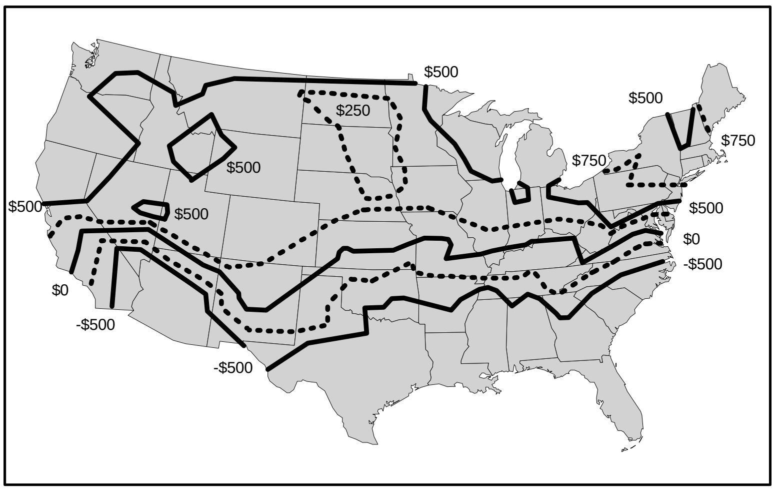

Fig. 41. Allowable installed cost premiums for Vuilleumier cycle heat pumps.

The installed cost premiums in Fig. 41 are calculated using the "scaled observed" efficiencies in Table 30 with electrical use of 320 W/ton for fans, blowers, and the secondary fluid pump and an annual maintenance cost $25 below the baseline gas system (the low pressure differentials across the displacers in the cylinders should result in low maintenance costs). The results are similar to the engine-driven heat pumps, although the economics are not quite as favorable. Installed costs can be from $0 to $500 per ton higher than the gas baseline system outside of the southern tier of states and can be over $500 per ton in the northeast and some regions in the west and $750 per ton in New York.

This cycle eliminates the electric motor and compressor of a conventional electric heat pump or air conditioner saving both equipment and maintenance costs. In their stead, however, is a secondary fluid heat transfer system and possibly a low torque displacer motor. The data in Table 31 show the installed cost premiums for the northern states for three and five year paybacks assuming that the average annual maintenance cost is $25 less than that for the gas furnace and electric air conditioner baseline. These results indicate that the Vuilleumier cycle heat pump should be economically viable (accepting the Sanyo COPs) at installed equipment costs slightly higher than the baseline gas furnace and electric air conditioner combination.

Table 31. Installed Cost Premiums for a Vuilleumier Cycle Heat Pump for 3 and 5 Year Paybacks.

Region	3 Year Payback ($/ton)	5 Year Payback ($/ton)
Northeast	$120	$200
Midwest	$65	$100
Northern Plains	$30	$50
Rocky Mountain	$65	$100
Pacific Northwest	$220	$290
California	$30	$50

Contacts and Sources of Information

Toshikazu Ishihara, Yoshiaki Kurosawa, Yonezou Ikumi, and Junji Matsue
Sanyo Electric Co., Ltd
Environmental Systems R&D Center
Sakata 1-1-1, Oizumi-Machi, Oura-Gun
Gunma 370-05, Japan

Rakesh Vidyadharan (student) and Ivan Maldonado (professor)
Iowa State University
Ames, Iowa
e-mail: rakeshv@iastate.edu
e-mail: maldonad@iastate.edu

H. Carlsen, Technical University of Denmark

H. Kühl, University of Dortmund, Germany

S. Schulz, University of Dortmund, Germany

Stirling and Vuilleumier Heat Pumps Design & Application, J. Wurm, J. Kinast, T. Roose, and W. Staats, McGraw-Hill, Inc. 1991.

Obvious Holes in Knowledge, Understanding, Information

Understanding of differences between theoretical calculations and Sanyo measurements; also the results of the Sanyo field test -- were the systems produced and sold? Was performance too low for a viable product? If so, why? Requests for information from Sanyo have not been successful, probably due to lack of contact with the appropriate person at Sanyo.

ABSORPTION CYCLES

Basic Concept Description

The absorption cycle is typically employed in cooling applications, though development of the GAX cycle is directed toward providing both high efficiency heating and cooling. Most absorption cycles use an electric pump to raise the pressure of a liquid solution of absorbent and absorbate. An external heat source, a gas burner in a direct fired system, steam in an indirect fired system, or waste heat, is used in the generator (or desorber) to cause the refrigerant to desorb from the absorbent creating a high pressure vapor. In cases where a volatile absorbent is used, such as when the working pair is ammonia-water, a rectifier is needed to reduce the concentration of the volatile absorbent (e.g. water) in the vapor to the condenser. The refrigerant vapor flows through a condenser, expansion valve, and evaporator providing useful heating or cooling. The high temperature and pressure liquid solution remaining in the generator has a relatively low concentration of the refrigerant (i.e. ammonia in an ammonia-water system or water in a lithium bromide-water system). This weak solution flows through a pressure valve to the absorber where it is recombined with the refrigerant vapor leaving the evaporator. Heat is generated during the absorption process and the absorber needs to be cooled in order for sufficient vapor to be absorbed into the solution to have adequate refrigerant flow. Various improvements are possible to the basic absorption cycle to boost its efficiency with the addition of heat exchangers to make use of heat rejected at the absorber, the weak solution leaving the generator, etc. Some possibilities are illustrated below.

Background Information

Single- and double-effect absorption cycle machines have been produced commercially for waste heat and “large” chiller applications. Development work in ongoing for triple-effect chillers for commercial buildings and GAX absorption systems for residential and light commercial applications.

Single-effect cycle: the single-effect absorption cycle is pictured in Fig. 42. Waste heat, steam from a boiler, or heat from a direct-fired burner is added (Q_{desorb}) to separate the refrigerant (generally water or ammonia) from the solution. The refrigerant passes through a condenser where heat is rejected from the cycle (Q_{cond}) either to be used for space conditioning for a heat pump or to the ambient for a chiller or air conditioner. The refrigerant passes through an expansion valve and into the evaporator where heat (Q_{evap}) is added to the cycle providing useful cooling or providing energy from the ambient for heat pumping. The high pressure, hot solution

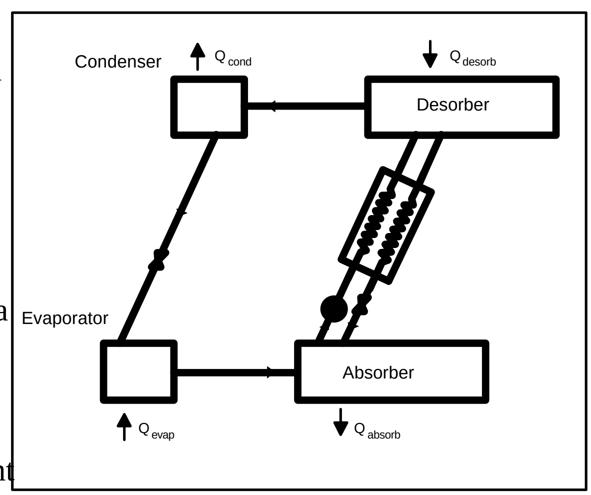

Fig. 42. Single-effect absorption cycle.

from the desorber (or generator) with a weak concentration of the refrigerant is passed through an internal heat exchanger and pressure valve to the absorber. The refrigerant and weak solution are combined in the absorber, heat is rejected to the ambient (Q_{absorb}) and the resulting strong solution pumped back to the desorber to complete the cycle.

GAX cycle: Several different R&D projects are currently underway to develop GAX chillers and heat pumps. Servel is developing a direct fired GAX ammonia-water chiller for light commercial and residential applications; they are represented in the U.S. by Robur Corporation. This system has a cooling COP of 0.62; an optional boiler can be added with a heating efficiency of 81%. Five ton modules can be combined to provide 10 to 25 ton light commercial units. Electrical consumption is on the order of 220 W/ton. This unit is scheduled to enter the commercial market in 1999.

The GAX cycle is a single-effect absorption cycle that employs heat energy recovered within the "power cycle" (as opposed to refrigeration cycle) to generate additional refrigerant vapor. A GAX cycle is shown in Fig. 43. The top of the absorber is relatively hot compared to the solution entering the top of the generator. Various methods have been developed to recover the heat from the top of the absorber to preheat the solution into the generator. This internal heat recovery can be viewed as generating more refrigerant vapor for a given energy input or requiring less energy input from an external source to generate a fixed flow of vapor.

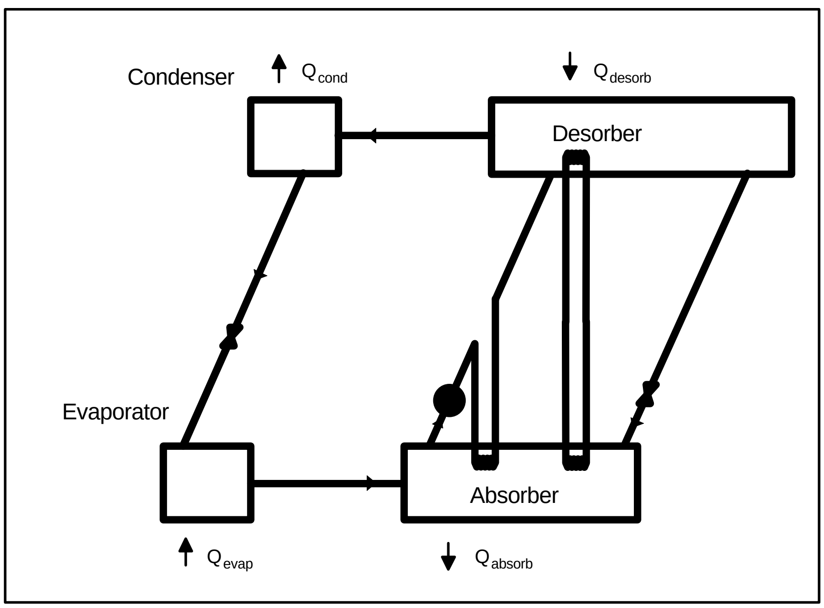

Fig. 43. GAX absorption cycle.

development programs have been pursued in the past both in North America, Europe, and Japan. Heating COPs are theoretically in the range of 1.4 to 1.5 and cooling COPs in the neighborhood of 0.70. At low ambient heating temperatures, the evaporator temperature and pressure is forced down, removing the overlap of temperature between the absorber and desorber. In that event there is no heat of absorption that can be employed to provide part of the energy input to the desorber and the cycle functions as a single-effect absorption cycle.

Double-effect cycle: a double effect absorption cycle is shown in Fig. 44. The condensing temperature in the high pressure condenser at the top is higher than the temperature required to drive the medium pressure desorber in the middle. The energy of condensation is used to generate additional vapor for the refrigeration cycle.

Many direct-fired double effect absorption machines are commercially available for large chiller applications. American Yazaki has a series of 30 to 100 ton chillers that may compete in the commercial unitary market. These systems have cooling COPs at full load of 1.00 and electrical power consumption on the order of 25 to 35 W/ton.

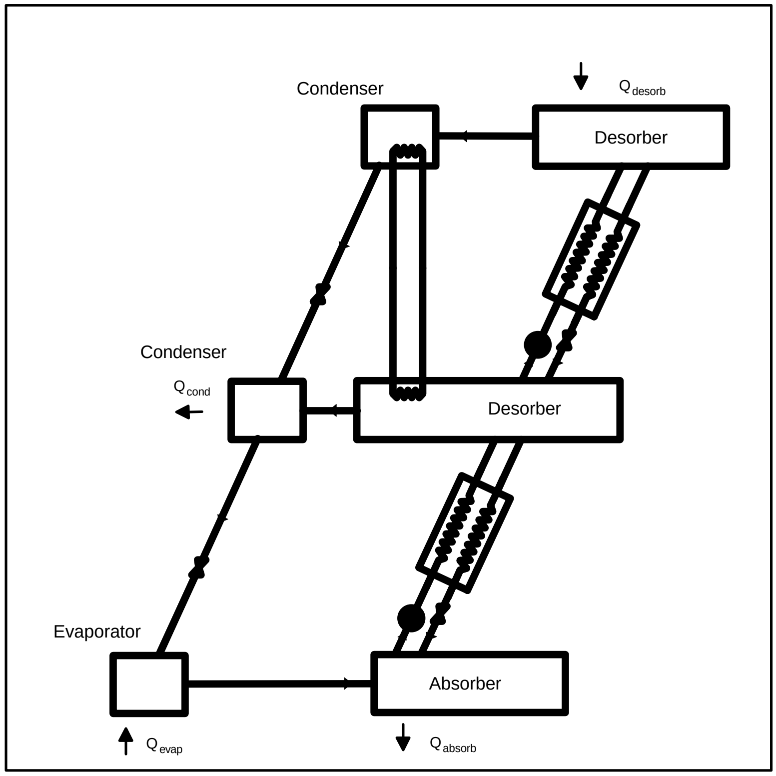

Fig. 44. Double effect absorption cycle (lithium bromide / water).

Secondary System Requirements

Traditionally, absorption systems have been applied as water chillers and consequently they require a hydronic distribution system. The GAX system developments have all used ammonia as the refrigerant, necessitating the isolation of the refrigerant in the outdoor package and a secondary brine loop between the indoor and outdoor units.

Efficiency Data

Absorption theoretical and observed efficiency data are summarized in Table 32. The assumed operating temperatures for the theoretical gCOPs of each cycle are listed in Table 39 on page B-3.

Single-effect cycles: the gCOP of a single-effect chiller is calculated for an ammonia-water working pair using a computer model by Herold, Radermacher, and Klein (1995). Results are listed only for cooling mode, since this cycle is only employed in cooling. The burner combustion and pump efficiencies are assumed to be 80% and 50%, respectively, and the effectiveness of the internal heat exchangers 100%. The ammonia concentration in the refrigerant circuit is set at 99.96%. The calculated gCOPs at 82E and 95EF are 0.58 and 0.53, with an annual performance factor of 0.56. Servel markets a direct-fired single effect chiller with a gCOP at conditions for the 95EF rating point of 0.48; Yazaki markets an indirect-fired single-effect chiller with an efficiency of 0.60 (combustion efficiency not included).

Table 32. Calculated and Observed Efficiencies for Ammonia Absorption Cycle Heat Pumps.

	Heating			Cooling		
Cycle Efficiency	47EF	17EF	Seasonal gCOP	82EF	95EF	Seasonal gCOP
Single Effect: theoretical observed				0.58	0.53 0.48	0.56
GAX: theoretical observed	1.52	1.50	1.36	0.71	0.64 0.62 to 0.71	0.67

notes: theoretical steady-state COPs include 80% burner efficiency, seasonal heating COPs include 50% waste heat recovery. Blank entries denote absence of calculated or measured information, calculated and observed cycle efficiencies do not apply for the shaded seasonal boxes

GAX cycles: extensive development work has been done for the application of the GAX cycle in small capacity heat pumping equipment. Field test prototypes of a cooling only unit were introduced in the in 1997 in 3 and 5 ton capacities with 110,000 to 165,000 Btu/h heat from an 80% to 82% AFUE gas burner (Servel 1998). Of the five models available, one has a gCOP of 0.62 at 55EF return water temperature and a supply water temperature of 45EF. The gCOP for the other four units is 0.48. The higher efficiency model requires 740 W in cooling mode and 300 W in heating (245 W/ton and 100 W/ton); the other models require up to 425 W/ton in cooling and 138 W/ton in heating.

Technical Advantages/Benefits

Absorption chillers can be a cost effective way of providing gas-fired cooling. Single effect chillers are most economically attractive when driven by process waste heat; advances in efficiency improvements and cost reductions for double-effect chillers have caused them to displace single-effect chillers in almost all other applications. The GAX cycle has the potential to provide significantly higher heating efficiency than a gas furnace in the residential and commercial unitary market. All absorption systems share the advantages of low emissions, quiet operation, low vibrations, and energy savings.

Technical Disadvantages

Absorption equipment is at a disadvantage to electric driven equipment in that absorption chillers must reject significantly more heat than electrically driven equipment and consequently require more heat exchanger surface. Larger heat exchangers translate into higher cost and overall size of the equipment package for absorption machines compared to conventional electric-driven heat pumps.

Technical Barriers

Single- and double-effect chillers are established technologies so they are not discussed in this section. Heat pumping applications, as opposed to water chilling, require a pair of working fluids that can operate below 32EF; ammonia-water is considered most seriously for GAX development. The use of ammonia creates potential corrosion problems for heat exchangers, piping, and the solution pump that must be resolved at acceptable cost. There may also be problems associated with system controls.

Economic Analysis

GAX cycle heat pump: There is poor agreement between the modeled COPs for the GAX cycle and those reported as observed in prototype testing. Results of the economic analysis are reported using the observed, prototype efficiencies. The results in Fig.45 show the installed cost premiums that would give the same life cycle cost as the baseline gas system. The data for the northeast indicate that costs could be as much as $1000 per ton higher than the baseline system with $1500 per ton or higher justified in northern Pennsylvania, throughout New York, and all of New England. Most of the Midwest, plains, Rocky Mountain region, and California have allowable first cost increments of at least $500 per ton for the GAX system. Most of the southeast and south central states would have to have lower installed costs than the gas furnace baseline to achieve equal life cycle costs. Figure 46 shows similar results in the southeast for a comparison of the GAX heat pump with a conventional electric heat pump.

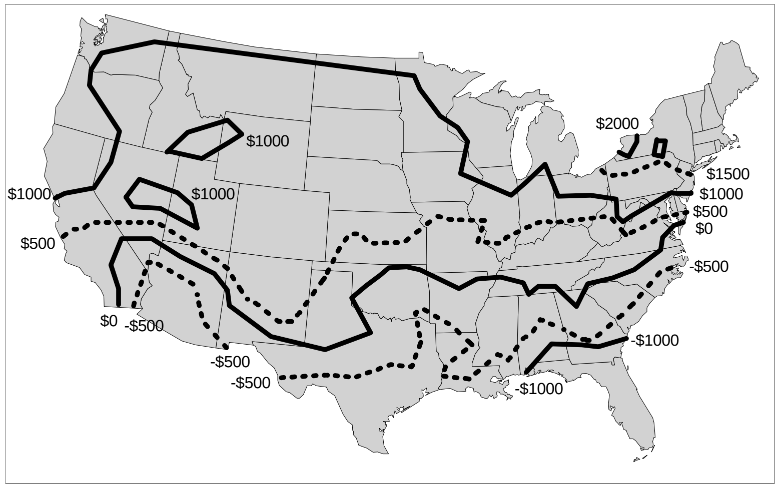

Fig. 45. Allowable first cost premium for GAX heat pump for equal life cycle cost with gas furnace baseline (equal maintenance costs).

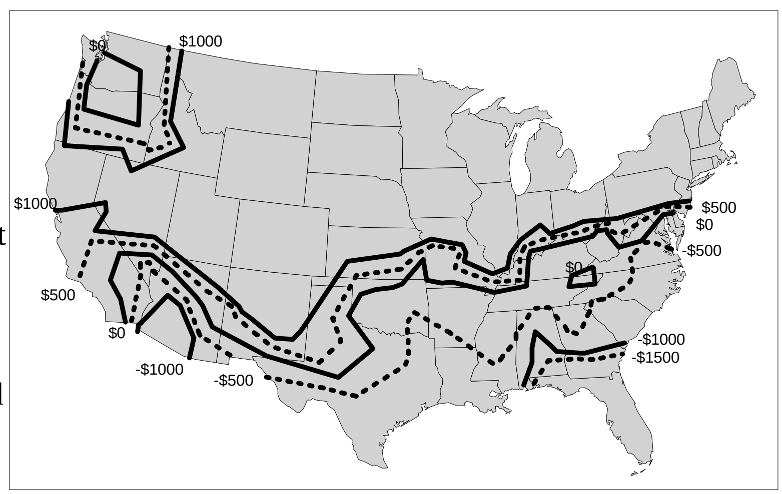

Fig. 46. Allowable first cost premium for GAX heat pump for same life cycle cost as an electric heat pump (equal maintenance costs).

There is some uncertainty concerning the annual maintenance cost differentials between the baseline furnace and air conditioner and the GAX absorption heat pump. The sensitivity of the results are shown in Fig. 47 in each of the nine geographic regions. The GAX system is expected to have the same maintenance cost as the gas furnace / electric air conditioner baseline ($0 /y differential), in which case it would have the same life cycle cost as the gas baseline at installed cost price differentials of $550 to $1600 per ton in California, the Northern Plains, the Rocky Mountain states, the Midwest, the Pacific Northwest, and the Northeast. Reasonable installed cost premiums are possible in these six regions even when the maintenance costs are $25 to $50 per year higher than those of the gas baseline. Installed costs would need to be $50 to $500 per ton lower in the Southeast, South Central, and Southwestern states even with the same maintenance costs as the gas baseline. The comparison of the GAX and the electric heat pump baseline in these three regions is similar to the comparison to the gas furnace and electric air conditioner; installed cost premiums are about $25 lower than those shown in Fig. 47. Although the installed cost premiums for equal life cycle costs are fairly high in much of the country, the allowable cost premiums for three and five year paybacks are fairly low as shown in Table 33.

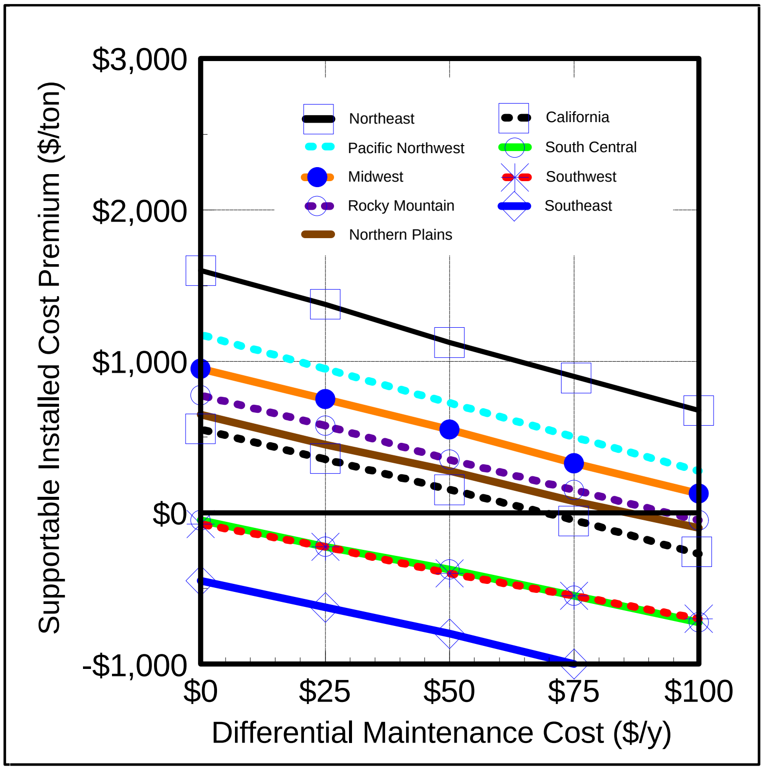

Fig. 47. Allowable installed cost premiums for GAX heat pumps.

It is not clear how actual equipment costs will compare between a GAX heat pump and the gas furnace baseline system. The GAX requires more heat transfer surfaces, a secondary loop, and both brine and solution pumps. All refrigerant tubing will need to be iron or steel at a higher cost than

Table 33. Installed Cost Premiums for a GAX Heat Pump for 3 and 5 Year Paybacks.

Region	3 Year Payback ($/ton)	5 Year Payback ($/ton)
Northeast	$345	$550
Midwest	$205	$320
Northern Plains	$140	$220
Rocky Mountain	$165	$260
Pacific Northwest	$290	$400
California	$115	$190

copper tubing. The GAX heat pump will not include cost of the compressor and motor for a net cost saving. Further cost information is needed.

Contacts and Sources of Information

Herold, K., Radermacher, R., and Klein, S., 1995. Absorption Chillers and Heat Pumps, CRC Press, Boca Raton, New York, London, and Tokyo.

Robert DeVault
Oak Ridge National Laboratory
P.O. Box 2008, MS-6070
Oak Ridge, Tennessee 37831
(423) 574-0738

Servel 1998, Product literature: “Servel: The Chiller-Heater, Advanced Absorption Cooling Technology, Sand and Efficient Hot Water Heating.”

Robur Corporation North American Headquarters
2300 Lynch Road
Evansville, IN 47711-2951
ph: 1-812-424-1800
fax: 1-812-422-5117

Obvious Holes in Knowledge, Understanding, Information

No major gaps in knowledge for the GAX cycle. It is unfortunate that there is such a difference between the modeled and observed efficiencies, but the measured values are at the desired rating points and are considered to be of comparable “quality” to the efficiencies stated for the gas and electric baseline equipment.

ADSORPTION HEAT PUMPS

Basic Concept Description

Some solids such as activated carbon and zeolites have an affinity to adsorb vapor onto or into their surface structure. If the materials (solid and gas) undergo adsorption in a reversible thermal reaction the pair can be used in a heat pump. Such a cycle is illustrated in Fig. 48. At "low" temperatures, molecular forces cause these gases to attach to the surface or move into the crystalline structure of the solid. The adsorption of the gas creates a pressure gradient and heat is also released. The process is reversed through the addition of heat which causes the refrigerant gas to desorb from the solid at high temperature and pressure. The high temperature, high pressure vapor can be circulated through a condenser, expansion device, and evaporator to provide useful heating or cooling.

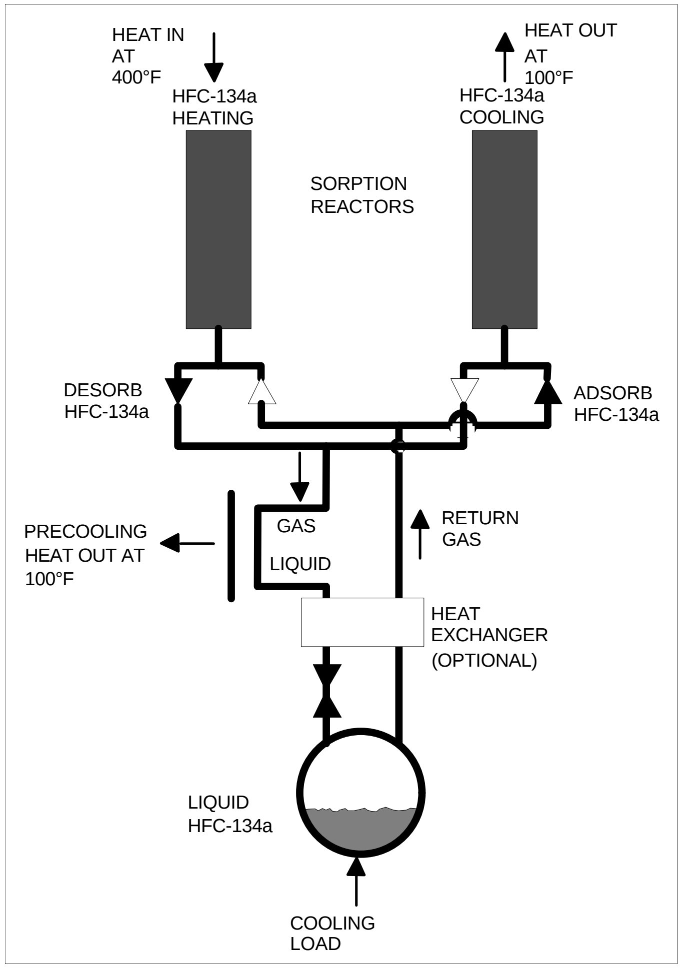

Fig. 48 Schematic of an adsorption cycle heat pump using R-134a.

The adsorption/desorption is not a continuous process, as are vapor compression or absorption. A sorption "bed" is charged with refrigerant at low temperature and pressure; when adsorption stops or slows down, the sorption bed is heated and high temperature and pressure gas is released from it. Pairs of beds are used with one bed adsorbing vapor (charging) while the other is desorbing vapor (regenerating) to provide "continuous" heating or cooling (actually oscillating between high and low cooling rates). An adsorption system with two pairs of beds is shown in Fig. 49. The addition of more sorption beds allows a steadier heating or cooling rate and also permits the use of heat rejected from the adsorption process to be used as part of the energy input for regenerating fully charged beds. These "advanced" cycles improve efficiency at the cost of adding a pump and heat recovery loops.

Background Information

Concepts for adsorption heat pumps differ fundamentally in the adsorbent-adsorbate pairs that are chosen and the molecular forces underlying the interaction of the pair. Commonly discussed adsorption pairs are:

! ammonia-carbon,
! water-zeolite,
! metal hydride, and
! organic salts or complex compounds.

Each pair has its advantages and disadvantages which may be shared with other pairs or may be unique to a particular pair.

Ammonia-carbon: activated carbon and ammonia adsorption systems use less exotic materials than most proposed adsorption heat pumps.

Water-Zeolite Adsorption: water has been used as the refrigerant in adsorption air-conditioning systems but cannot be used in a heat pump operating near 0EC (32EF). Zeolite adsorption systems are distinguished from many other adsorption processes because they employ the adsorption of a vapor into a solid crystalline structure instead of using surface effects. The adsorption of refrigerant vapor on surface adsorbents (e.g. silica gel, activated carbon) depends exponentially on H/RT where H is the energy of adsorption, R is the universal gas constant, and T is the absolute temperature. The adsorption of vapor into the crystalline structure of the zeolite depends exponentially on the second to fifth powers of H/RT. This makes zeolites well suited for heat pumping applications by reducing the influence of condensation temperature and pressure on the COP of the cycle. When it is heated, the zeolite desorbs most of the refrigerant vapor even at high vapor pressure. This behavior allows the adsorption system to operate at high temperatures without a cooling tower with little loss in performance. Zeolites are used in heat exchangers with copper tubing.

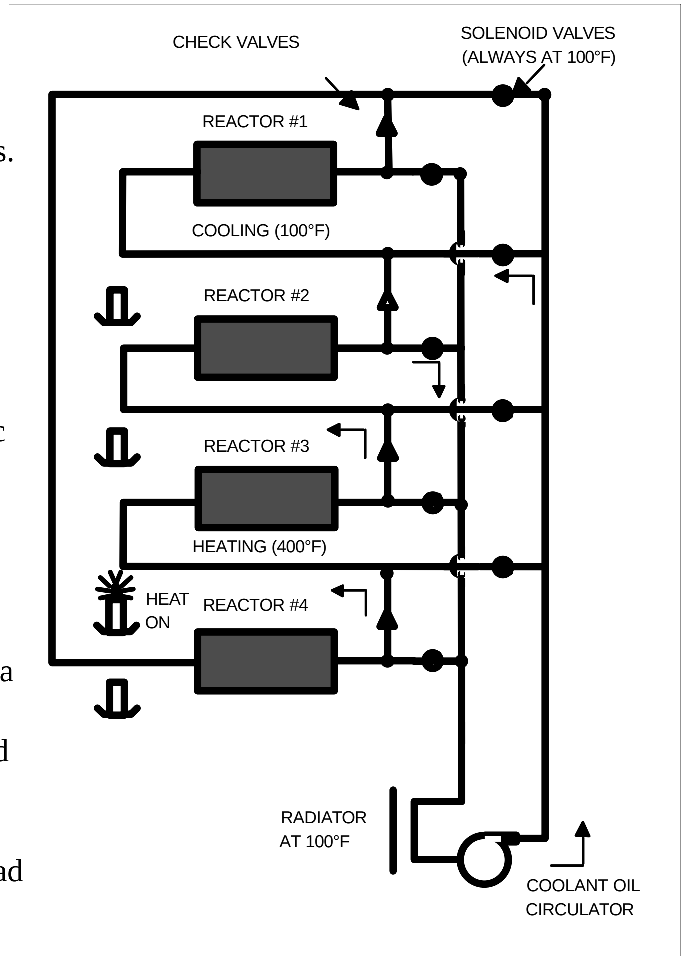

Fig. 49. Adsorption system using two pairs of adsorbent beds for “continuous” output and regeneration for high COP.

Metal-Hydride Adsorption: "there are a number of metals that possess the remarkable ability to adsorb large quantities of hydrogen gas. The hydrogen combines with the metal to form a 'solid solution' which is, in effect, a new metal alloy. Hydrogen adsorption occurs under specific temperature and pressure conditions. The hydrogen is released (desorbed) when the alloy temperature is elevated or the pressure is reduced. The metal hydride alloys are used in powdered form within stainless steel tubes. Ergenics has miniaturized the design of a metal hydride air conditioner in order to get a ton of cooling from a mechanical package weighing less than 50 lb. A major factor in the size and weight reductions is due to obtaining cycle times on the order of 15 seconds, allowing the use of fewer adsorption beds.

Organic salts or complex compounds: this adsorption concept employs a complex organic salt as the adsorbent and ammonia as the adsorbate and refrigerant. "A specific salt will adsorb or desorb [ammonia] at a specific temperature over an entire 'coordination sphere.' If a salt has three 'coordination spheres,' this means that the ammonia can array itself around the salt in three ways. The first molecules of ammonia form a 'shell' or 'coordination sphere' around the salt molecule. If more ammonia molecules are added once the first shell is filled, they arrange themselves further from the salt in a second coordination sphere. Some salts may form as many as three of these coordination spheres at increasing distances from the salt. (Ryan 1993)" These systems lend themselves well to high efficiency cycles because the outer coordination spheres can be regenerated at the relatively low temperatures of heat recovered from the charging adsorbent beds..

Secondary System Requirements

High efficiency systems require regenerator loops with circulating oils; this adds an electric parasitic to the gas-fired system. Metal hydride systems would require secondary loops to isolate the explosive hydrogen gas from the conditioned space.

Efficiency Data

Very little information has been located on the efficiencies of adsorption heat pumps and no independent modeling has been performed as part of this project. The data that are available are listed in Table 34. The published COPs rarely include any discussion or explanation of the operating conditions.

Ammonia-carbon: Vasiliev et al. (1977) reported on calculated and prototype measurements on a carbon fiber-ammonia adsorption device providing capacity measurements and predictions across a range of evaporator and condenser temperatures. They cite a COP "greater than 1" and a cooling capacity or 200 W/kg carbon fiber. Wave Air Corporation was funded to develop an ammonia-carbon heat pump with seasonal heating and cooling gCOPs of 1.30 and 1.00, respectively (AGCC 1996); the status of this project is unknown.

Water-Zeolite Adsorption: Tchernev and Emerson (1988) reported measured seasonal gCOPs of 1.8 heating and 1.2 cooling on a regenerative prototype system. Two 45 pound zeolite heat exchangers provided 6000 Btu/h of cooling; 82 kg zeolite/ton capacity.

Metal-Hydride Adsorption: Ergenics constructed a prototype metal hydride heat pump using 27 lb of alloy with a net cooling capacity of 8172 Btu/h; 18 kg/ton capacity. The Japan Metals and Chemicals Company has cooling only metal hydride air conditioners using LaNi and MmNi[1] alloys with gCOPs of 0.45 providing 50EF air at 4 cycles per hour. They also have a $LmNi_3$ heat pump with a gCOP of 1.6 (presumed to be heating efficiency) at 8.5 cycles per hour providing water at either 113E or 59EF.

Organic salts or complex compounds: Rockenfeller (1992) reported that a residential sized adsorption heat pump with complex compounds would have a gCOP of 1.0 at “rating conditions” and heating gCOP of approximately 1.7 at 30EF.

Technical Advantages/Benefits

“The absence of the liquid phase in the generator makes corrosion a much slower process than with liquids [absorption]. Corrosion studies of ammoniates in aluminum have been favorable up to 400EF (DOE 1993, p. A-27).”

Water-Zeolite Adsorption: regeneration of the adsorbent beds can begin at temperatures as low as 100EF, this allows some of the heat of adsorption to be used to regenerate the adsorbent in multiple bed regenerative systems. Water can be a very desirable refrigerant because of its benign environmental properties.

Metal-hydride: the metal hydride pair employs a process in which hydrogen is adsorbed into the crystalline structure of the metal. The lattice work of the crystals allow large masses of hydrogen to be adsorbed providing greater capacity per unit mass of adsorbent than may be possible with adsorption pairs that use a surface effect.

Organic salts or complex compounds: the nature of the “coordination spheres” of complex compounds provide opportunities for high efficiency for this adsorption pair through heat transfer for regenerating adsorption beds. Each coordination sphere has its own regeneration energy requirement; the further the sphere is from the salt molecule, the less energy is required to desorb the ammonia. Heat recovered from sorbent beds adsorbing ammonia can be used effectively to desorb ammonia from the outer coordination spheres in a second bed. External heat sources may be needed only to desorb ammonia from the innermost coordination sphere.

---

[1] Mm - mixed metal, Lm - lanthanum-rich mixed metal

Technical Disadvantages

Adsorption heat pumping is an inherently cyclical process and multiple adsorbent beds are

Tble 34. Calculated and Observed Efficiencies for Adsorption Cycles.

Adsorption Cycle	Heating			Cooling		
	47EF	17EF	Seasonal gCOP	82EF	95EF	Seasonal gCOP
Water/Zeolite theoretical observed			1.8			0.7† to 1.2
Ammoniated Carbon theoretical observed			1.3			0.7† to 1.0
Metal Hydride theoretical observed			1.6			0.45 to 0.7†
Organic Salts: Complex Compounds theoretical observed	1.7			1.0		
Open Cycle theoretical observed						

notes: blank entries denote absence of calculated or measured information, calculated and observed cycle efficiencies do not apply for the shaded seasonal boxes

† one reviewer reported that the cooling season gCOP of 0.7 is more likely for water/zeolite, ammoniated carbon, and metal hydride adsorption systems than the values the authors reported from other sources.

necessary to provide approximately continuous capacity. Adsorption systems inherently require large heat transfer surfaces to transfer heat to and from the adsorbent materials which automatically makes cost an issue. High efficiency systems require that heat of adsorption be recovered to provide part of the heat needed to regenerate the adsorbent. These regenerative cycles consequently need multiples of two-bed heat exchangers and complex heat transfer loops and controls to recover and use waste heat as the heat exchangers cycle between adsorbing and desorbing refrigerant. This exacerbates issues concerning first cost and also adds an electric parasitic.

Performance can deteriorate over numerous adsorption cycles because of decrepitation and surface contamination.

Ammonia-carbon: materials compatibility issues with ammonia, stainless steel heat exchanger tubes and pipes. Ammonia is not universally accepted as a refrigerant in residential applications because it is toxic and flammable in some concentrations; precautions must be made to isolate ammonia from the occupied space and to contain it within a machine room or disperse it in the atmosphere safely if a leak occurs.

Water-Zeolite Adsorption: size and cost are both factors working against zeolite adsorption heat pumps. A three ton heat pump would require 240 kg of zeolite and large amounts of copper. ADL estimated that materials and components alone for a three ton system would cost $2500 exclusive of labor, overheads, dealer markups, and installation costs (DOE 1993).

Metal-Hydride Adsorption: flammability of the refrigerant (i.e. hydrogen).

Organic salts or complex compounds: materials compatibility issues with ammonia, stainless steel heat exchanger tubes and pipes. Rocky Research has reported that absorbent salts have shown no change in properties over thousands of cycles (DOE 1993, p. A-28).

Economic Analysis

The absence of efficiency data for any of the solid/vapor pairs makes it impossible to perform any kind of analysis for annual energy use or any economic comparisons. Rockenfeller projected that the <u>manufacturing</u> cost of a complex compound, residential heat pump would be less than $400 per ton (1992);

Technical Barriers

Not known at this time.

Contacts and Sources of Information

AGCC 1996. <u>Natural Gas Cooling Equipment Guide</u>, American Gas Cooling Center, 1515 Wilson Boulevard, Arlington, Virginia 22209, April 1996, p. 153.

DaCosta D., 1993. “Metal Hydride Heat Pumps,” Proceedings of the 1993 Refrigeration, Heat Pump, and Air Conditioning Workshop, Breckenridge, CO, June.

DOE 1993. “A Research Needs Assessment: Energy Efficient Alternatives to Chlorofluorocarbons (CFCs),” DOE/ER/30115-H1, June.

Rockenfeller, U., Kirol, L, and Ryan, W., 1992. “Solid-gas chemisorption: Efficient HVAC&R Without CFCs,” ASHRAE Journal, March 1992, pp. 54-58.

Ryan, W., 1993. “CFC-Free Chemisorption Heat Pumps and Refrigeration,” Proceedings of the 1993 Refrigeration and Air-Conditioning Technology Workshop, Breckenridge, Colorado, June 23-25.

Tchernev, D.I. and Emerson, D. T. 1988. “High-Efficiency Regenerative Zeolite Heat Pump,” *ASHRAE Transactions, Vol 94, Pt. 2,* pp. 2024-2032.

Vasliev, L., et al. 1996. “Adsorption Heat Pump Using Carbon Fiber/NH_3 and Heat Pipes,” Heat Pump 96: Proceedings of the 5th International Energy Agency Conference on Heat Pumping Technologies, September 22-26, Toronto, Canada.

Obvious Holes in Knowledge, Understanding, Information

Efficiency data at rating points and also status of past and current R&D projects.

DUPLEX STIRLING HEAT PUMP

Basic Concept Description

This technology combines a Stirling engine with a Stirling cycle cooler. The following description is from the Ohio University Internet site:

> "In a Stirling machine, a confined volume of gas is repeatedly expanded at one temperature and recompressed at another with the result that heat energy is absorbed from the environment during expansion and rejected to the environment during compression. Regardless of whether energy is being absorbed or rejected, more is transferred at a higher temperature than at a lower temperature. Thus, the difference between the amount of energy absorbed at high temperature and rejected at a warm temperature by a Stirling engine appears as the mechanical, hydraulic, or electrical power it delivers to a load. Conversely, the difference between the amount of energy absorbed at a low temperature and rejected at a warm temperature by a Stirling cooler or heat pump must be provided to the machine in order to keep it operating. In a duplex Stirling cooler, this power is provided by a directly coupled Stirling engine. (Ohio 1998)"

Stirling engines can transfer their output to a load with either a mechanical linkage using a crank and piston rods or with pistons and displacers acting as harmonic mechanical oscillators in a hermetically sealed cylinder. The performance of the Stirling engine is proportional to the mean operating pressure of the working gas, and leakage of gas around the shaft seals of the kinematic machine (mechanical linkages) progressively degrades performance. In addition, unbalanced forces acting on the drive mechanism can lead to greater wear than is experienced with the free-piston machine and the lubricant necessary for the piston rods in the kinematic machine fouls heat exchanger surfaces requiring periodic maintenance. By contrast the free-piston Stirling engine employs balanced forces in a sealed cylinder using inertial, spring, and damping forces to control the frequency and phase of the piston oscillations without an external drive mechanism.

Background Information

Dr. William Beale and Sunpower, Inc. of Athens, Ohio have been strong advocates of duplex Stirling heat pumps. The U.S. Department of Energy and NASA have both supported work on free-piston Stirling engines. Duplex Stirling cryocoolers are commercially available for remote sensing applications. Silena Germany is a distributor for alpha-, beta -, and gamma- spektrometer, including the CoCoS HPGe and X-ray detextion device with duplex Stirling cooler. Duplex Stirling machines have been proposed for refrigeration and space conditioning applications, but have not been developed commercially. Much of the related R&D performed since the mid-1970's has focused on basic understanding of the forces and hysterisis effects of the Stirling cycle in order to apply it to heating and air conditioning applications. During the late 1980's, DOE funded work at the Massachusetts Institute of Technology to study Stirling cycle processes in support of contracted work on engine/compressor couplings for free-piston Stirling engine/Rankine cycle heat pumps at Mechanical Technology Inc. and Sunpower.

Secondary System Requirements

Heat pipes or secondary heat transfer loops will be necessary to provide useful heating or cooling with a Stirling device. The working volume of gas in the Stirling cooler is a fundamental design property of the machine. Additional internal volume as would be necessary to circulate the working gas through either an indoor or outdoor heat exchanger represents increased void volume that reduces efficiency or makes operation impossible altogether..

Efficiency Data

ADL derived comparable efficiencies for electric driven reverse Rankine and Stirling cycle heat pumps at three of the ARI rating points (82EF was omitted). Duplex Stirling COPs were derived by using the relative performance of R-22 and Stirling cycle from the ADL report (1993, p. A-47), the theoretical R-22 cycle efficiency with an 80% compression efficiency, 95% transmission efficiency, and a 28% Stirling engine efficiency. The resulting gCOPs, HSPF, and SEER are listed in Table 35.

Table 35. Calculated and Observed Efficiencies for Duplex Stirling Heat Pumps.

		Heating			Cooling		
Cycle Efficiency	conversion efficiency	47EF	17EF	Seasonal gCOP	82EF	95EF	Seasonal gCOP
Cycle COP	28%	4.98	3.08		5.30	3.98	
theoretical (ADL)		1.57	1.48	1.3		0.96	0.91
theoretical (ORNL)		1.69	1.19	1.3	1.41	1.06	1.3
observed							

Notes: gCOPs computed using relationship between Stirling COPs listed in ADL (1993, p. A-47) and R-22 cycle COPs with 80% compression efficiency. Blank entries denote absence of calculated or measured information, calculated and observed cycle efficiencies do not apply for the shaded seasonal boxes

Technical Advantages/Benefits

The Stirling cycle is claimed to have higher efficiency than the Rankine cycle, although this has not yet been demonstrated in laboratory or prototype equipment suitable for HVAC applications. Likewise, the Stirling engine has potential for long life that also has not been demonstrated.

Technical Disadvantages

Requires secondary heat transfer loop, very high regenerator effectiveness, understanding complex relationships between power and displacer pistons, gas springs, etc.

Technical Barriers

ADL (1993, p. 2-12) identified several research needs that for Stirling cycle refrigeration in general:

! accurate cycle modeling capability,

! improved regenerator performance to achieve higher effectiveness, lower pressure drop, lower void volume, lower cost, and less susceptibility to contaminant plugging.

! reduction in log mean temperature difference for the hot and cold heat exchangers where high density heat transfer is required, and

! improvement of secondary heat transfer loops.

Economic Analysis

used in the economic analysis because they are believed to be more accurate than the COPs modeled for this project; the COP at 82EF is assumed to be the same as the value ADL estimated for the 95EF condition. This latter assumption overestimates the energy use in cooling mode and may result in misleading economic comparisons in the southern states. This is not perceived as a major error since as a rule the gas-fired systems are most competitive in the predominantly heating climates. The supportable installed cost premiums for duplex Stirling heat pumps relative to the gas baseline are shown in Fig. 50 for a difference in maintenance costs of $25 per year. A higher installed cost could be supported

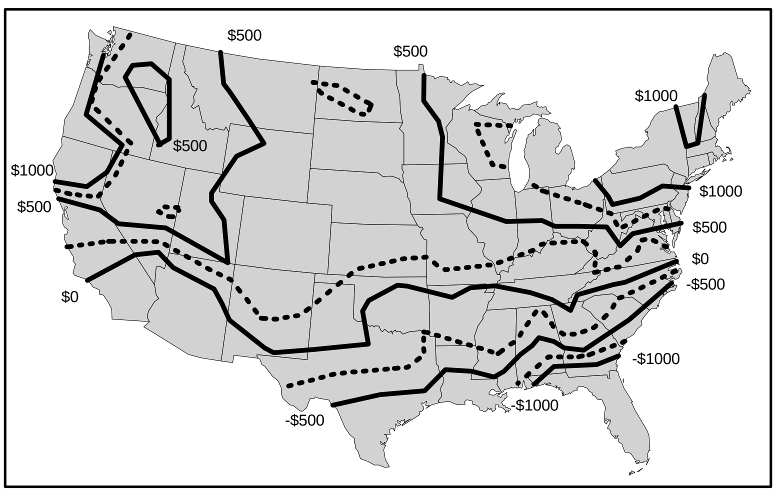

Fig. 50. Allowable installed cost premiums for duplex Stirling heat pumps relative to the gas furnace baseline.

outside of the southern tier of states, ranging from $0 to $500 throughout the central parts of the country, $500 to $100 per ton in the northeast and northwest, and above $1000 per ton in New York, parts of New England, and the Pacific Northwest. Installed costs significantly below the baseline system would be necessary in the southern states.

The duplex Stirling heat pump should have a long life with low maintenance requirements, though this has not been demonstrated or disproved through hardware testing. In this system, the compressor and electric motor of a conventional heat pump have been replaced by the duplex Stirling module and a secondary heat transfer loop has been added. The Stirling module must include a regenerator with high effectiveness, a complex heater head, and more complicated controls than an electric heat pump. Each of these factors increases materials and manufacturing costs negating the savings from eliminating the motor and compressor and possibly resulting in a more expensive machine than the baseline electric heat pump. Since the installed costs of the gas and electric baseline systems are comparable, the duplex Stirling system will be more expensive than the gas furnace and electric air conditioner system.

The installed cost premiums permitting three and five year paybacks for the duplex Stirling heat pump are listed in Table 36 for an annual maintenance cost $25 higher than that of the gas furnace baseline. A higher maintenance cost is selected because of the addition of a secondary heat transfer loop and the high reliability of the motor/compressor in a conventional air conditioner. These results show that reasonable paybacks can be achieved with the duplex Stirling heat pump, but the increase in installed costs must be on the order of $100 to $175 per ton in much of the country.

Table 36. Installed Cost Premiums for a Duplex Stirling Heat Pump.

Region	3 Year Payback ($/ton)	5 Year Payback ($/ton)	Equal Life Cycle Cost ($/ton)
Northeast	$267	$423	$1173
Southeast	-$66	-$108	-$370
South Central	$10	$14	-$8
South West	-$4	$12	$24
Midwest	$138	$219	$609
Northern Plains	$87	$136	$369
Rocky Mountain	$117	$184	$493
Pacific Northwest	$234	$322	$892
California	$98	$153	$413

Contacts and Sources of Information

ADL 1993. Energy Efficient Alternatives to Chlorofluorocarbons (CFCs): A Research Needs Assessment Final Report, U.S. Department of Energy, Office of Energy Research, DOE/ER/30115-H1, June.

Ohio 1998. http://www.cns.ohiou.edu/~mcab/260.html

Obvious Holes in Knowledge, Understanding, Information

Measured COPs at ARI rating conditions or direct reference to simulated COPs.

EJECTOR HEAT PUMPS

Basic Concept Description

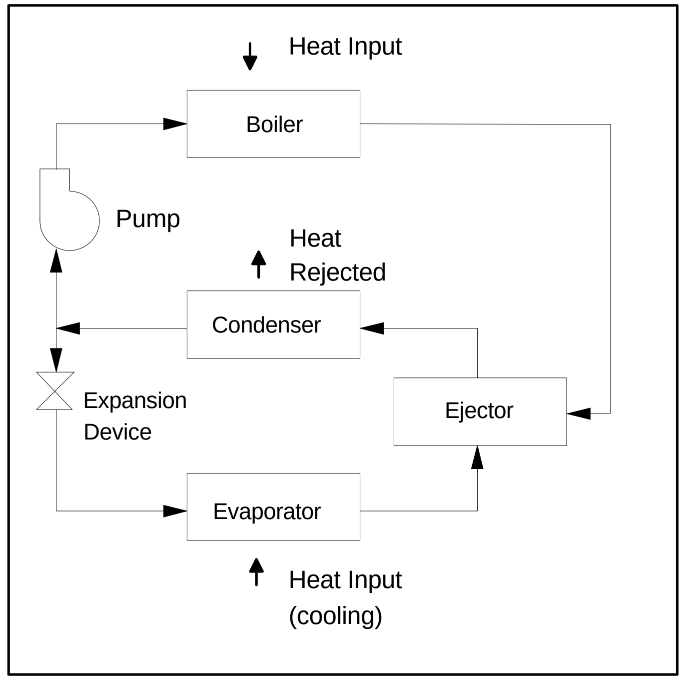

Fig. 51. Schematic of an ejector heat pump.

reverse Rankine cycle in that it includes a condenser, evaporator, and expansion valve; the compressor is replaced by a pump, a boiler, and an ejector. The pump uses relatively little energy to raise the pressure of most of the liquid from the condenser to a higher pressure where additional heat is added at the boiler to create a high pressure, high temperature vapor. The vapor is expanded through a jet ejector, where it entrains some low pressure vapor from the evaporator, with the combined reduced pressure stream of vapor flowing to the condenser. Heat is rejected at the condenser, the resulting high pressure liquid flow is split, with most of it flowing back to the circulating pump and part flowing through an expansion valve to the evaporator. Heat is absorbed in the evaporator either providing useful cooling or energy for heat pumping in heating mode. The cycle is illustrated in Fig. 51.

Background Information

A steam-jet ejector was first used some time prior to 1901 by LeBlanc in France and by Parsons in England; Parsons used water as the refrigerant. C. T. Hsu investigated ejectors for heat pump applications for DOE and ORNL while he was a graduate student at the University of Tennessee in the 1980s. Hsu found that the COP is proportional to the boiler temperature and that the boiler temperature could be increased up to the critical temperature of the refrigerant (1984). Charan looked at the application of fluorocarbon refrigerants in ejector refrigeration systems at conditions for cold food storage and air conditioning (1990). Khalidy (1995) accepted Hsu’s conclusion on the relationship of boiler temperature and efficiency, but concluded through analytical and experimental investigations that the condenser temperature is the most significant variable in ejector heat pump COP, especially at low evaporator temperatures.

Secondary System Requirements

No secondary systems are required. Electric parasitics would include air handling equipment for the evaporator and condenser and a pump to circulate liquid refrigerant from the evaporator back to the boiler.

Efficiency Data

Charan (1990) calculated COPs for ejector systems at evaporator temperatures from 0E to 40EF, a 200EF boiler temperature and 90EF condensing temperature for five fluorocarbon refrigerants. The COPs at 40EF ranged from 0.63 to 0.79 for a system that does not include a pump to supply high pressure liquid to the boiler. Charan's COPs are a factor of 3 to 4 higher than values calculated by Hsu (1984) and measured by Khalidy (1995) under similar conditions.

Hsu (1984) published a model for an ejector heat pump and presented parametric results for several fluorocarbon refrigerants. Khalidy (1995) built upon Hsu's model and also constructed and tested an ejector heat pump using R-113, a solar concentrator to power the boiler, and a 2 kW electric heater to supplement the solar concentrator on cloudy days. Khalidy presents his analytical results in terms of ejector efficiency and COPs from observations. The results in Table 37 are from Hsu's model using the evaporating and condensing conditions in Table 3.

Table 37. Calculated and Observed Efficiencies for Ejector Heat Pumps.

		Heating			Cooling		
Cycle Efficiency	conversion efficiency	47EF	17EF	Seasonal gCOP	82EF	95EF	Seasonal gCOP
Cycle COP theoretical observed	0.80 1.00	1.052	1.036	0.98	0.293 0.25	0.214 0.26	0.27

Notes: boiler temperature set at 200EF, with nozzle and diffuser efficiencies of 0.97 and 0.75, refrigerant is R-22, pump power excluded from calculations. The observed COPs are from Khalidy (1995) at similar though not identical conditions excluding solar panel efficiencies. Blank entries denote absence of calculated or measured information, calculated and observed cycle efficiencies do not apply for the shaded seasonal boxes

Technical Advantages/Benefits

One feature of the ejector heat pump is that the boiler can operate at relatively low temperatures which enables them to be driven with waste heat or solar energy. An ejector heat pump using a low pressure refrigerant (e.g. R-11, R-123) can operate effectively with a boiler temperature of about 200EF. Ejector heat pumps should also have high reliability and low equipment costs.

Technical Disadvantages

Ejector heat pumps have very low efficiencies relative to conventional compression systems and are best employed where low quality heat is available at little or low cost.

Technical Barriers

There are considerable losses associated with the mixing of the high velocity gas from the boiler and the low velocity gas from the evaporator. The gas also goes through shock waves which add additional losses. The mixing and shock processes are irreversible losses (ADL 1993).

Economic Analysis

The very low heating and cooling efficiencies make gas-fired ejector heat pumps compare extremely unfavorably with the gas furnace baseline in every part of the U.S. Some reductions in equipment cost would be possible as a result of replacing the air conditioner compressor with an relatively inexpensive ejector and pump. Both systems, however, employ gas burners and air handling equipment at comparable costs. This technology could be more attractive if driven by waste heat or solar energy.

Contacts and Sources of Information

ADL 1993. Energy Efficient Alternatives to Chlorofluorocarbons (CFCs): A Research Needs Assessment Final Report, U.S. Department of Energy, Office of Energy Research, DOE/ER/30115-H1, June.

Charan, V. 1990. *"A Comparative Performance of Freon Ejector Refrigeration Systems,"* Proceedings of the 1990 USNC/IIR-Purdue Refrigeration Conference, July 17-20, pp. 55-60.

Hsu, C. T. 1984. Investigation of an Ejector Heat Pump by Analytical Methods, Oak Ridge National Laboratory, ORNL/CON-144, July.

Khalidy, N., and Zayonia, A., 1995. *"Design and Experimental Investigation of an Ejector In an Air-Conditioning and Refrigeration System,"* ASHRAE Transactions, Vol 101, Pt 2, pp. 383-391.

Obvious Holes in Knowledge, Understanding, Information

Modeled performance at ARI rating conditions.

CONCLUSIONS

This project was initiated by the Department of Energy in response to a request from the HVAC industry for consolidated information about alternative heating and cooling cycles and for objective comparisons of those cycles in space conditioning applications. Twenty-seven different heat pumping technologies are compared on energy use and operating costs using consistent operating conditions and assumptions about component efficiencies for all of them. This report provides a concise summary of the underlying principals of each technology, its advantages and disadvantages, obstacles to commercial development, and economic feasibility. Both positive and negative results in this study are valuable; the fact that many of the cycles investigated are not attractive for space conditioning avoids any additional investment of time or resources in evaluating them for this application. In other cases, negative results in terms of the cost of materials or in cycle efficiencies identify where significant progress needs to be made in order for a cycle to become commercially attractive.

Although reverse Rankine cycle heat pumps using hydrocarbons have similar energy use to conventional electric-driven heat pumps, there are no significant energy savings due to the minor differences in estimated steady-state performance; higher costs would be required to accommodate the use of a flammable refrigerant. Magnetic and compressor-driven metal hydride heat pumps may be able to achieve efficiencies comparable to reverse Rankine cycle heat pumps, but they are likely to have much higher life cycle costs because of high costs for materials and peripheral equipment. Both thermoacoustic and thermionic heat pumps could have lower life cycle costs than conventional electric heat pumps because of reduced equipment and maintenance costs although energy use would be higher.

There are strong opportunities for gas-fired heat pumps to reduce both energy use and operating costs outside of the high cooling climates in the southeast, south central states, and the southwest. Diesel and IC (Otto) engine-driven heat pumps are commercially available and should be able to increase their market share relative to gas furnaces *on a life cycle cost basis*; the cost premiums associated with these products, however, make it difficult to achieve three or five year paybacks which adversely affects their use in the U.S. Stirling engine-driven and duplex Stirling heat pumps have been investigated in the past as potential gas-fired appliances that would have longer lives and lower maintenance costs than diesel and IC engine-driven heat pumps at slightly lower efficiencies. These potential advantages have not been demonstrated and there has been a low level of interest in Stirling engine-driven heat pumps since the late 1980's. GAX absorption heat pumps have high heating efficiencies relative to conventional gas furnaces and are viable alternatives to furnace/air conditioner combinations in all parts of the country outside of the southeast, south central states, and desert southwest. Adsorption heat pumps may be competitive with the GAX absorption system at a higher degree of mechanical complexity; insufficient information is available to be more precise in that assessment.

APPENDIX A: METAL HYDRIDE CALCULATIONS

Quoting (and paraphrasing) from Feldman[1]:

"For a frictionless, adiabatic, isentropic process of an ideal gas with constant specific heats, pv^k is constant, where "k" is the ratio of specific heats, $k=C_p/C_v$; k=1.4 for hydrogen. In a process between states 1 and 2, $p_1v_1^k = p_2v_2^k$, and with pv=RT:

$$\frac{T_2}{T_1} = \left[\frac{p_2}{p_1}\right]^{\frac{k-1}{k}} = \left[\frac{p_2}{p_1}\right]^{\frac{R}{c_p}} \qquad (17)$$

The compression work may be determined for a steady flow process in an open compressor system from,

$$w_c = -\int_2^1 v\,dp = \frac{RT_1}{E_c}\cdot\frac{k}{k-1}\cdot\left[\left(\frac{p_2}{p_1}\right)^{\frac{k-1}{k}} - 1\right] \qquad (18)$$

where E_c is the total compressor efficiency, v is the specific volume, and R is the gas constant.

At temperature T_c the hydrogen gas pressure desorbing from the cold hydride is given by the van't Hoff equation, where ΔH and ΔS are the heat and entropy of desorption, respectively:

$$R\ln p_c = \frac{\Delta H}{T_c} - \Delta S \qquad (19)$$

and at the temperature T_m the hydrogen gas pressure absorbing into the warm hydride is,

$$R\ln p_m = \frac{\Delta H}{T_m} - \Delta S \qquad (20)$$

Combining equations 19 and 20, we obtain the pressure ratio,

$$\frac{p_m}{p_c} = \exp\left[\frac{\Delta H}{R}\left(\frac{1}{T_m} - \frac{1}{T_c}\right)\right] \qquad (21)$$

---

[1] K.T. Feldman, Jr., K. J. Kim, T. R. Way, G. Lloyd, A. Razani, "Compressor Driven Metal Hydride Heat Pumps," Conference Proceedings, 1996.

For the hydrides the pressure and temperature of the gas are described by the van't Hoff equations 19? and 20?. Equation 21? May be combined with equation 11? to give,

$$W = \frac{RT}{E} \cdot \frac{k}{k-1} \cdot \left(\exp\left[\frac{k-1}{k} \cdot \frac{\Delta H}{R} \cdot \left(\frac{1}{T} - \frac{1}{T} \right) \right] - 1 \right) \tag{22}$$

Equation 22 includes the assumption that the hydrogen flowing out of the compressor is cooled from T_h to T_m. To determine the efficiency, we must calculate the amount of cooling produced per mole of hydrogen,

$$q = -\Delta H - q_{loss} \tag{23}$$

where q_{loss} is the parasitic heat loss per mole of hydrogen due to heating and cooling the mass (m_c+m_{cont}),

$$q_{loss} = \frac{1}{n}\left(m_c C_p + m_{cont} C'_p\right)\left(T - T\right) \tag{24}$$

where the mass of the hydride is m_c with specific heat C_p, and the mass of the hydride container is m*cont* with specific heat C'_p, the amount of cooling per mole of hydrogen is given by $\bar{m} = m/n$ and

$m_{cont} = m/R_m$, where R_m accounts for the mass of the container with fins, and n is the number of moles of hydrogen desorbed per cycle. Thus equation 23 becomes,

$$q = -\Delta H - \bar{m}\left(C_p + \frac{C'_p}{R_m} \right)\left(T - T\right) \tag{25}$$

The COP can then be calculated from equations 27 and 11. For example, a hydride air conditioner operating with $LaNi_5$, where ΔH = -7380 cal/mole, C_p = 0.1 cal/g-K, C'_p = 0.11 cal/g-K, R_m = 2 (for a thin wall finned tube), $\bar{m} = 175.8$ g/mole hydrogen, T_m= 46°C, T_c= 8°C (the "standard" rating temperatures for air conditioners, including an 11°C temperature drop across each heat exchanger coil), and the cooling per mole is,

$$q = -(-7380) - (175.8)\cdot(0.1 + 0.11/2)\cdot(46 - 8)$$

(26)

$$= \text{[illegible] cal/mole hydrogen}$$

For isentropic compression, the efficiency for cooling is given by,

$$COP = \frac{q_c}{w_{cm}} = 5.76 \tag{27}$$

$$W_{cm} = (1.97)\cdot(283\ K)\cdot\frac{1.4}{1.4-1}\left[\exp\left(\frac{1.4-1}{1.4}\cdot\frac{-730}{1.97}\left[\frac{1}{309}-\frac{1}{283}\right]\right)-1\right] \tag{28}$$

$$w_{cm} = 12\ kJ/mole\ hydrogen$$

APPENDIX B: TABULATED ASSUMPTIONS

Table 38. Specified Conversion Efficiencies, Temperatures and) Ts for Electric Driven Heat Pump Cycle Calculations.

Technology	47EF Rating Point						17EF Rating Point						82EF Rating Point						95EF Rating Point					
	source	HX	) T	HX	sin k	) T	source	HX	) T	HX	sin k	) T	source	HX	) T	HX	sin k	) T	source	HX	) T	HX	sin k	) T
Electric Reverse Rankine Cycle	47	29	18	100	68	32	17	-14	31	85	68	17	80	49	31	105	82	23	80	49	31	120	95	25
Rankine Cycle (Hydrocarbon)	47	29	18	100	68	32	17	-14	31	85	68	17	80	49	31	105	82	23	80	49	31	120	95	25
Transcritical CO_2	47	33	14	73	68	5	17	-10	27	78	68	10	80	49	31	85	82	3	80	49	31	100	95	5
Brayton Cycle	47	29	18	100	68	32	17	10	7	85	68	17	80	49	31	105	82	23	80	49	31	120	95	25
Stirling Cycle	47	29	18	100	68	32	17	-14	31	10 0	68	32	80	49	31	105	82	23	80	49	31	120	95	25
Thermoelectric	47	29	18	100	68	32	17	-14	31	85	68	17	80	49	31	105	82	23	80	49	31	120	95	25
Thermoacoustic	47	29	18	100	68	32	17	-14	31	85	68	17	80	49	31	105	82	23	80	49	31	120	95	25
Pulse Tube	47	29	18	100	68	32	17	-14	31	85	68	17	80	49	31	105	82	23	80	49	31	120	95	25
Magnetic Cooling	47	29	18	105	68	37	17	5	12	90	68	22	80	44	36	110	82	28	80	44	36	125	95	30
Compressor Driven Metal Hydride	47	29	18	100	68	32	17	-14	31	10 0	68	32	80	49	31	105	82	23	80	49	31	120	95	25

Table 39. Specified Conversion Efficiencies, Temperatures and) Ts for Gas-Fired Heat Pump Cycle Calculations.

Technology	Conversion Efficiency	47EF Rating Point						17EF Rating Point						82EF Rating Point						95EF Rating Point					
		source	HX	) T	HX	sink	) T	source	HX	) T	HX	sink	) T	source	HX	) T	HX	sink	) T	source	HX	) T	HX	sink	) T
Gas Furnace / Electric Air Conditioner	0.80													80	49	31	105	82	23	80	49	31	120	95	25
Diesel Engine Driven	0.35	47	29	18	100	68	32	17	-14	31	85	68	17	80	49	31	120	82	38	80	49	31	135	95	40
IC Engine Driven HP	0.30	47	29	18	100	68	32	17	-14	31	85	68	17	80	49	31	120	82	38	80	49	31	135	95	40
Stirling Engine Driven	0.28	47	29	18	100	68	32	17	-14	31	85	68	17	80	49	31	120	82	38	80	49	31	135	95	40
Brayton Engine Driven	0.27	47	29	18	100	68	32	17	-14	31	85	68	17	80	49	31	120	82	38	80	49	31	135	95	40
Rankine Engine Driven	0.24	47	29	18	100	68	32	17	-14	31	85	68	17	80	49	31	120	82	38	80	49	31	135	95	40
Fuel Cell Powered HP	0.40	47	29	18	100	68	32	17	-14	31	85	68	17	80	49	31	105	82	23	80	49	31	120	95	25
Vuilleumier Cycle HP	0.80	47	29	18	102	68	34	17	10	7	72	68	4	80	49	31	137	82	55	80	49	31	150	95	55
Absorption Cycle																									
single-effect	0.80	47	29	18	100	68	32	17	10	7	85	68	17	80	49	31	105	82	23	80	49	31	120	95	25
double-effect	0.80	47	29	18	100	68	32	17	10	7	85	68	17	80	49	31	105	82	23	80	49	31	120	95	25
GAX	0.80	47	29	18	100	68	32	17	10	7	85	68	17	80	49	31	105	82	23	40	49	31	120	95	25
Duplex Stirling	0.28	47	29	18	100	68	32	17	-14	31	85	68	17	80	49	31	120	82	38	80	49	31	135	95	40
Ejector Heat Pump	0.80	47	29	18	101	68	33	17	-14	31	101	68	33	80	49	31	105	82	23	80	49	31	120	95	25

APPENDIX C: MODELED, OBSERVED, AND REPORTED EFFICIENCIES (REALITY CHECK)

Table 40. Comparison of Modeled and Reported COPs and Efficiencies.

Technology	Temperature Condition	Modeled Value	Observed Value	Source
Thermoacoustic Cooling	95EF	0.39	2.3 to 2.5	Steve Garrett, personal communication
	95EF	0.39	1.7 to 2.0	Greg Swift, personal communication
IC-Engine Driven HP	gCOP(heat)	1.45	1.3	Nowakowski 1996, p. 46
	gCOP(heat)	1.45	1.27	Nowakowski 1995, p. 1386
	gCOP(cool)	0.89	1.1	Nowakowski 1996, p. 46
	95EF	0.88	0.9	Nowakowski 1995, p. 1384
	IPLV		0.77	ThermoKing Brochure, p. 25
	gCOP(cool)	0.89	0.72	Aisin Brochure, back cover
Diesel Engine Driven HP	gCOP(heat)	1.57	1.3	Yanmar Brochure (Y4GPB-PRC)
	gCOP(cool)	1.05	0.9	Yanmar Brochure (Y4GPB-PRC)
Stirling Engine Driven HP	47EF	1.63	1.09	Aisin Seiki
	47EF	1.63	1.57	Aisin Seiki (70% heat recovery)
	47EF	1.63	1.80	SPS
	47EF	1.63	1.36	Sunpower (90% heat recovery)
	15EF	1.56	1.08	Sunpower (90% heat recovery)
	95EF	0.70	0.91	Aisin Seiki
	95EF	0.70	1.10	SPS
	95EF	0.70	0.42	Sunpower
	85EF	0.88	1.0	Sunpower
Brayton Engine Driven HP	47EF	1.59	1.2 to 1.4	GRI/DOE
	95EF	0.68	1.0	GRI/DOE
Single-Effect Absorption	heating	1.30	0.81	Servel
	cooling	0.56	0.5 to 0.6	Servel
	cooling	0.56	0.62	DeVault
Double-Effect Absorption	IPLV	0.94	0.96	DeVault
Adsorption: Complex Compounds	30EF		1.7	Rockenfeller 1992
	gCOP(cool)		1.0	Rockenfeller 1992
	gCOP(heat)		1.5	Bill Ryan 1992
	gCOP(cool)		1.0	Bill Ryan 1992
Adsorption: Ammoniated Carbon	gCOP(heat)		1.30	WaveAir
	gCOP(cool)		1.00	WaveAir
	47EF		1.9 to 2.4	JPL
	95EF		1.0 to 1.7	JPL
	17EF		1.5 to 1.8	JPL
	82EF		1.3 to 1.6	JPL
Adsorption: Water Zeolite	gCOP(heat)		1.8	Tchernev 1988
	gCOP(cool)		1.2	Tchernev 1988

Table 41. Comparison of Modeled and Reported COPs and Efficiencies (cont).

Technology	Temperature Condition	Modeled Value	Observed Value	Source
Adsorption: Water / Zeolite	gCOP(cool) gCOP(cool) gCOP(heat)		0.4 to 0.5 1.2 1.8	Tchernev 1988 (w/o regeneration) Tchernev 1988 (w/ regeneration) Tchernev 1988 (w/ regeneration)
Electric Heat Pump	47EF 17EF 95EF 82EF HSPF SEER	3.83 2.60 3.21 4.02 8.2 11.9	3.84 2.60 2.66 8.3 12.0	Carrier Product literature Carrier Product literature Carrier Product literature Carrier Product literature Carrier Product literature
Geothermal Heat Pumps	HSPF SEER		2.7 to 3.6 9.6 to 12.6	L'Ecuyer 1993 L'Ecuyer 1993
Compressor Driven Metal Hydride	95EF	3.12	3.22	Kim 1997
Transcritical CO_2	47EF 95EF	3.78 2.32	2.49 2.27	Bullock 1997 Bullock 1997
Brayton Cycle	47EF 17EF 95EF 82EF HSPF SEER	1.73 1,71 0.92 0.98 5.0 2.9		
Stirling Cycle	47EF 17EF 95EF 82EF HSPF SEER	1.67 1.50 0.86 0.93 4.7 2.7		
Thermoelectric	47EF 17EF 95EF 82EF HSPF SEER	1.40 1.31 0.62 0.86 4.4 2.9		

APPENDIX D: TABULATED ASSUMPTIONS

Average price of natural gas (\$ per 1000 ft^3) to residential customers in 1997 listed by state (Energy Information Agency (EIA) Form-176, "Annual Report of Natural Gas Supply and Disposition):

Alabama	$8.35	Louisana	$7.16	Ohio	$6.75
Alaska	$3.77	Maine	$8.47	Oklahoma	$6.23
Arizona	$7.83	Maryland	$8.36	Oregon	$6.21
Arkansas	$6.67	Massachusetts	$9.43	Pennsylvania	$8.33
California	$6.81	Michigan	$5.20	Rhode Island	$9.61
Colorado	$4.81	Minnesota	$5.76	South Carolina	$8.37
Connecticut	$10.33	Mississippi	$6.35	South Dakota	$5.75
Delaware	$8.36	Missouri	$6.61	Tennessee	$6.91
Florida	$11.90	Montana	$5.05	Texas	$6.32
Georgia	$7.41	Nebraska	$5.69	Utah	$5.13
Hawaii	$21.74	Nevada	$6.27	Vermont	$6.41
Idaho	$5.12	New Hampshire	$8.48	Virginia	$8.60
Illinois	$5.95	New Jersey	$7.93	Washington	$5.64
Indiana	$6.37	New Mexico	$5.87	West Virginia	$6.81
Iowa	$6.17	New York	$9.73	Wisconsin	$6.43
Kansas	$6.42	North Carolina	$8.98	Wyoming	$4.58
Kentucky	$6.37	North Dakota	$4.99	U.S. Average	$6.94

Data taken from an electronic document located at:

ftp://ftp.eia.doe.gov/pub/oil_gas/natural_gas/data_publications/natural_gas_annual/current/pdf/table_024.pdf

Estimated U.S. Electric Utility Revenue From Residential Consumers (¢ per kWh) for 1998 (Energy Information Administration, Form EIA-286, “Monthly Electric Utility Sales and Revenue Report with State Distribution).

Alabama	7.0	Louisiana	7.1	Ohio	8.7
Alaska	11.6	Maine	12.8	Oklahoma	6.7
Arizona	8.8	Maryland	8.6	Oregon	5.9
Arkansas	7.3	Massachusetts	10.5	Pennsylvania	10.0
California	10.5	Michigan	8.8	Rhode Island	11.2
Colorado	7.4	Minnesota	7.4	South Carolina	7.5
Connecticut	12.0	Mississippi	7.0	South Dakota	7.2
Delaware	9.2	Missouri	7.2	Tennessee	6.3
Florida	7.9	Montana	6.6	Texas	7.7
Georgia	7.7	Nebraska	6.6	Utah	6.9
Hawaii	13.9	Nevada	7.0	Vermont	11.5
Idaho	5.3	New York	14.1	Virginia	7.7
Illinois	10.0	New Jersey	11.7	Washington	5.0
Indiana	7.1	New Mexico	9.0	West Virginia	6.3
Iowa	8.6	New Hampshire	13.6	Wisconsin	7.2
Kansas	7.7	North Dakota	6.5	Wyoming	6.4
Kentucky	5.7	North Carolina	8.1	U.S. Average	8.31

Electricity costs for residential cosumers was taken from an electronic document located at http://www.eia.doe.gov/cneaf/electricity/epm/epmt55.txt

Energy cost ratios by state (1000 Btu natural gas per $ / 1000 Btu electric per $):

Alabama	2.52	Indiana	3.35	Nebraska	3.48
Alaska	9.24	Iowa	4.19	Nevada	3.35
Arizona	3.38	Kansas	3.60	New Hampshire	4.82
Arkansas	3.29	Kentucky	2.69	New Jersey	4.43
California	4.63	Louisiana	2.98	New Mexico	4.60
Colorado	4.62	Maine	4.54	New York	4.35
Connecticut	3.49	Maryland	2.98	North Carolina	2.71
Delaware	3.30	Massachusetts	3.34	North Dakota	3.91
Florida	1.99	Michigan	5.08	Ohio	3.87
Georgia	3.12	Minnesota	3.86	Oklahoma	3.23
Hawaii	1.92	Mississippi	3.31	Oregon	2.85
Idaho	3.11	Missouri	3.27	Pennsylvania	3.61
Illinois	5.05	Montana	3.93	Rhode Island	3.50

South Carolina	2.69
South Dakota	3.76
Tennessee	2.74
Texas	3.66
Utah	4.04
Vermont	5.39
Virginia	2.69
Washington	2.66
West Virginia	2.78
Wisconsin	3.36
Wyoming	4.20
U.S. Average	3.60

APPENDIX E: ECONOMIC ANALYSIS

Seasonal performance factors and economic analyses are performed for the following 117 cities using typical weather year data and state-wide averages for gas and electric rates. The distribution of these cities across the U.S. is shown in Fig. 52. Building loads are computed for a two-story, 2000 ft^2 home with "typical" insulation (using binned temperature data from the Air Force Weather Manual for each of the following cities:

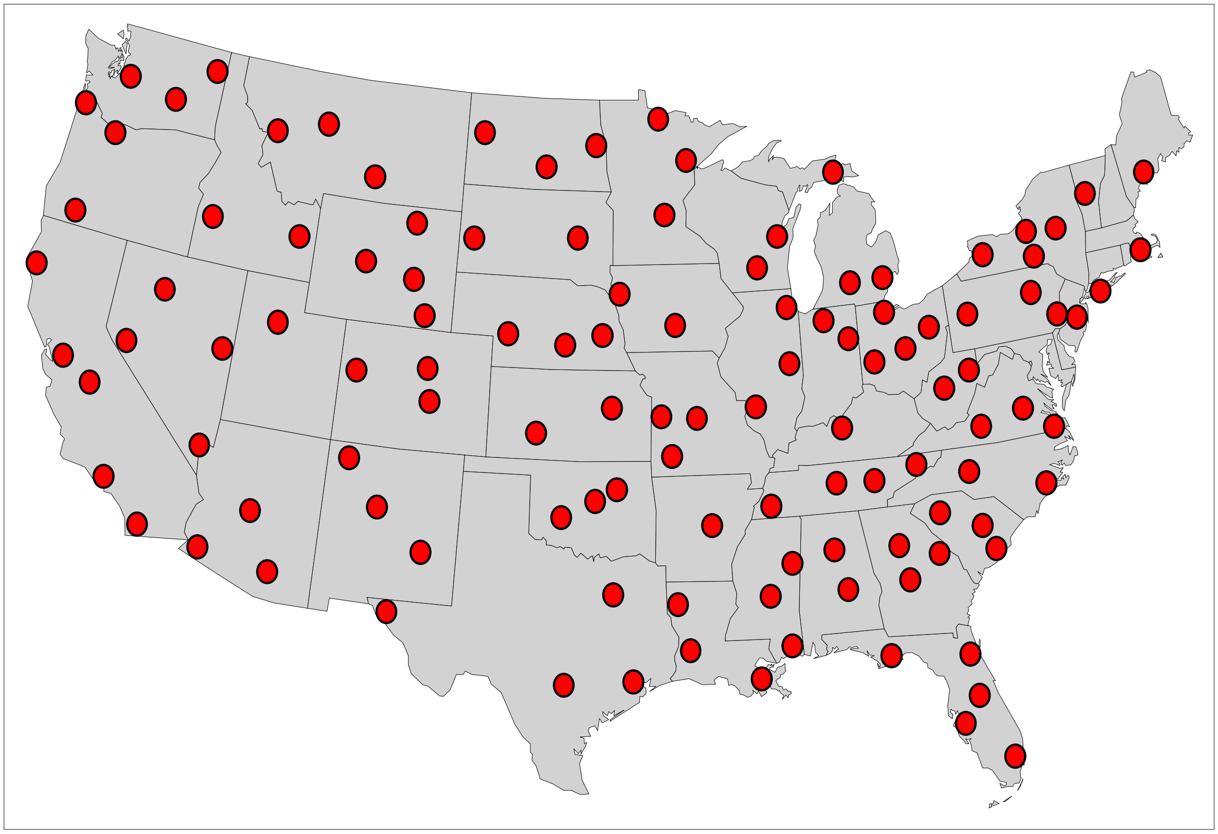

Fig. 52. Distribution of weather data across the U.S. for heating and cooling calculations.

Birmingham, Alabama
Montgomery, Alabama
Phoenix, Arizona
Tucson, Arizona
Yuma, Arizona
Little Rock, Arkansas
Arcata, California
Los Angeles, California
Merced, California
Oakland, California
San Diego, California
Colorado Springs, Colorado

Denver, Colorado
Grand Junction, Colorado
Appalachicola, Florida
Jacksonville, Florida
Miami, Florida
Orlando, Florida
Tampa, Florida
Atlanta, Georgia
Augusta, Georgia
Macon, Georgia
Des Moines, Iowa

Sioux City, Iowa
Boise, Idaho
Idaho Falls, Idaho
Champaigne-Urbana, Illinois
Chicago, Illinois
East St. Louis, Illinois
Fort Wayne, Indiana
South Bend, Indiana
Dodge City, Kansas
Topeka, Kansas
Louisville, Kentucky
Lake Charles, Louisiana
New Orleans, Louisiana
Shreveport, Louisiana
Portland, Maine
Falmouth, Massachusetts
Battle Creek, Michigan
Detroit, Michigan
Sault Ste Marie, Michigan
Duluth, Minnesota
International Falls, Minnesota
Minneapolis, Minnesota
Biloxi, Mississippi
Columbus, Mississippi
Jackson, Mississippi
Columbia, Missouri
Kansas City, Missouri
Springfield, Missouri
Billings, Montana
Great Falls, Montana
Missoula, Montana
Grand Island, Nebraska
Lincoln, Nebraska
North Platte, Nebraska
Ely, Nevada
Las Vegas, Nevada
Reno, Nevada
Winnemucca, Nevada
Trenton, New Jersey
Albuquerque, New Mexico
Farmington, New Mexico
Roswell, New Mexico
Albany, New York
Binghamton, New York
Niagara Falls, New York
Syracuse, New York
Westhampton Beach, New York
Greensboro, North Carolina
New Bern, North Carolina
Bismarck, North Dakota
Grand Forks, North Dakota
Williston, North Dakota
Akron, Ohio
Columbus, Ohio
Dayton, Ohio
Toledo, Ohio
Altus, Oklahoma
Oklahoma City, Oklahoma
Tulsa, Oklahoma
Astoria, Oregon
Medford, Oregon
Portland, Oregon
Philadelphia, Pennsylvania
Pittsburgh, Pennsylvania
Wilkes-Barre, Pennsylvania
Charleston, South Carolina
Greenville, South Carolina
Sumter, South Carolina
Huron, South Dakota
Rapid City, South Dakota
Bristol, Tennessee
Knoxville, Tennessee
Memphis, Tennessee
Nashville, Tennessee
El Paso, Texas
Fort Worth, Texas
Houston, Texas
San Antonio, Texas
Salt Lake City, Utah
Burlington, Vermont
Norfolk, Virginia
Richmond, Virginia
Roanoke, Virginia
Moses Lake, Washington
Seattle, Washington
Spokane, Washington
Charleston, West Virginia
Elkins, West Virginia
Green Bay, Wisconsin
Madison, Wisconsin
Casper, Wyoming
Cheyenne, Wyoming
Lander, Wyoming
Sheridan, Wyoming

The results for economic comparisons depend on system efficiencies for the baseline and alternative technologies, heating and cooling loads and climate variables, energy costs, and the relative costs of gas and electricity. Appendix D tabulates the average costs of gas and electricity in each state in the U.S. and the ratio of energy costs (i.e. Btus that can be purchased for $1.00 spent on natural gas divided by the number of Btus that can be purchased for a $1.00 spent on electricity). In general, gas-fired systems compare more favorably with the electric heat pump baseline in the cities where the “heat content” of a dollar of natural gas is high compared to the “heat content” of a dollar of electricity. Burlington, Vermont; Albuquerque, Roswell, and Farmington, New Mexico; Albany, Binghamton, Niagara Falls, Syracuse, and Westhampton Beach, New York; and Portland, Maine are good locations for efficient gas-fired equipment based on the gas and electric rates.

APPENDIX F: MAINTENANCE COST ASSUMPTIONS

Electric-Driven Heat Pumps

1.	Reverse Rankein Cycle Heat Pump	
	a) R-22	$100
	b) Propane	$100
	c) Transcritical CO_2	$100
2.	Brayton Cycle	$100
3.	Stirling Cycle	$100
4.	Thermoelectric Cooling	$25
5.	Thermionic Cooling	$25
6.	Thermoacoustic Cooling	$100
7.	Pulse Tube Refrigeration	$100
8.	Magnetic Refrigeration	$125
9.	Compressor Driven Metal Hydride Heat Pump	$110

Gas-Fired Heat Pumps

10.	Gas Furnace and Electric Air Conditioner	$100
11.	Engine Driven Rankine Cycle Heat Pumps	
	a) IC engine	$125
	b) Diesel Engine	$125
	c) Stirling Engine	$125
	d) Brayton Engine	$125
	e) Rankine Engine	$125
12.	Fuel Cell Powered Rankine Cycle Heat Pump	$200
13.	Absorption Cycles	
	a) Single Effect	$100
	b) GAX Cycle	$100
	c) Double Effect	$100
14.	Vuilleumier Cycle Heat Pump	$75
15.	Duplex Stirling Heat Pump	$125

APPENDIX G: BUILDING LOAD CALCULATIONS

Heating and cooling loads are computed using the ORNL APF / Loads Model with binned weather data from the Air Force Weather Manual[1] . The ORNL APF / Loads Model is documented in an unpublished draft report by C. K. Rice and S. K. Fischer in the Building Equipment Research Program of the Energy Division at Oak Ridge National Laboratory. The APF / Loads Model was written to compute seasonal and annual performance factors for single- and variable-speed electric heat pumps. It incorporated FORTRAN subroutines to compute building heating and cooling loads from the MAD[2] program for the design of Annual Cycle Energy Systems; MAD in turn used subroutines from the NBSLD[3] program from the National Bureau of Standards. The loads calculation from NBSLD is treated as a black box and is taken as sufficiently accurate for the comparisons of annual energy use performed in the current project.

Building specification data are used for a two-story, 2000 ft^2 home with typical levels of insulation, window glazing, and air infiltration. The walls are assumed to be of frame construction with R-11 fiberglass batt insulation and ½ in. polyurethane sheathing; the overall roof R-value is 20; the floor R-value is 10; there are single pane windows; and one air change per hour. The average monthly internal sensible heat source rates are set at 4300 Btu/h. The building walls are defined as:

- North - 426 ft^2 including 54 ft^2 of windows;
- East - 204 ft^2 including 36 ft^2 of windows;
- South - 426 ft^2 including 54 ft^2 of windows;
- West - 204 ft^2 including 36 ft^2 of windows;

The summer and winter thermostat settings are assumed to be 78E and 70E, respectively, and the design wet bulb temperature is 66EF.

The main program from the APF model was modified to loop through a list of weather data files, store the name of each city, the corresponding design heating and cooling loads, and the annual binned temperatures and hours. These data are written into an ASCII data file that can be imported into EXCEL for analysis; each column of the data file corresponds to the binned loads and temperatures for a single city. The data were organized to group cities by DOE climate region. This appeared to be a meaningful way to structure the economic analysis which turned out to be less useful than expected. FORTRAN programs used in this analysis are stored in the file folder “C:\NIK Technologies\APF & Loads Calculations\Source.” The main program is in file “LDSCAL2.FOR” and the list of subroutines needed to compile and like the program are in “LODFILES.FOR.” The latter file also contains the

---

[1] *Engineering Weather Data*, Departments of the Air Force, the Army, and the Navy, AFM 88-29, TM 5-785, NAVFAC P-89, July 1978.

[2] *MAD: A Computer Program for ACES Design Using Monthly Thermal Loads*, M. L. Ballou, E. A. Nephew, and L. A. Abbatiello, ORNL/CON-51, March 1981.

[3] NBSLD: *The Computer Program for Heating and Cooling Loads in Buildings*, T. Kusuda, NBS Building Science Series 69, July 1976.

control specification to compile and load the program using the SVS FORTRAN compiler. All of the FORTRAN subroutines for this program use "INCLUDE" statements to incorporate COMMON blocks; these statements point to the included files using subdirectory or folder names that need to be changed to correspond to how the files are stored.

APPENDIX H: THERMIONIC CONVERTERS

Theory of a Thermionic Converter

Labinov assembled a derivation of the theoretical efficiency of thermionic converters from multiple sources. Heat is transfered by the current flowing between the electrodes and the current density is given by Richardson's formula:

$$J = A T^{2} e^{-\varphi_0 / KT} \tag{29}$$

where A is the thermionic constant (120 A/cm^2·K^2), T is the absolute temperature of the electrode (K), K is the Boltzmann constant (1.3806 x 10^{-23} W/K sec), and φ_0 is the work function of an electron (eV). The heat transfered is then given by:

$$Q = \frac{\varphi_0 + 2KT}{e_0} J \tag{30}$$

where e_0 is the charge of an electron (1.602 x 10^{-13} Coulomb). It follows that both the current, J, and heat transfer, Q, increase as the temperature, T, increases. The net current between two electrodes is the difference between the current from the hot electrode to the cold electrode and the current in the opposite direction:

$$J = J_{h-c} - J_{c-h} \tag{31}$$

where J_{h-c} is the current from the hot electrode to the cold electrode and J_{c-h} is the current in the opposite direction.

If φ_0 is the same for both electrodes, then other things being equal the electrons will move from the hot electrode to the cold electrode and the thermionic converter will operate as an electrogenerator. At least two conditions must be met to make a thermionic converter operate as a refrigeration device:

- the current specific density must be great enough to provide the necessary heat transfer. Figure 53 shows the relationship of φ_0 and T assuming that a current specific density of 1 A/cm^2 is the minimum acceptable value for practical purposes. This dependence is practically linear and φ_0 should be 0.3 eV to provide the specified current density at a temperature below 250 K (-10°F).
- when electrons move in the interelectrode space, a space charge is formed of the voltage ΔV_1. The voltage ΔV_1 applied to the electrodes must overcome that charge and also the potential barrier of the hot electrode (collector) surface, then:

$$J = J - J\, e^{\frac{\cdot}{\cdot\, C}} \qquad (32)$$

$$Q = \frac{(\phi + 2KT)}{e} J - \frac{(\phi + 2KT)}{e} J\, e^{-} \qquad (33)$$

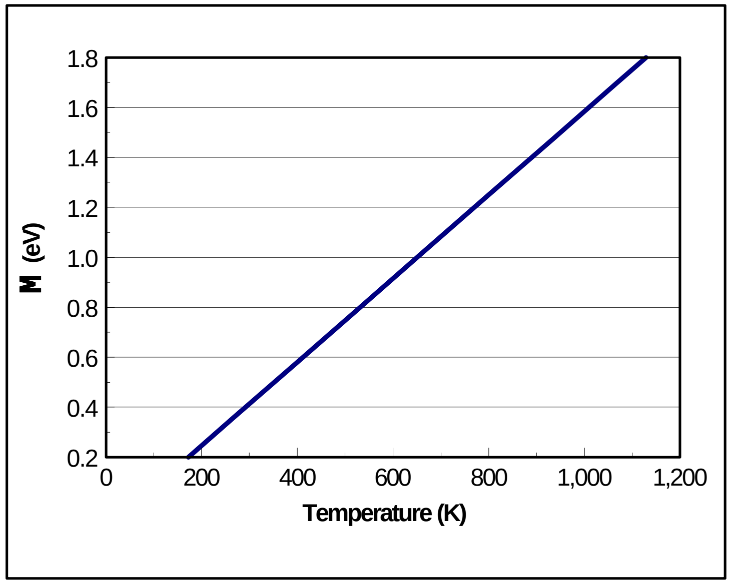

Fig. 53. Relationship between the work function and electrode temperature for a Richardson current of 1 amp/cm^2.

So the total voltage applied to a thermionic refrigerator should consist of two parts:

$$V = \Delta V + \Delta V \qquad (34)$$

where ΔV_1 is the voltage drop across the interelectrode space and ΔV_2 is the voltage drop of an external circuit. Not only the value of current may change depending on the value of the electric field voltage of the interelectrode space, but the direction of current and heat transfer may change as well.

The preceding equations show that for fixed temperatures T_C and T_E, the efficiency depends on N_0 and ΔV. Current strength grows as N_0 decreases, but Q is decreasing at the same time as N_0 »KT. The total current increases as ΔV increases, but the energy consumption of the process increases at the same time.

Model of a Thermionic Converter

Figure 54 illustrates the components and electron flow of an operating thermionic cooling device using ballistic electrons (Edelson) or the tunneling effect (Mahan). Electrical energy is required so the heat flow going from an external source to the cathode can be transferred from the electrode at a lower temperature (the emitter) to the electrode at a higher temperature (collector) where it can be rejected to the ambient. The electron cooling rate (Watts) is given by:

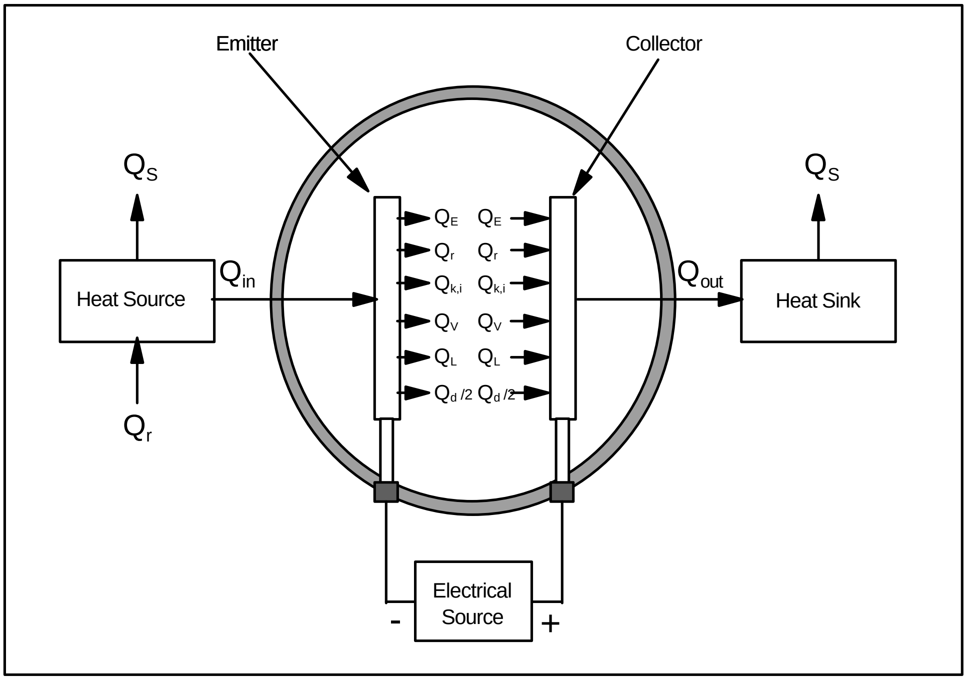

Fig. 54. Energy transfer rates in a thermionic refrigerator.

$$Q_E = SJ_E\,\frac{\phi_E + 2KT_E}{e} - SJ_C\,\frac{\phi_E + 2KT_C}{e}\,e^{\frac{\cdots}{\cdots C}} \qquad (35)$$

where:

S is the emitter surface area (cm^2),

T_E is the emitter temperature (K),

T_C is the collector temperature (K),

J_E is the current formed by the electrons emitted by the cathode at temperature T_E ($A/sec\cdot cm^2$), and

J_C is the current formed by the electrons emitted by the anode at temperature T_C ($A/sec\cdot cm^2$).

The rate of interelectrode thermal radiation is given by:

$$Q_r = S\sigma_0\,\varepsilon\left(T_E^4 - T_C^4\right) \qquad (36)$$

where:

σ_0 is the Stephan-Boltzmann radiation constant (5.67 x 10-12 $W/cm^2\cdot K^4$), and

ε is the net effective thermal emissivity ($\varepsilon \leq 1$).

This expression for Q_r does not include any thermal radiation energy transfer through surface areas of electrodes other than those facing the interelectrode space. The value of ε may be used to account for the influence of a thin layer of a dielectric placed between the two electrodes. Nobody has examined how a superthin film which is easily penetrated by electrons affects radiant heat flow.

The heat conduction rate through the electrical leads associated with the emitter consists of the sum of two terms: $Q_L+½Q_d$. The first term, Q_L, is the rate heat would be conducted through the lead when there is no current flow. This is given by:

$$Q_L = K_L \frac{S_L}{l_L}\left(T - T\right) \tag{37}$$

where:

K_L is the lead thermal conductivity,
S_L is the lead cross-sectional area, and
l_L is the length of the electrical leads.

The second term in the conduction heat transfer arises because half of the Joule heat rate, Q_d, generated in the electrical leads is transfered back to the collector. This term is given by the relationship:

$$\frac{1}{2}Q_d = \frac{1}{2}SJV_L = \frac{1}{2}S J \rho_L \frac{l_L}{S_L} \tag{38}$$

where:

V_L is the voltage drop across the leads and
ρ_L is the electrical resistivity of the leads.

If the heat conduction rate through the structural components connected to the collector are designated as $Q_{k,i}$ and the heat conduction rate through the interelectrode space as Q_v (when there is a semiconductor film between the electrodes), then:

$$Q_k = Q_{k,i} + Q_v = g_k\left(T - T\right) \tag{39}$$

where g_k is the sum of the thermal conductivities, g_i, of the interelectrode space and the structural materials connected to the emitter. The total heat transferred to the anode (collector) should be equal to the total quantity of heat transfered to the external source (Q_0), that is:

$$Q_0 = Q + Q + Q + Q + \frac{1}{2}Q_d + Q \tag{40}$$

and the electrical energy suppled to transfer the heat is:

$$W = S \cdot J \cdot V \tag{41}$$

where $V=V_T+V_L$ and

V_T is the space charge voltage drop across the interelectrode space and

V_L is the voltage drop across the external circuit.

The efficiency of the thermionic converter is then:

$$0 \; ' \; \frac{Q}{W} \; ' \; \frac{Q \,\%Q \,\%Q \,\% \frac{1}{2} Q \,\%Q}{S@J@V} \qquad (42)$$

Defining the “electronic efficiency” as the maximum possible efficiency associated with strictly electronic processes under ideal conditions of transport in the interelectrode space:

$$\Theta \; ' \; \frac{Q}{S@J@V} \qquad (43)$$

Figure 55 shows the calculated efficiency for T_E = 500 K, T_C = 700K, and N0 = 0.7 eV for both electrodes. The changes in efficiency The change in efficiency is shown against the change of voltage applied between the electrodes ( ) V_1). The figure also shows that the direction of heat flow changes at the critical value of) V = 0.323 V, and the process of heat transfer from the cold electrode (emitter) to the hot electrode (collector) begins. The maximum value of calculated COP is 2.08 while the theoretical value is 2.5 in this case. Under these circumstances, the specific density of the transfered heat is 1W/cm^2. The maximum efficiency of the thermionic converter is 80% of that of the Carnot cycle.

The practical value of COP is much lower than that shown in Fig. 55 because of the losses in a real device. It is clear from the relations above that these losses will be reduced for a lower temperature drop in the electrodes and for a smaller interelectrode space. The relative efficiency is given by:

$$0 \; ' \; \frac{0}{0} \qquad (44)$$

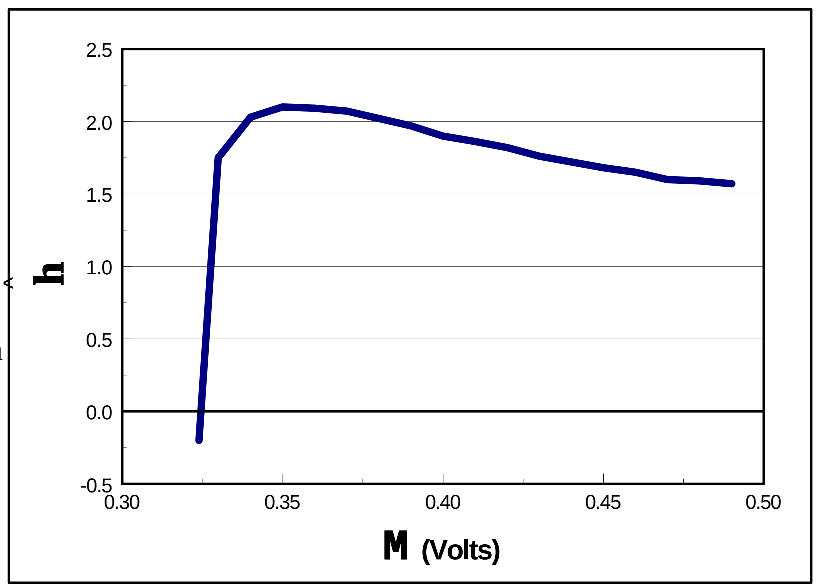

Fig. 55. Theoretical efficiency of a thermionic converter.

where

0_r is the real value of a thermionic converter efficiency including heat losses and

0_c is the Carnot efficiency at the same temperatures.

Figure 56 shows the relative efficiency against the integral factor that characterizes the thermal resistance of the thermionic converter. It is clear that the real efficiency decreases with the thermal resistance N and approaches 5 to 10% of Carnot efficiency.

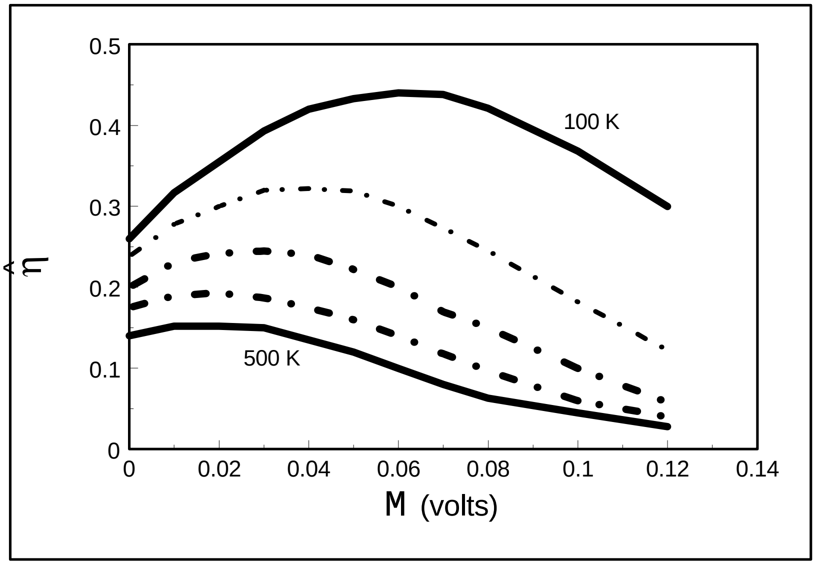

Fig. 56. Reduction in real efficiency for a thermionic converter.

APPENDIX I: MALONE REFRIGERATION

An examination of the thermodynamic relationships provides some insights into the Malone cycle. First, the first and second laws of thermodynamics give:

$$TdS = dU + pdV \tag{45}$$

and for adiabatic compression (TdS = 0), this becomes:
As V=f(p,T), then:

$$dU = -pdV \tag{46}$$

$$dV = \left(\frac{\partial V}{\partial p}\right)_T dp + \left(\frac{\partial V}{\partial T}\right)_p dT \tag{47}$$

where

$$\left(\frac{\partial V}{\partial p}\right)_T = K_p \tag{48}$$

is the coefficient of isothermic compression and

$$\left(\frac{\partial V}{\partial T}\right)_p = \beta_T \tag{49}$$

is the coefficient of isobaric compression. Substitution of the ideal gas equation (pV=RT) gives $K_p=RT/p^2$ and $\beta_T=R/p$. So, K_p depends on the absolute value of the pressure than β_T does. This principal depends holds for gases as well as liquids, although the total pressure includes internal and external pressures. The external pressures are similar for liquids and gases, but the internal pressures of a liquid is caused by surface tension and depends on its temperature and chemical composition; the liquid internal pressure can be hundreds or thousands of atmospheres of pressure. So the values of K_p and β_T are much lower for a liquid than a gas; a liquid is practically incompressible. As a result, the adiabatic compression of a gas requires considerably greater work than the adiabatic compression of a liquid under the same pressure drop. On the contrary, a considerably larger amount of power is released with gas expansion than with liquid expansion.

Heat transfer in an isobaric process (the Brayton cycle) is given by:

$$
\begin{aligned}
&\delta Q = T\,dS + p\,dV \\
&\Rightarrow \\
&T\,dS = C_p\,dT + p\,dV \\
&\Rightarrow \\
&T\left(\frac{\partial S}{\partial T}\right)_p = C_p + p\left(\frac{\partial V}{\partial T}\right)_p
\end{aligned}
\tag{50}
$$

and

$$
\begin{aligned}
&Q = C_p \int dT + p \int \left(\frac{\partial V}{\partial T}\right)_p dT \\
&\Rightarrow \\
&Q = C_p\left(T_2 - T_1\right) + p\beta_T \left(T_2 - T_1\right)
\end{aligned}
\tag{51}
$$

So the heat transfer for the isobaric process in the Brayton cycle Malone system depends on β_T but not on K_p. It can also be shown that heat transfer for the Stirling cycle process depends on the coefficient of isobaric compression, β_T, but not on the coefficient of isothermic compression, K_p. Figure 57 shows lines of constant isothermic (dashed) and isobaric (solid) compression coefficients for carbon dioxide; the labels on the lines show how K_p changes slowly from 0.01 to 0.02 away from the critical point on the left of the drawing, but rapidly from 0.20 to 1.0 near the critical point on the right. Similar changes can be seen for β_T.

Under normal conditions, β_T is much smaller for a liquid than it is for a gas because of the exclusively strong compression resulting from surface tension forces. As the critical point is approached, however, the density of the liquid and the density of the equilibrium gas approach each other very quickly and the surface tension forces begin to decrease and become zero at the critical point. As a result, β_T and K_p increase as the critical point is approached from the liquid side.

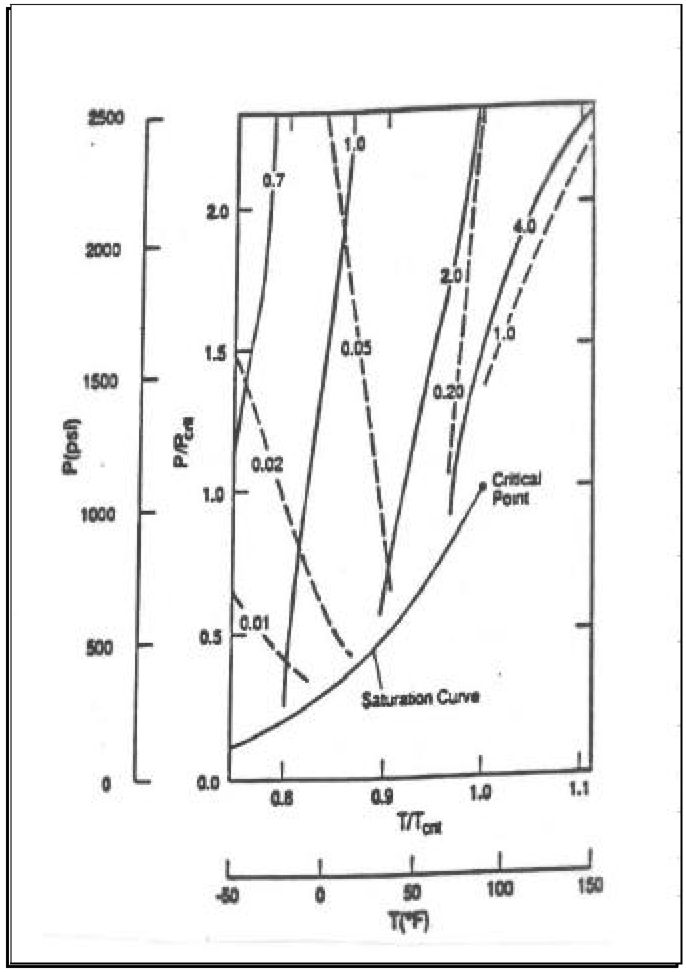

Fig. 57. K_p (dashed lines) and $\$_T$ (solid lines) near the critical point of CO_2.

APPENDIX J: GAS AND ELECTRICAL CONSUMPTION FOR EACH TECHNOLOGY

State and City	Electric Heat Pump (kWh/y)	Electric Heat Pump (therms/y)	Gas Furnace/Electric AC (kWh/y)	Gas Furnace/Electric AC (therms/y)	Hydrocarbon Heat Pump (kWh/y)	Hydrocarbon Heat Pump (therms/y)	Transcritical CO_2 Heat Pump (kWh/y)	Transcritical CO_2 Heat Pump (therms/y)
Alabama								
Birmingham	7,294	0	3,870	463	7,316	0	8,364	0
Montgomery	7,095	0	4,597	362	7,118	0	8,318	0
Arizona								
Phoenix	9,261	0	7,688	253	9,300	0	11,939	0
Tucson	7,787	0	5,998	280	7,815	0	9,572	0
Yuma	9,399	0	8,408	169	9,443	0	12,433	0
Arkansas								
Little Rock	7,763	0	4,205	501	7,788	0	9,006	0
California								
Arcata	5,627	0	518	729	5,615	0	5,700	0
Los Angeles	3,629	0	2,254	226	3,628	0	3,824	0
Merced	6,627	0	3,856	428	6,640	0	7,680	0
Oakland	4,189	0	1,473	438	4,179	0	4,284	0
San Diego	2,949	0	1,806	197	2,947	0	3,062	0
Colorado								
Colorado Springs	14,585	0	2,000	1,154	14,620	0	15,335	0
Denver	14,454	0	1,990	1,137	14,487	0	15,223	0
Grand Junction	11,278	0	2,991	945	11,319	0	12,353	0
Florida								
Appalachicola	6,461	0	5,221	191	6,483	0	7,659	0
Jacksonville	6,481	0	5,190	199	6,504	0	7,753	0
Miami	7,128	0	6,982	23	7,161	0	8,739	0
Orlando	6,227	0	5,462	119	6,250	0	7,470	0
Tampa	6,689	0	6,151	84	6,716	0	8,162	0
Georgia								
Atlanta	7,475	0	3,128	562	7,495	0	8,301	0
Augusta	7,174	0	4,149	428	7,197	0	8,314	0
Macon	6,948	0	4,384	374	6,970	0	8,102	0
Idaho								
Boise	11,150	0	2,395	1,054	11,184	0	12,046	0
Idaho Falls	18,976	0	1,750	1,475	19,019	0	19,761	0
Illinois								
Champaigne-Urbana	15,043	0	2,530	1,177	15,087	0	15,985	0
Chicago	15,297	0	1,924	1,265	15,336	0	16,106	0
East St. Louis	11,435	0	3,188	905	11,474	0	12,495	0
Indiana								
Fort Wayne	13,586	0	2,204	1,140	13,626	0	14,445	0
South Bend	14,537	0	2,091	1,205	14,578	0	15,373	0
Iowa								
Des Moines	17,312	0	2,360	1,250	17,355	0	18,239	0
Sioux City	18,402	0	2,663	1,306	18,454	0	19,476	0
Kansas								
Dodge City	12,086	0	3,284	926	12,128	0	13,299	0
Topeka	12,933	0	3,205	985	12,977	0	14,066	0
Kentucky								
Louisville	9,640	0	3,278	767	9,672	0	10,647	0
Louisiana								
Lake Charles	6,676	0	5,047	246	6,697	0	7,936	0
New Orleans	6,126	0	4,812	201	6,146	0	7,278	0
Shreveport	7,526	0	4,623	410	7,550	0	8,816	0

State and City	Electric Heat Pump (kWh/y)	Electric Heat Pump (therms/y)	Gas Furnace/Electric AC (kWh/y)	Gas Furnace/Electric AC (therms/y)	Hydrocarbon Heat Pump (kWh/y)	Hydrocarbon Heat Pump (therms/y)	Transcritical CO_2 Heat Pump (kWh/y)	Transcritical CO_2 Heat Pump (therms/y)
Maine								
Portland	16,743	0	1,490	1,349	16,778	0	17,379	0
Massachusetts								
Falmouth	12,390	0	1,386	1,087	12,411	0	12,861	0
Michigan								
Battle Creek	14,437	0	2,027	1,230	14,482	0	15,285	0
Detroit	15,483	0	1,994	1,273	15,527	0	16,286	0
Sault Ste Marie	26,637	0	1,215	1,777	26,676	0	27,263	0
Minnesota								
Duluth	31,461	0	1,174	1,949	31,499	0	32,065	0
International Falls	34,783	0	1,178	2,040	34,820	0	35,372	0
Minneapolis	22,354	0	1,981	1,513	22,402	0	23,218	0
Mississippi								
Biloxi	6,537	0	4,949	240	6,559	0	7,769	0
Columbus	7,795	0	4,138	495	7,820	0	8,979	0
Jackson	7,255	0	4,480	400	7,277	0	8,471	0
Missouri								
Columbia	11,678	0	3,137	908	11,715	0	12,749	0
Kansas City	11,275	0	3,518	854	11,316	0	12,487	0
Springfield	11,049	0	3,141	864	11,084	0	12,073	0
Montana								
Billings	16,638	0	2,009	1,277	16,673	0	17,439	0
Great Falls	20,870	0	1,700	1,476	20,899	0	21,526	0
Missoula	16,856	0	1,505	1,417	16,895	0	17,601	0
Nebraska								
Grand Island	16,601	0	2,672	1,232	16,650	0	17,680	0
Lincoln	16,520	0	2,489	1,209	16,566	0	17,495	0
North Platte	16,699	0	2,403	1,281	16,750	0	17,744	0
Nevada								
Ely	18,865	0	2,091	1,460	18,913	0	19,781	0
Las Vegas	9,367	0	6,709	400	9,405	0	11,766	0
Reno	12,163	0	2,426	1,125	12,203	0	13,015	0
Winnemucca	14,029	0	2,762	1,161	14,072	0	15,109	0
New Jersey								
Trenton	10,754	0	2,221	937	10,781	0	11,460	0
New Mexico								
Albuquerque	8,654	0	3,261	703	8,682	0	9,648	0
Farmington	11,886	0	2,977	965	11,927	0	12,908	0
Roswell	8,625	0	4,143	585	8,656	0	9,961	0
New York								
Albany	16,312	0	1,668	1,276	16,349	0	17,028	0
Binghamton	19,084	0	1,435	1,413	19,119	0	19,697	0
Niagara Falls	16,228	0	1,722	1,323	16,266	0	16,936	0
Syracuse	15,864	0	1,748	1,258	15,900	0	16,579	0
Westhampton Beach	10,781	0	1,672	989	10,805	0	11,305	0
North Carolina								
Greensboro	7,990	0	2,940	641	8,013	0	8,821	0
New Bern	6,918	0	4,201	396	6,937	0	7,909	0

	Electric Heat Pump		Gas Furnace/Electric AC		Hydrocarbon Heat Pump		Transcritical CO_2 Heat Pump	
State and City	(kWh/y)	(therms/y)	(kWh/y)	(therms/y)	(kWh/y)	(therms/y)	(kWh/y)	(therms/y)
North Dakota								
Bismarck	28,116	0	2,027	1,750	28,162	0	28,985	0
Grand Forks	33,185	0	1,818	1,960	33,231	0	33,967	0
Williston	24,514	0	1,946	1,584	24,562	0	25,370	0
Ohio								
Akron	14,144	0	1,834	1,180	14,178	0	14,850	0
Columbus	10,854	0	2,295	968	10,886	0	11,656	0
Dayton	11,849	0	2,610	967	11,883	0	12,727	0
Toledo	15,612	0	2,065	1,256	15,654	0	16,448	0
Oklahoma								
Altus	9,230	0	4,551	605	9,265	0	10,767	0
Oklahoma City	9,438	0	4,037	660	9,471	0	10,718	0
Tulsa	9,438		4,176	645	9,472		10,785	
Oregon								
Astoria	7,220	0	704	832	7,212	0	7,333	0
Medford	8,404	0	2,567	836	8,422	0	9,129	0
Portland	7,152	0	1,545	806	7,153	0	7,468	0
Pennsylvania								
Philadelphia	10,266	0	2,052	925	10,292	0	10,918	0
Pittsburgh	13,990	0	1,798	1,154	14,022	0	14,666	0
Wilkes-Barre	13,310	0	1,755	1,130	13,343	0	13,993	0
South Carolina								
Charleston	6,664	0	4,057	382	6,683	0	7,626	0
Greenville	6,930	0	3,208	518	6,949	0	7,799	0
Sumter	6,712		3,914	405	6,731		7,702	
South Dakota								
Huron	23,699	0	2,383	1,579	23,755	0	24,768	0
Rapid City	18,167	0	2,157	1,305	18,207	0	19,028	0
Teennessee								
Bristol	8,400	0	2,625	700	8,423	0	9,147	0
Knoxville	7,798	0	2,835	634	7,818	0	8,545	0
Memphis	8,333	0	4,038	569	8,360	0	9,516	0
Nashville	9,004	0	3,292	686	9,032	0	9,993	0
Texas								
El Paso	7,716	0	4,567	442	7,742	0	9,038	0
Fort Worth	8,417	0	5,408	423	8,447	0	10,080	0
Houston	7,052	0	5,551	228	7,077	0	8,479	0
San Antonio	7,286	0	6,006	196	7,314	0	8,993	0
Utah								
Salt Lake City	11,880	0	2,328	1,065	11,917	0	12,761	0
Vermont								
Burlington	21,493	0	1,512	1,524	21,534	0	22,183	0
Virginia								
Norfolk	7,640	0	3,187	616	7,661	0	8,450	0
Richmond	7,822	0	3,083	635	7,844	0	8,675	0
Roanoke	8,527	0	2,705	734	8,549	0	9,319	0
Washington								
Moses Lake	11,411	0	2,563	1,036	11,446	0	12,330	0
Seattle	7,903	0	1,270	913	7,904	0	8,179	0
Spokane	13,311	0	1,764	1,253	13,347	0	14,038	0

State and City	Electric Heat Pump (kWh/y)	(therms/y)	Gas Furnace/Electric AC (kWh/y)	(therms/y)	Hydrocarbon Heat Pump (kWh/y)	(therms/y)	Transcritical CO_2 Heat Pump (kWh/y)	(therms/y)
West Virginia								
Charleston	9,252	0	2,611	779	9,278	0	10,054	0
Elkins	12,910	0	1,640	1,061	12,935	0	13,484	0
Wisconsin								
Green Bay	21,208	0	1,632	1,526	21,253	0	21,957	0
Madison	19,252	0	1,901	1,398	19,295	0	20,066	0
Wyoming								
Casper	17,654	0	2,039	1,394	17,701	0	18,581	0
Cheyenne	17,521	0	1,685	1,388	17,558	0	18,244	0
Lander	17,700	0	1,736	1,360	17,750	0	18,516	0
Sheridan	18,088	0	2,053	1,381	18,134	0	19,002	0

State and City	Brayton Cycle Heat Pump (kWh/y)	Brayton Cycle Heat Pump (therms/y)	Stirling Cycle Heat Pump (kWh/y)	Stirling Cycle Heat Pump (therms/y)	Thermoelectric Heat Pump (max ZT) (kWh/y)	Thermoelectric Heat Pump (max ZT) (therms/y)	Thermoacoustic Heat Pump (kWh/y)	Thermoacoustic Heat Pump (therms/y)
Alabama								
Birmingham	19,510	0	13,006	0	11,006	0	9,575	0
Montgomery	20,655	0	13,116	0	10,717	0	9,269	0
Arizona								
Phoenix	27,562	0	16,001	0	13,262	0	12,154	0
Tucson	23,649	0	14,234	0	11,494	0	10,135	0
Yuma	28,508	0	16,003	0	13,211	0	12,308	0
Arkansas								
Little Rock	20,753	0	13,805	0	11,800	0	10,230	0
California								
Arcata	11,287	0	9,868	0	8,930	0	7,332	0
Los Angeles	11,884	0	7,868	0	5,852	0	4,568	0
Merced	18,337	0	12,175	0	10,184	0	8,636	0
Oakland	11,326	0	8,563	0	6,944	0	5,367	0
San Diego	9,658	0	6,475	0	4,799	0	3,690	0
Colorado								
Colorado Springs	24,223	0	20,212	0	19,420	0	17,861	0
Denver	23,848	0	19,916	0	19,171	0	17,661	0
Grand Junction	22,950	0	17,525	0	16,432	0	14,655	0
Florida								
Appalachicola	21,404	0	12,745	0	9,696	0	8,410	0
Jacksonville	21,074	0	12,551	0	9,677	0	8,482	0
Miami	25,947	0	14,392	0	10,408	0	9,280	0
Orlando	21,518	0	12,456	0	9,259	0	8,087	0
Tampa	23,400	0	13,280	0	9,830	0	8,726	0
Georgia								
Atlanta	18,454	0	12,998	0	11,261	0	9,780	0
Augusta	19,922	0	13,020	0	10,876	0	9,473	0
Macon	20,070	0	12,857	0	10,546	0	9,075	0
Idaho								
Boise	22,070	0	17,511	0	16,584	0	14,570	0
Idaho Falls	28,770	0	24,992	0	24,508	0	22,822	0
Illinois								
Champaigne-Urbana	25,840	0	21,104	0	20,283	0	18,606	0
Chicago	25,039	0	21,142	0	20,557	0	18,874	0
East St. Louis	23,363	0	17,712	0	16,441	0	14,637	0
Indiana								
Fort Wayne	23,807	0	19,487	0	18,736	0	17,075	0
South Bend	24,590	0	20,440	0	19,770	0	18,091	0
Iowa								
Des Moines	27,451	0	22,975	0	22,265	0	20,798	0
Sioux City	29,213	0	24,319	0	23,667	0	22,144	0
Kansas								
Dodge City	23,928	0	18,155	0	17,034	0	15,451	0
Topeka	24,815	0	19,154	0	18,035	0	16,311	0
Kentucky								
Louisville	21,641	0	15,831	0	14,291	0	12,576	0

State and City	Brayton Cycle Heat Pump (kWh/y)	Brayton Cycle Heat Pump (therms/y)	Stirling Cycle Heat Pump (kWh/y)	Stirling Cycle Heat Pump (therms/y)	Thermoelectric Heat Pump (max ZT) (kWh/y)	Thermoelectric Heat Pump (max ZT) (therms/y)	Thermoacoustic Heat Pump (kWh/y)	Thermoacoustic Heat Pump (therms/y)
Louisiana								
Lake Charles	21,114	0	12,809	0	10,017	0	8,742	0
New Orleans	19,843	0	11,915	0	9,185	0	7,960	0
Shreveport	21,240	0	13,655	0	11,342	0	9,869	0
Maine								
Portland	25,731	0	22,423	0	21,893	0	20,189	0
Massachusetts								
Falmouth	20,691	0	17,655	0	16,879	0	15,273	0
Michigan								
Battle Creek	24,284	0	20,287	0	19,786	0	18,114	0
Detroit	25,274	0	21,348	0	20,802	0	19,112	0
Sault Ste Marie	34,486	0	31,720	0	31,540	0	30,187	0
Minnesota								
Duluth	38,930	0	36,289	0	36,124	0	34,895	0
International Falls	41,829	0	39,277	0	39,127	0	38,063	0
Minneapolis	31,641	0	27,758	0	27,373	0	26,000	0
Mississippi								
Biloxi	20,610	0	12,501	0	9,791	0	8,539	0
Columbus	20,693	0	13,784	0	11,725	0	10,286	0
Jackson	20,592	0	13,260	0	10,970	0	9,501	0
Missouri								
Columbia	23,443	0	17,827	0	16,566	0	14,895	0
Kansas City	23,595	0	17,511	0	16,192	0	14,462	0
Springfield	22,740	0	17,143	0	15,807	0	14,175	0
Montana								
Billings	26,478	0	22,458	0	21,735	0	20,039	0
Great Falls	30,134	0	26,564	0	25,800	0	24,182	0
Missoula	26,642	0	23,010	0	22,493	0	20,665	0
Nebraska								
Grand Island	27,446	0	22,547	0	21,866	0	20,297	0
Lincoln	26,710	0	22,174	0	21,515	0	19,996	0
North Platte	27,059	0	22,551	0	22,075	0	20,482	0
Nevada								
Ely	29,360	0	25,122	0	24,606	0	22,835	0
Las Vegas	26,060	0	15,937	0	13,661	0	12,355	0
Reno	23,261	0	18,747	0	17,883	0	15,679	0
Winnemucca	25,575	0	20,488	0	19,616	0	17,748	0
New Jersey								
Trenton	20,581	0	16,382	0	15,329	0	13,729	0
New Mexico								
Albuquerque	20,334	0	14,658	0	13,125	0	11,426	0
Farmington	23,491	0	18,120	0	16,999	0	15,220	0
Roswell	21,472	0	14,636	0	12,890	0	11,351	0
New York								
Albany	25,149	0	21,676	0	21,173	0	19,671	0
Binghamton	27,349	0	24,270	0	23,839	0	22,409	0
Niagara Falls	25,448	0	21,910	0	21,386	0	19,785	0
Syracuse	24,961	0	21,359	0	20,782	0	19,245	0
Westhampton Beach	19,814	0	16,312	0	15,393	0	13,658	0

State and City	Brayton Cycle Heat Pump (kWh/y)	Brayton Cycle Heat Pump (therms/y)	Stirling Cycle Heat Pump (kWh/y)	Stirling Cycle Heat Pump (therms/y)	Thermoelectric Heat Pump (max ZT) (kWh/y)	Thermoelectric Heat Pump (max ZT) (therms/y)	Thermoacoustic Heat Pump (kWh/y)	Thermoacoustic Heat Pump (therms/y)
North Carolina								
Greensboro	18,785	0	13,568	0	12,019	0	10,488	0
New Bern	20,187	0	13,094	0	10,628	0	9,032	0
North Dakota								
Bismarck	37,323	0	33,469	0	33,070	0	31,787	0
Grand Forks	41,658	0	38,213	0	37,945	0	36,813	0
Williston	33,579	0	29,767	0	29,410	0	28,091	0
Ohio								
Akron	23,451	0	19,741	0	19,071	0	17,495	0
Columbus	21,193	0	16,746	0	15,734	0	14,016	0
Dayton	22,700	0	17,807	0	16,668	0	15,020	0
Toledo	25,546	0	21,462	0	20,849	0	19,203	0
Oklahoma								
Altus	22,864	0	15,456	0	13,685	0	12,176	0
Oklahoma City	22,423	0	15,651	0	13,917	0	12,312	0
Tulsa	22,626		15,666		13,914		12,328	
Oregon								
Astoria	13,814	0	11,935	0	10,886	0	9,238	0
Medford	19,246	0	14,672	0	13,277	0	11,165	0
Portland	16,005	0	12,859	0	11,516	0	9,380	0
Pennsylvania								
Philadelphia	19,805	0	15,805	0	14,791	0	13,168	0
Pittsburgh	23,062	0	19,448	0	18,753	0	17,209	0
Wilkes-Barre	22,349	0	18,769	0	18,122	0	16,533	0
South Carolina								
Charleston	19,423	0	12,580	0	10,213	0	8,754	0
Greenville	17,789	0	12,338	0	10,628	0	9,114	0
Sumter	19,004		12,447		10,271		8,806	
South Dakota								
Huron	33,850	0	29,400	0	29,056	0	27,664	0
Rapid City	27,914	0	23,770	0	23,120	0	21,594	0
Teennessee								
Bristol	18,686	0	13,895	0	12,500	0	10,917	0
Knoxville	18,506	0	13,414	0	11,795	0	10,137	0
Memphis	21,280	0	14,503	0	12,562	0	10,924	0
Nashville	20,586	0	14,861	0	13,289	0	11,693	0
Texas								
El Paso	21,268	0	13,812	0	11,612	0	10,110	0
Fort Worth	23,641	0	14,958	0	12,544	0	11,024	0
Houston	22,495	0	13,451	0	10,495	0	9,284	0
San Antonio	23,187	0	13,585	0	10,684	0	9,626	0
Utah								
Salt Lake City	22,488	0	17,995	0	17,128	0	15,313	0
Vermont								
Burlington	30,023	0	26,786	0	26,444	0	25,000	0
Virginia								
Norfolk	19,112	0	13,574	0	11,793	0	10,060	0
Richmond	18,945	0	13,579	0	11,963	0	10,303	0
Roanoke	19,094	0	14,220	0	12,813	0	11,161	0

State and City	Brayton Cycle Heat Pump (kWh/y)	Brayton Cycle Heat Pump (therms/y)	Stirling Cycle Heat Pump (kWh/y)	Stirling Cycle Heat Pump (therms/y)	Thermoelectric Heat Pump (max ZT) (kWh/y)	Thermoelectric Heat Pump (max ZT) (therms/y)	Thermoacoustic Heat Pump (kWh/y)	Thermoacoustic Heat Pump (therms/y)
Washington								
Moses Lake	22,584	0	17,829	0	16,844	0	14,756	0
Seattle	16,256	0	13,525	0	12,353	0	10,368	0
Spokane	23,567	0	19,714	0	19,016	0	16,992	0
West Virginia								
Charleston	19,700	0	14,893	0	13,601	0	11,993	0
Elkins	21,527	0	18,113	0	17,306	0	15,825	0
Wisconsin								
Green Bay	30,141	0	26,670	0	26,327	0	24,887	0
Madison	28,577	0	24,744	0	24,249	0	22,840	0
Wyoming								
Casper	27,757	0	23,653	0	23,210	0	21,534	0
Cheyenne	27,050	0	23,409	0	22,827	0	21,125	0
Lander	27,004	0	23,293	0	22,971	0	21,382	0
Sheridan	28,091	0	23,973	0	23,483	0	21,860	0

State and City	Pulse Tube Heat Pump		Magnetic Heat Pump (¼ HP Pump)		Compressor Driven Metal Hydride HP		Diesel Engine Driven Heat Pump	
	(kWh/y)	(therms/y)	(kWh/y)	(therms/y)	(kWh/y)	(therms/y)	(kWh/y)	(therms/y)
Alabama								
Birmingham	46,377	0	6,446	0	8,361	0	917	546
Montgomery	50,777	0	6,322	0	7,728	0	958	563
Arizona								
Phoenix	68,022	0	8,777	0	9,468	0	1,314	827
Tucson	58,805	0	7,165	0	8,022	0	1,099	660
Yuma	70,980	0	9,014	0	9,385	0	1,357	865
Arkansas								
Little Rock	48,795	0	6,832	0	8,882	0	981	593
California								
Arcata	20,119	0	5,226	0	6,789	0	560	305
Los Angeles	29,583	0	3,173	0	3,644	0	513	266
Merced	42,765	0	5,962	0	7,185	0	860	495
Oakland	24,641	0	3,768	0	4,517	0	518	284
San Diego	23,773	0	2,574	0	2,935	0	413	227
Colorado								
Colorado Springs	44,685	0	13,063	0	17,896	0	1,094	754
Denver	43,624	0	12,997	0	17,647	0	1,074	750
Grand Junction	47,630	0	9,611	0	14,331	0	1,091	685
Florida								
Appalachicola	56,381	0	5,839	0	6,640	0	974	554
Jacksonville	55,196	0	5,894	0	6,737	0	970	557
Miami	72,050	0	6,506	0	7,020	0	1,170	658
Orlando	57,866	0	5,654	0	6,250	0	973	550
Tampa	63,641	0	6,140	0	6,680	0	1,066	604
Georgia								
Atlanta	42,288	0	6,567	0	8,868	0	871	525
Augusta	48,249	0	6,389	0	8,136	0	941	556
Macon	48,978	0	6,150	0	7,613	0	928	547
Idaho								
Boise	43,837	0	9,488	0	14,307	0	1,061	669
Idaho Falls	49,338	0	17,089	0	23,189	0	1,268	918
Illinois								
Champaigne-Urbana	48,769	0	13,240	0	18,612	0	1,173	802
Chicago	45,141	0	13,577	0	19,025	0	1,142	790
East St. Louis	48,537	0	9,813	0	14,157	0	1,087	718
Indiana								
Fort Wayne	45,336	0	11,914	0	17,119	0	1,107	733
South Bend	45,657	0	12,795	0	18,230	0	1,131	761
Iowa								
Des Moines	49,306	0	15,617	0	20,854	0	1,206	871
Sioux City	52,568	0	16,469	0	22,242	0	1,283	929
Kansas								
Dodge City	49,381	0	10,546	0	15,009	0	1,126	751
Topeka	50,082	0	11,205	0	15,962	0	1,142	736
Kentucky								
Louisville	47,336	0	8,328	0	11,848	0	1,025	622

State and City	Pulse Tube Heat Pump (kWh/y)	Pulse Tube Heat Pump (therms/y)	Magnetic Heat Pump (¼ HP Pump) (kWh/y)	Magnetic Heat Pump (¼ HP Pump) (therms/y)	Compressor Driven Metal Hydride HP (kWh/y)	Compressor Driven Metal Hydride HP (therms/y)	Diesel Engine Driven Heat Pump (kWh/y)	Diesel Engine Driven Heat Pump (therms/y)
Louisiana								
Lake Charles	54,476	0	6,070	0	7,012	0	977	562
New Orleans	51,539	0	5,539	0	6,310	0	905	518
Shreveport	51,589	0	6,698	0	8,354	0	993	589
Maine								
Portland	43,950	0	15,056	0	20,442	0	1,136	822
Massachusetts								
Falmouth	37,355	0	11,154	0	15,251	0	946	616
Michigan								
Battle Creek	44,951	0	12,560	0	18,447	0	1,127	772
Detroit	45,708	0	13,628	0	19,408	0	1,151	806
Sault Ste Marie	50,869	0	24,922	0	30,706	0	1,333	1,153
Minnesota								
Duluth	54,558	0	29,814	0	35,344	0	1,391	1,346
International Falls	56,775	0	33,226	0	38,423	0	1,415	1,497
Minneapolis	51,641	0	20,463	0	26,345	0	1,315	1,081
Mississippi								
Biloxi	53,072	0	5,917	0	6,868	0	949	547
Columbus	49,276	0	6,936	0	9,005	0	984	587
Jackson	50,017	0	6,456	0	8,015	0	961	568
Missouri								
Columbia	48,615	0	10,178	0	14,410	0	1,096	724
Kansas City	49,697	0	9,713	0	13,845	0	1,100	725
Springfield	47,967	0	9,625	0	13,665	0	1,068	695
Montana								
Billings	46,578	0	15,018	0	19,959	0	1,165	849
Great Falls	48,942	0	19,437	0	24,062	0	1,227	1,001
Missoula	46,496	0	15,051	0	20,911	0	1,206	861
Nebraska								
Grand Island	50,678	0	14,730	0	20,348	0	1,233	863
Lincoln	48,380	0	14,732	0	20,043	0	1,183	840
North Platte	49,002	0	14,721	0	20,721	0	1,220	858
Nevada								
Ely	51,402	0	16,857	0	23,127	0	1,305	935
Las Vegas	62,071	0	8,683	0	10,066	0	1,254	797
Reno	45,201	0	10,181	0	15,594	0	1,093	694
Winnemucca	49,551	0	12,224	0	17,569	0	1,197	787
New Jersey								
Trenton	41,279	0	9,460	0	13,488	0	973	606
New Mexico								
Albuquerque	45,087	0	7,442	0	10,620	0	972	581
Farmington	48,114	0	10,183	0	14,939	0	1,097	698
Roswell	49,148	0	7,549	0	10,179	0	1,022	635
New York								
Albany	43,547	0	14,723	0	19,895	0	1,113	807
Binghamton	44,680	0	17,531	0	22,776	0	1,155	847
Niagara Falls	44,692	0	14,549	0	20,106	0	1,147	796
Syracuse	43,986	0	14,268	0	19,450	0	1,115	792
Westhampton Beach	38,022	0	9,407	0	13,565	0	924	584

State and City	Pulse Tube Heat Pump (kWh/y)	Pulse Tube Heat Pump (therms/y)	Magnetic Heat Pump (¼ HP Pump) (kWh/y)	Magnetic Heat Pump (¼ HP Pump) (therms/y)	Compressor Driven Metal Hydride HP (kWh/y)	Compressor Driven Metal Hydride HP (therms/y)	Diesel Engine Driven Heat Pump (kWh/y)	Diesel Engine Driven Heat Pump (therms/y)
North Carolina								
Greensboro	42,002	0	6,957	0	9,730	0	894	545
New Bern	49,530	0	6,090	0	7,599	0	930	543
North Dakota								
Bismarck	57,074	0	26,296	0	31,962	0	1,462	1,328
Grand Forks	59,997	0	31,339	0	37,081	0	1,545	1,524
Williston	52,994	0	22,627	0	28,371	0	1,352	1,178
Ohio								
Akron	42,980	0	12,591	0	17,654	0	1,075	717
Columbus	42,717	0	9,400	0	13,784	0	1,008	634
Dayton	45,810	0	10,399	0	14,718	0	1,059	674
Toledo	46,430	0	13,835	0	19,402	0	1,159	797
Oklahoma								
Altus	52,402	0	8,135	0	10,911	0	1,096	687
Oklahoma City	50,508	0	8,228	0	11,281	0	1,059	665
Tulsa	51,188	0	8,246	0	11,238		1,071	673
Oregon								
Astoria	25,228	0	6,703	0	8,732	0	670	354
Medford	40,244	0	7,173	0	10,370	0	929	362
Portland	31,705	0	6,188	0	8,649	0	764	453
Pennsylvania								
Philadelphia	39,607	0	8,956	0	12,981	0	935	576
Pittsburgh	41,978	0	12,520	0	17,305	0	1,050	717
Wilkes-Barre	41,041	0	11,787	0	16,647	0	1,029	685
South Carolina								
Charleston	48,011	0	5,902	0	7,406	0	902	522
Greenville	40,891	0	6,052	0	8,102	0	840	505
Sumter	46,062		5,931		7,501		885	518
South Dakota								
Huron	55,840	0	21,622	0	27,979	0	1,419	1,180
Rapid City	48,409	0	16,476	0	21,628	0	1,207	897
Teennessee								
Bristol	40,467	0	7,259	0	10,328	0	880	529
Knoxville	40,919	0	6,742	0	9,337	0	862	507
Memphis	49,213	0	7,271	0	9,721	0	1,002	612
Nashville	45,457	0	7,832	0	10,897	0	969	607
Texas								
El Paso	50,847	0	6,855	0	8,626	0	996	602
Fort Worth	57,009	0	7,548	0	9,234	0	1,109	670
Houston	58,702	0	6,469	0	7,418	0	1,050	605
San Antonio	60,432	0	6,797	0	7,591	0	1,094	641
Utah								
Salt Lake City	44,362	0	10,230	0	15,207	0	1,070	681
Vermont								
Burlington	47,855	0	19,748	0	25,391	0	1,243	1,001
Virginia								
Norfolk	43,356	0	6,567	0	9,143	0	899	541
Richmond	42,424	0	6,746	0	9,455	0	898	529
Roanoke	41,219	0	7,405	0	10,504	0	910	544

State and City	Pulse Tube Heat Pump		Magnetic Heat Pump (¼ HP Pump)		Compressor Driven Metal Hydride HP		Diesel Engine Driven Heat Pump	
	(kWh/y)	(therms/y)	(kWh/y)	(therms/y)	(kWh/y)	(therms/y)	(kWh/y)	(therms/y)
Washington								
Moses Lake	44,743	0	9,664	0	14,421	0	1,067	702
Seattle	31,214	0	7,029	0	9,812	0	793	471
Spokane	43,946	0	11,513	0	17,075	0	1,115	745
West Virginia								
Charleston	41,811	0	8,017	0	11,494	0	932	568
Elkins	39,579	0	11,647	0	15,803	0	977	644
Wisconsin								
Green Bay	49,203	0	19,390	0	25,347	0	1,270	997
Madison	48,704	0	17,552	0	23,137	0	1,230	933
Wyoming								
Casper	48,951	0	15,739	0	21,824	0	1,249	904
Cheyenne	46,699	0	15,816	0	21,346	0	1,195	860
Lander	46,636	0	15,671	0	21,870	0	1,190	897
Sheridan	49,095	0	16,219	0	22,080	0	1,246	905

State and City	IC Engine-Driven Heat Pump (kWh/y)	IC Engine-Driven Heat Pump (therms/y)	Stirling Engine-Driven Heat Pump (kWh/y)	Stirling Engine-Driven Heat Pump (therms/y)	Brayton Engine Driven Heat Pump (kWh/y)	Brayton Engine Driven Heat Pump (therms/y)	Rankine Engine Driven Heat Pump (kWh/y)	Rankine Engine Driven Heat Pump (therms/y)
Alabama								
Birmingham	965	625	917	665	917	688	917	760
Montgomery	984	648	958	691	958	716	958	794
Arizona								
Phoenix	1,317	960	1,314	1,026	1,314	1,063	1,314	1,190
Tucson	1,104	763	1,099	816	1,099	845	1,099	942
Yuma	1,353	1,006	1,357	1,076	1,357	1,115	1,357	1,251
Arkansas								
Little Rock	1,032	678	981	723	981	747	981	826
California								
Arcata	558	342	560	359	560	370	560	400
Los Angeles	497	305	513	325	513	337	513	372
Merced	871	568	860	605	860	626	860	693
Oakland	495	323	518	343	518	354	518	388
San Diego	397	260	413	277	413	287	413	317
Colorado								
Colorado Springs	1,258	845	1,094	872	1,094	894	1,094	964
Denver	1,232	838	1,074	866	1,074	888	1,074	956
Grand Junction	1,268	776	1,091	812	1,091	836	1,091	912
Florida								
Appalachicola	977	640	974	686	974	711	974	792
Jacksonville	976	644	970	689	970	714	970	796
Miami	1,169	766	1,170	822	1,170	854	1,170	954
Orlando	971	638	973	684	973	710	973	792
Tampa	1,063	702	1,066	753	1,066	782	1,066	873
Georgia								
Atlanta	932	597	871	634	871	654	871	719
Augusta	981	637	941	680	941	704	941	779
Macon	957	628	928	670	928	694	928	769
Idaho								
Boise	1,229	752	1,061	790	1,061	813	1,061	885
Idaho Falls	1,485	1,029	1,268	1,045	1,268	1,069	1,268	1,144
Illinois								
Champaigne-Urbana	1,386	907	1,173	926	1,173	948	1,173	1,022
Chicago	1,339	886	1,142	910	1,142	932	1,142	1,002
East St. Louis	1,254	802	1,087	847	1,087	871	1,087	948
Indiana								
Fort Wayne	1,298	826	1,107	854	1,107	876	1,107	948
South Bend	1,332	859	1,131	882	1,131	905	1,131	976
Iowa								
Des Moines	1,403	979	1,206	993	1,206	1,016	1,206	1,089
Sioux City	1,539	1,052	1,283	1,058	1,283	1,082	1,283	1,159
Kansas								
Dodge City	1,300	839	1,126	886	1,126	911	1,126	993
Topeka	1,340	849	1,142	865	1,142	889	1,142	966
Kentucky								
Louisville	1,143	707	1,025	744	1,025	766	1,025	840

State and City	IC Engine-Driven Heat Pump (kWh/y)	IC Engine-Driven Heat Pump (therms/y)	Stirling Engine-Driven Heat Pump (kWh/y)	Stirling Engine-Driven Heat Pump (therms/y)	Brayton Engine Driven Heat Pump (kWh/y)	Brayton Engine Driven Heat Pump (therms/y)	Rankine Engine Driven Heat Pump (kWh/y)	Rankine Engine Driven Heat Pump (therms/y)
Louisiana								
Lake Charles	985	649	977	694	977	720	977	801
New Orleans	909	599	905	641	905	665	905	740
Shreveport	1,030	677	993	722	993	747	993	828
Maine								
Portland	1,315	916	1,136	938	1,136	959	1,136	1,027
Massachusetts								
Falmouth	1,060	703	946	719	946	738	946	798
Michigan								
Battle Creek	1,352	859	1,127	895	1,127	918	1,127	991
Detroit	1,367	897	1,151	929	1,151	952	1,151	1,024
Sault Ste Marie	1,490	1,285	1,333	1,273	1,333	1,295	1,333	1,365
Minnesota								
Duluth	1,535	1,479	1,391	1,462	1,391	1,483	1,391	1,551
International Falls	1,553	1,619	1,415	1,605	1,415	1,625	1,415	1,688
Minneapolis	1,549	1,176	1,315	1,203	1,315	1,225	1,315	1,297
Mississippi								
Biloxi	959	632	949	676	949	700	949	779
Columbus	1,036	672	984	715	984	739	984	817
Jackson	993	652	961	696	961	720	961	798
Missouri								
Columbia	1,254	810	1,096	854	1,096	878	1,096	956
Kansas City	1,262	812	1,100	859	1,100	884	1,100	965
Springfield	1,213	780	1,068	823	1,068	846	1,068	923
Montana								
Billings	1,343	947	1,165	966	1,165	987	1,165	1,056
Great Falls	1,362	1,099	1,227	1,114	1,227	1,135	1,227	1,202
Missoula	1,413	954	1,206	986	1,206	1,009	1,206	1,083
Nebraska								
Grand Island	1,471	980	1,233	992	1,233	1,016	1,233	1,093
Lincoln	1,410	955	1,183	961	1,183	983	1,183	1,054
North Platte	1,478	973	1,220	985	1,220	1,009	1,220	1,084
Nevada								
Ely	1,539	1,051	1,305	1,068	1,305	1,093	1,305	1,171
Las Vegas	1,283	920	1,254	982	1,254	1,016	1,254	1,133
Reno	1,299	790	1,093	816	1,093	838	1,093	910
Winnemucca	1,403	894	1,197	921	1,197	945	1,197	1,025
New Jersey								
Trenton	1,103	687	973	716	973	737	973	802
New Mexico								
Albuquerque	1,071	659	972	698	972	721	972	791
Farmington	1,281	791	1,097	823	1,097	847	1,097	922
Roswell	1,103	723	1,022	769	1,022	794	1,022	876
New York								
Albany	1,286	901	1,113	922	1,113	943	1,113	1,011
Binghamton	1,302	967	1,155	964	1,155	985	1,155	1,054
Niagara Falls	1,327	899	1,147	917	1,147	940	1,147	1,011
Syracuse	1,288	887	1,115	909	1,115	930	1,115	999
Westhampton Beach	1,059	658	924	684	924	703	924	762

State and City	IC Engine-Driven Heat Pump (kWh/y)	IC Engine-Driven Heat Pump (therms/y)	Stirling Engine-Driven Heat Pump (kWh/y)	Stirling Engine-Driven Heat Pump (therms/y)	Brayton Engine Driven Heat Pump (kWh/y)	Brayton Engine Driven Heat Pump (therms/y)	Rankine Engine Driven Heat Pump (kWh/y)	Rankine Engine Driven Heat Pump (therms/y)
North Carolina								
Greensboro	976	618	894	655	894	676	894	742
New Bern	956	623	930	664	930	688	930	761
North Dakota								
Bismarck	1,689	1,423	1,462	1,449	1,462	1,471	1,462	1,543
Grand Forks	1,780	1,616	1,545	1,638	1,545	1,659	1,545	1,726
Williston	1,594	1,268	1,352	1,296	1,352	1,317	1,352	1,387
Ohio								
Akron	1,246	811	1,075	832	1,075	854	1,075	922
Columbus	1,160	714	1,008	748	1,008	769	1,008	837
Dayton	1,209	764	1,059	793	1,059	816	1,059	887
Toledo	1,365	899	1,159	919	1,159	941	1,159	1,013
Oklahoma								
Altus	1,184	782	1,096	832	1,096	859	1,096	949
Oklahoma City	1,161	754	1,059	801	1,059	826	1,059	909
Tulsa	1,171	763	1,071	811	1,071	837	1,071	922
Oregon								
Astoria	687	402	670	416	670	428	670	464
Medford	1,012	405	929	424	929	435	929	471
Portland	807	509	764	538	764	554	764	604
Pennsylvania								
Philadelphia	1,069	651	935	682	935	701	935	764
Pittsburgh	1,205	807	1,050	830	1,050	851	1,050	918
Wilkes-Barre	1,196	773	1,029	795	1,029	816	1,029	881
South Carolina								
Charleston	929	599	902	639	902	662	902	733
Greenville	890	575	840	612	840	632	840	696
Sumter	916	594	885	634	885	656	885	726
South Dakota								
Huron	1,713	1,272	1,419	1,312	1,419	1,336	1,419	1,414
Rapid City	1,405	1,007	1,207	1,015	1,207	1,037	1,207	1,107
Teennessee								
Bristol	976	600	880	632	880	651	880	712
Knoxville	937	576	862	608	862	628	862	688
Memphis	1,072	697	1,002	742	1,002	766	1,002	845
Nashville	1,070	685	969	727	969	749	969	821
Texas								
El Paso	1,038	689	996	735	996	760	996	842
Fort Worth	1,148	772	1,109	822	1,109	851	1,109	945
Houston	1,058	700	1,050	749	1,050	776	1,050	864
San Antonio	1,098	743	1,094	795	1,094	824	1,094	920
Utah								
Salt Lake City	1,248	768	1,070	802	1,070	825	1,070	896
Vermont								
Burlington	1,432	1,105	1,243	1,118	1,243	1,139	1,243	1,208
Virginia								
Norfolk	969	614	899	653	899	674	899	741
Richmond	976	600	898	637	898	657	898	722
Roanoke	1,003	616	910	651	910	671	910	736

State and City	IC Engine-Driven Heat Pump (kWh/y)	IC Engine-Driven Heat Pump (therms/y)	Stirling Engine-Driven Heat Pump (kWh/y)	Stirling Engine-Driven Heat Pump (therms/y)	Brayton Engine Driven Heat Pump (kWh/y)	Brayton Engine Driven Heat Pump (therms/y)	Rankine Engine Driven Heat Pump (kWh/y)	Rankine Engine Driven Heat Pump (therms/y)
Washington								
Moses Lake	1,241	781	1,067	825	1,067	848	1,067	921
Seattle	847	529	793	557	793	574	793	624
Spokane	1,311	827	1,115	867	1,115	889	1,115	961
West Virginia								
Charleston	1,046	644	932	676	932	697	932	761
Elkins	1,099	732	977	749	977	768	977	830
Wisconsin								
Green Bay	1,473	1,105	1,270	1,120	1,270	1,143	1,270	1,215
Madison	1,422	1,037	1,230	1,057	1,230	1,080	1,230	1,153
Wyoming								
Casper	1,477	1,002	1,249	1,035	1,249	1,059	1,249	1,137
Cheyenne	1,378	961	1,195	984	1,195	1,007	1,195	1,079
Lander	1,444	983	1,190	1,017	1,190	1,039	1,190	1,109
Sheridan	1,472	1,017	1,246	1,030	1,246	1,054	1,246	1,128

Stata and City	Fuel Cell Powered Rankine Heat Pump		Vuilleumier Cycle Heat Pump		GAX Absorption Heat Pump		Duplex Stirling Cycle Heat Pump	
	(kWh/y)	(therms/y)	(kWh/y)	(therms/y)	(kWh/y)	(therms/y)	(kWh/y)	(therms/y)
Alabama								
Birmingham	0	527	1,670	932	757	890	1,618	719
Montgomery	0	529	1,702	991	721	957	1,649	752
Arizona								
Phoenix	0	731	2,278	1,390	853	1,352	2,207	975
Tucson	0	598	1,909	1,156	752	1,124	1,849	845
Yuma	0	752	2,341	1,450	829	1,417	2,268	999
Arkansas								
Little Rock	0	576	1,786	996	813	951	1,730	763
California								
Arcata	0	327	965	489	714	422	935	407
Los Angeles	0	242	860	507	405	487	833	408
Merced	0	458	1,506	849	706	806	1,459	643
Oakland	0	298	856	512	527	470	829	418
San Diego	0	225	687	428	334	412	665	350
Colorado								
Colorado Springs	0	800	2,176	1,077	1,237	980	2,108	918
Denver	0	795	2,131	1,065	1,215	971	2,064	906
Grand Junction	0	709	2,194	1,042	1,122	959	2,125	849
Florida								
Appalachicola	0	495	1,691	1,027	634	1,010	1,638	778
Jacksonville	0	497	1,689	1,020	636	1,001	1,636	767
Miami	0	560	2,023	1,257	646	1,256	1,959	941
Orlando	0	482	1,680	1,035	593	1,024	1,627	780
Tampa	0	521	1,839	1,137	624	1,129	1,782	849
Georgia								
Atlanta	0	522	1,613	869	787	822	1,562	689
Augusta	0	528	1,696	960	750	921	1,643	734
Macon	0	518	1,654	958	713	924	1,603	730
Idaho								
Boise	0	709	2,126	1,001	1,168	912	2,060	825
Idaho Falls	0	991	2,568	1,253	1,509	1,125	2,488	1,096
Illinois								
Champaigne-Urbana	0	855	2,397	1,150	1,297	1,043	2,322	978
Chicago	0	846	2,317	1,108	1,327	1,000	2,244	951
East St. Louis	0	745	2,170	1,080	1,098	1,012	2,102	883
Indiana								
Fort Wayne	0	776	2,244	1,061	1,240	962	2,174	895
South Bend	0	813	2,304	1,088	1,289	981	2,232	926
Iowa								
Des Moines	0	920	2,428	1,209	1,352	1,098	2,352	1,042
Sioux City	0	997	2,661	1,291	1,428	1,167	2,578	1,111
Kansas								
Dodge City	0	770	2,249	1,114	1,131	1,043	2,179	902
Topeka	0	776	2,318	1,116	1,173	1,014	2,246	920
Kentucky								
Louisville	0	622	1,977	989	987	921	1,915	793

	Fuel Cell Powered Rankine Heat Pump		Vuilleumier Cycle Heat Pump		GAX Absorption Heat Pump		Duplex Stirling Cycle Heat Pump	
Stata and City	(kWh/y)	(therms/y)	(kWh/y)	(therms/y)	(kWh/y)	(therms/y)	(kWh/y)	(therms/y)
Louisiana								
Lake Charles	0	507	1,703	1,022	667	998	1,650	770
New Orleans	0	467	1,572	953	602	934	1,523	719
Shreveport	0	557	1,782	1,022	768	983	1,726	776
Maine								
Portland	0	892	2,274	1,127	1,366	1,014	2,203	985
Massachusetts								
Falmouth	0	673	1,834	909	1,120	807	1,777	779
Michigan								
Battle Creek	0	826	2,339	1,085	1,302	988	2,266	925
Detroit	0	865	2,365	1,123	1,339	1,021	2,291	965
Sault Ste Marie	0	1,253	2,577	1,470	1,667	1,314	2,496	1,339
Minnesota								
Duluth	0	1,446	2,655	1,655	1,748	1,500	2,573	1,529
International Falls	0	1,587	2,686	1,784	1,777	1,642	2,602	1,665
Minneapolis	0	1,139	2,680	1,387	1,552	1,282	2,596	1,233
Mississippi								
Biloxi	0	495	1,659	994	649	972	1,607	750
Columbus	0	563	1,792	997	811	952	1,736	766
Jackson	0	538	1,717	989	745	951	1,663	752
Missouri								
Columbia	0	745	2,169	1,086	1,104	1,016	2,102	886
Kansas City	0	744	2,182	1,099	1,077	1,033	2,114	885
Springfield	0	713	2,098	1,057	1,064	990	2,033	860
Montana								
Billings	0	904	2,323	1,172	1,341	1,064	2,251	1,012
Great Falls	0	1,056	2,355	1,319	1,455	1,205	2,281	1,169
Missoula	0	928	2,444	1,183	1,443	1,071	2,368	1,024
Nebraska								
Grand Island	0	923	2,544	1,220	1,360	1,104	2,465	1,038
Lincoln	0	904	2,439	1,180	1,320	1,064	2,363	1,013
North Platte	0	928	2,557	1,199	1,381	1,079	2,477	1,026
Nevada								
Ely	0	1,007	2,661	1,289	1,523	1,159	2,578	1,118
Las Vegas	0	730	2,219	1,306	904	1,258	2,149	932
Reno	0	759	2,247	1,037	1,225	932	2,177	870
Winnemucca	0	835	2,427	1,156	1,301	1,048	2,351	960
New Jersey								
Trenton	0	632	1,908	921	1,054	839	1,848	765
New Mexico								
Albuquerque	0	576	1,853	935	922	874	1,795	742
Farmington	0	727	2,215	1,054	1,137	969	2,146	868
Roswell	0	623	1,908	1,031	882	981	1,849	794
New York								
Albany	0	867	2,225	1,109	1,313	1,002	2,156	963
Binghamton	0	924	2,252	1,163	1,401	1,025	2,181	1,028
Niagara Falls	0	862	2,296	1,118	1,362	999	2,224	968
Syracuse	0	851	2,227	1,103	1,307	995	2,158	954
Westhampton Beach	0	624	1,832	870	1,057	784	1,775	737

Stata and City	Fuel Cell Powered Rankine Heat Pump (kWh/y)	Fuel Cell Powered Rankine Heat Pump (therms/y)	Vuilleumier Cycle Heat Pump (kWh/y)	Vuilleumier Cycle Heat Pump (therms/y)	GAX Absorption Heat Pump (kWh/y)	GAX Absorption Heat Pump (therms/y)	Duplex Stirling Cycle Heat Pump (kWh/y)	Duplex Stirling Cycle Heat Pump (therms/y)
North Carolina								
Greensboro	0	550	1,689	882	845	829	1,636	704
New Bern	0	519	1,654	956	726	921	1,602	740
North Dakota								
Bismarck	0	1,385	2,921	1,632	1,745	1,528	2,830	1,477
Grand Forks	0	1,585	3,079	1,805	1,886	1,701	2,983	1,667
Williston	0	1,236	2,758	1,470	1,605	1,372	2,672	1,321
Ohio								
Akron	0	765	2,155	1,028	1,244	923	2,088	879
Columbus	0	661	2,006	955	1,090	874	1,944	790
Dayton	0	697	2,091	1,017	1,117	932	2,025	843
Toledo	0	854	2,361	1,124	1,332	1,012	2,287	964
Oklahoma								
Altus	0	668	2,048	1,107	934	1,054	1,984	844
Oklahoma City	0	660	2,009	1,065	944	1,011	1,946	833
Tulsa	0	664	2,026	1,079	943	1,025	1,962	839
Oregon								
Astoria	0	380	1,188	558	831	480	1,151	469
Medford	0	385	1,750	535	974	464	1,696	453
Portland	0	494	1,396	730	868	659	1,353	602
Pennsylvania								
Philadelphia	0	602	1,849	876	1,027	797	1,791	729
Pittsburgh	0	770	2,084	1,025	1,215	925	2,019	878
Wilkes-Barre	0	735	2,069	982	1,192	883	2,005	839
South Carolina								
Charleston	0	494	1,608	925	703	892	1,557	715
Greenville	0	503	1,540	842	746	798	1,492	660
Sumter		496	1,585	905	707	869	1,535	698
South Dakota								
Huron	0	1,234	2,962	1,498	1,648	1,401	2,870	1,323
Rapid City	0	958	2,431	1,227	1,382	1,110	2,355	1,067
Teennessee								
Bristol	0	533	1,688	843	870	783	1,635	684
Knoxville	0	503	1,621	830	824	774	1,570	667
Memphis	0	602	1,855	1,013	862	964	1,797	787
Nashville	0	613	1,850	965	911	910	1,792	770
Texas								
El Paso	0	575	1,795	1,022	788	982	1,739	776
Fort Worth	0	629	1,987	1,148	838	1,105	1,924	856
Houston	0	538	1,831	1,099	696	1,077	1,774	822
San Antonio	0	562	1,900	1,149	702	1,127	1,841	843
Utah								
Salt Lake City	0	719	2,158	1,012	1,179	920	2,091	840
Vermont								
Burlington	0	1,076	2,477	1,302	1,510	1,180	2,400	1,163
Virginia								
Norfolk	0	548	1,676	894	833	843	1,624	712
Richmond	0	522	1,689	865	844	810	1,636	687
Roanoke	0	547	1,735	869	906	805	1,681	700

Stata and City	Fuel Cell Powered Rankine Heat Pump		Vuilleumier Cycle Heat Pump		GAX Absorption Heat Pump		Duplex Stirling Cycle Heat Pump	
	(kWh/y)	(therms/y)	(kWh/y)	(therms/y)	(kWh/y)	(therms/y)	(kWh/y)	(therms/y)
Washington								
Moses Lake	0	748	2,147	1,040	1,161	959	2,080	859
Seattle	0	514	1,464	743	943	663	1,419	618
Spokane	0	805	2,267	1,066	1,308	967	2,197	906
West Virginia								
Charleston	0	578	1,809	891	943	823	1,752	725
Elkins	0	685	1,901	941	1,122	843	1,842	804
Wisconsin								
Green Bay	0	1,072	2,548	1,312	1,529	1,188	2,468	1,165
Madison	0	993	2,460	1,257	1,440	1,143	2,383	1,099
Wyoming								
Casper	0	964	2,555	1,236	1,456	1,126	2,475	1,063
Cheyenne	0	926	2,384	1,188	1,418	1,071	2,309	1,032
Lander	0	960	2,498	1,191	1,407	1,092	2,420	1,043
Sheridan	0	972	2,546	1,241	1,447	1,118	2,466	1,075

Internal Distribution

1. V. D. Baxter
2. J. E. Christian
3. G. E. Courville
4. T. R. Curlee
5. R. C. DeVault
6. P. D. Fairchild

7-56. S. K. Fischer

57. P. W. Garland

58-67. S. D. Labinov

68. V. C. Mei
69. C. I. Moser
70. R. W. Murphy
71. C. K. Rice
72. J. R. Sand
73. R. B. Shelton
74. J. A. Shonder
75. J. J. Tomlinson
76. A. Zaltash
77. Central Research Library
78. Document Reference Section
79. Laboratory Records
80. Laboratory Records - RC

External Distribution

81. Dr. Lilia A. Abron, President Peer Consults P.C., 1460 Gulf Boulevard Apt. 1103, Clearwater, FL 33767
82. Karim Amrane, Air Conditioning and Refrigeration Technology Institute, 4301 N. Fairfax Drive, Suite 425, Arlington, VA 22203
83. Roland Ares, Ares Corporation, 1000 Wedgewood Drive, St. Charles, MO 63303
84. Dr. Douglas Bauer, Executive Director, Commission on Engineering and Technical Systems, National Research Council, Harris 280, 2001 Wisconsin Avenue NW, Washington, DC 20007
85. Don Bennett, Director of Engineering & Development, Outokumpu Copper Franklin, Inc., 4720 Bowling Green Road, P.O. Box 539, Franklin, KY 42135-0539
86. Don Bivens, E.I. du Pont de Nemours & Co., Fluorochemicals Laboratory, Chestnut Run Plaza, Building 711, Room 2106, Wilmington, DL 19880-0711
87. Mort Blatt, Electric Power Research Institute, P.O. Box 10412, Palo Alto, CA 94303
88. Jim Braun, 1077 Herrick Laboratories, Purdue University, West Lafayette, IN 47907-1077
89. Clark Bullard, 124 Mechanical Engineering Building, University of Illinois, MC 244, 1206 West Green, Urbana, IL 61801
90. Charles Bullock, Carrier Corporation, Carrier Parkway, P.O. Box 4808, Syracuse, NY 13221
91. Lee Burgett, Vice President, The Trane Company, Commercial Systems Group, 3600 Pammel Creek Road, LaCrosse, WI 54601-7599
92. Jean-Luc Caillat, Vice President, Research, Copeland Corporation, 1675 West Campbell Road, Sidney, OH 45365-0669
93. Richard Cawley, Manager Unitary Technology, The Trane Company, 6200 Troup Highway, P.O. Box 9010, Tyler, TX 75711
94. James Connell, Thermo-Technology Ventures, 85 First Avenue, Waltham, MA 03154
95. James Cowie, Manager Technical Programs, CDA, 260 Madison Avenue, New York, NY

10016

96. Titu Doctor, Crispaire, E-Tech Appl. Prod., 3285 Saturn Court, Norcross, GA 30092
97. Piotr Domanski, Group Leader Thermal Machinery Group, NIST, Building Environment Division, Building 226, Room B114, Gaithersburg, MD 20899
98. Don Erickson, President Energy Concepts Company, 627 Ridgely Avenue, Annapolis, MD 21401
99. Ron Fiskum, CE-422, 5H-048/FORS, U.S. Department of Energy, Washington, DC 20585
100. Fuel Cell Institute, P.O. Box 65481, Washington, DC 20035-5481
101. Steve Garrett, Graduate Program in Acoustics, Applied Research Laboratory, The Pennsylvania State University, P.O. Box 30, State College, PA 16804-0030
102. Paul Glamm, Engineering Manager, The Trane Company, 3600 Pammel Creek Road, Lacrosse, WI 54601-7599
103. Ken Hickman, Vice President Applied Systems Engineering, York International Corporation, 631 South Richland Avenue, P.O. Box 1592, Mail Code 191A, York, PA 17405-1592
104. Dr. Stephen G. Hildebrand, Director, Environmental Sciences Division, Oak Ridge National Laboratory, P.O. Box 2008, Oak Ridge, TN 37831-6037
105. Glen Hourahan, Air Conditioning and Refrigeration Institute, 4301 N. Fairfax Drive, Suite 425, Arlington, VA 22203
106. Michael Hughes, 195 Schultz Road, West Seneca, NY 14224
107. John Judge, Advanced Systems Engineering, York International Corporation, Heat Transfer Group, 631 South Richland Avenue, P.O. Box 1592, Mail Code 191A, York, PA 17405
108. Kwang Kim, Artificial Muscles Institute & Mechanical Engineering Department, University of New Mexico, Albuquerque, NM 87131

109-113. Esher Kweller, U.S. Department of Energy, CE-422, 5H048/FORS, 1000 Independence Avenue, S.W., Washington, DC 20585,

114. Jim Miller, Argonne National Laboratory, Building 205, 9700 Cass Avenue, Argonne, IL 60439-4837
115. Gary Nowakowski, Gas Research Institute, 8600 West Bryn Mawr Avenue, Chicago, IL 60631
116. Darin Nutter, University of Arkansas, Mechanical Engineering Department, Fayetteville, AR 72701
117. Reinhard Radermacher, A.J. Clark School of Engineering, University of Maryland, 3137 Engineering Classroom Building, College Park, MD 20742-3035
118. Wayne Reedy, Carrier Corporation, Carrier Parkway TR4, Syracuse, NY 13221-4808
119. Edward Reid, American Gas Cooling Center, 1515 Wilson Boulevard, Arlington, VA 22209
120. Mr. P. Richard Rittelmann, FAIA Executive Vice President, Burt Hill Kosar Rittelmann Associates, 400 Morgan Center, Butler, PA 16001-5977
121. Robert Rose, Fuel Cells 2000, 1625 K Street NW, Suite 790, Washington, DC 20006
122. John Ryan, U.S. Department of Energy, CE-422, 5H048/FORS, 1000 Independence Avenue, S.W., Washington, DC 20585,
123. William Ryan, Gas Research Institute, 8600 West Bryn Mawr Avenue, Chicago, IL 60631
124. Sam Shelton, Thermax, Inc., 290 14th Street NW, Atlanta, GA 30318
125. Richard Sweetser, Exergy Parners Corporation, 12020 Meadowville Court, Herndon, VA

20170

126. Greg Swift, Condensed Matter and Thermal Physics Group, Mail Stop K764, Los Alamos National Laboratory, Los Alamos, NM 87545
127. Dr. Susan F. Tierney, The Economic Resource Group, Inc., One Mifflin Place, Cambridge, MA 02138
128. Dr. C. Michael Walton, Ernest H. Cockrell Centennial Chair in Engineering, Department of Civil Engineering, University of Texas at Austin, Austin, TX 78712-1076
129. C. Wu, Department of Mechanical Engineering, U.S. Naval Academy, Annapolis, MD
130. Ed Wuesthoff, Americold, 2340 2nd Avenue NW, Cullman, AL 35058
131. Carl Zimm, Astronautics Corporation, Astronautics Technology Center, 5800 Cottage Grove Road, Madison, WI 53716-1387
132. OSTI , U.S. DOE, Oak Ridge, TN 37830